5-2018

Optimization Models for Sustainable Design and Management of Biopower Supply Chains

Hadi Karimi
Clemson University, hkarimi@clemson.edu

Optimization Models for Sustainable Design and Management of Biopower Supply Chains

---

A Dissertation
Presented to
the Graduate School of
Clemson University

In Partial Fulfillment
of the Requirements for the Degree
Doctor of Philosophy
Industrial Engineering

---

by
Hadi Karimi
May 2018

Accepted by:
Dr. Sandra D. Ekşioğlu, Committee Chair
Dr. Amin Khademi
Dr. Michael Carbajales-Dale
Dr. B. Rae Cho

Abstract

This dissertation presents optimization models to aid with the sustainable design and management of biopower (biomass cofiring) supply chains. We address three main challenges associated with today's biopower projects: i) high cost of biomass collection, storage and delivery, ii) inefficiency of the mechanisms used to incentivize biomass usage for generating electricity, and iii) lack of clear understanding about the trade-offs between economic and environmental impacts of biopower supply chains.

In order to address the high cost of delivering biomass, we present a novel mixed integer nonlinear program that integrates production and transportation decisions at power plants. Proposed model captures the loss in process efficiencies from using biomass, investment and operational costs associated with cofiring, and savings due to production tax credit (PTC), a major governmental incentive to support biopower. We develop a Lagrangian relaxation approach to provide upper bounds, and two linear approximations to provide lower bounds for the problem. An important finding is that the one-size-fits-all approach of PTC is not effective in motivating plants to utilize biomass and there is a need for sophisticated incentive schemes. In order to address the second issue, we propose alternatives for the existing PTC incentive. The proposed flexible alternatives are functions of plant capacity and biomass cofiring ratio. We use a resource allocation framework to model and analyze the profit-earning potentials and fairness of the proposed incentive schemes. Finally, in order to address the last challenge, we propose a stochastic biobjective optimization model to analyze the economic and environmental impacts of biopower supply chains. The economic objective function maximizes the potential profits in the supply chain and

the environmental objective function minimizes the life cycle greenhouse gasses (GHG). We use a life cycle assessment (LCA) approach to derive the emission factors for this objective function. We capture uncertainties of biomass quality and supply via the use of chance constraints.

The results of this dissertation work are useful for electric utility companies and policy makers. Utility companies can use the proposed models to identify ways to improve biopower production, have better environmental performance, and make use of the existing incentives. Policy makers would gain insights on designing incentive schemes for a more efficient utilization of biomass and a fairer distribution of tax-payers money.

Dedication

This dissertation is dedicated to my wonderful *parents*, my supportive *brothers*, and my lovely *niece* and *nephews*.

Acknowledgments

First and foremost, I would like to express my highest appreciation to my academic advisor, Dr. Sandra Duni Ekşioğlu. I am indebted to Dr. Ekşioğlu for her continuous support, guidance, and inspiration throughout my Ph.D. studies at Clemson University. Without her assistance and mentorship this dissertation would never have been accomplished. Additionally, I would like to thank other members of my dissertation committee: Dr. Amin Khademi, Dr. Michael Carbajales-Dale, and Dr. B. Rae Cho. I truly appreciate all of their time and assistance as I navigated through this process. I have had the honor of collaborating with Dr. Khademi and Dr. Carbajales-Dale in publishing and preparation of two journal papers. I also express my sincere gratitude to Dr. Burak Ekşioğlu for his collaboration in our first peer-reviewed paper published in *IIE Transactions*.

I would like to thank all my great friends and colleagues in the Industrial Engineering Department at Clemson University. Especially Zahra Azadi, Site Wang, Mowen Lu, Shasha Wang, Rob Curry, Farhad Hasankhani, Amirali Nasrollah-Zade, Abdelwahab Alwahishie, Josh Margolis, and Jon Lonski.

I acknowledge financial support from the National Science Foundation, grant CMMI 1462420. I appreciate Clemson University's Computing and Information Technology center (CCIT) for generous allotment of compute time on Palmetto cluster.

Finally, my eternal thanks to my parents, Haaj Hossein Karimi and Haajie Golnaz Niki, for their love, affection, and support. Words are never enough to express my love for them.

Table of Contents

List of Tables

List of Figures

Chapter 1

Introduction

1.1 Introduction

The large scale physical, social, and ecological impacts of global warming present increasing and certain threat for the future of our planet. The analysis conducted by the U.S. Environmental Protection Agency predicts that carbon-dioxide (CO_2) concentration in the atmosphere will reach 500 ppm by 2030 if we continue to consume fossil fuels at the current rate (EPA 2009). About 41% of global CO_2 emissions are due to electricity and heat generation, and 43% of these emissions are due to coal combustion in thermal power plants (IEA 2012). In the U.S., coal contributes to 71% of the total CO_2 emissions from the energy sector (U.S. Energy Information Administration (EIA), 2015). The increasing concerns about global warming and the depletion of fossil fuel reserves have motivated countries to decrease dependency on fossil fuels and incorporate renewable sources for securing environmentally friendly future.

The 5th Assessment Report (AR5) of the Intergovernmental Panel on Climate Change (IPCC) proposes different strategies to decrease the use of fossil fuels in the upcoming decades. Power plants can adopt one or a combination of the approaches proposed in order to meet the IPCC environmental goals. The approaches proposed by IPCC are (Change 2014): a) invest in improving the efficiency of the power generation system; b)

invest in carbon dioxide capture and storage (CCS) technology; and c)substitute fossil fuels with fuels which have low carbon content (e.g. natural gas) or are carbon neutral (e.g. hydro, nuclear, biomass, etc) fuels.

In this dissertation, we propose models that optimize the performance of biomass utilization in coal-fired power plants. Biomass is the name given to any organic matter which is derived from plants and animals. That is plant and animal materials such as wood from forests, crops, seaweed, material left over from agricultural and forestry processes, and organic industrial, human and animal wastes. Biomass is one of the earliest sources of energy used by humans. Biomass consists of carbohydrates and is considered a renewable energy source since its supply is renewable. Compared to other renewable technologies such as solar or wind, biomass energy can be easily stored.

There are two major ways that biomass can be used for generating electricity: gasification and direct firing. Biomass gasification systems operate by heating biomass in an environment where the solid biomass breaks down to form a flammable gas. The gas produced is cleaned, filtered, and then burned in a gas turbine for power generation. In direct firing, biomass is used as combustible fuel in a boiler to produce high-pressure steam that is used to power a steam turbine-driven power generator. Biomass at coal plants can be burned in a separate boiler or together with coal in the same boiler (cofiring). The primary focus of study in this dissertation is on the direct co-combustion of biomass and coal at existing power plants, referred to as *biomass cofiring* or *biopower* throughout the dissertation.

Biomass cofiring is shown to be an efficient and inexpensive alternative to mitigate harmful environmental impact of coal-fired power plants (Baxter 2005, Basua et al. 2011). Unlike CCS and natural gas technologies, biopower entails insignificant investment costs and implementation complexities. It is one of the best known near-term solutions that can help coal plants to meet environmental restrictions and obtain financial incentives and credits from state and federal governments. Currently, about 40 of the 560 coal-fired power plants in the U.S. are co-firing biomass.

Despite the well-known benefits, biopower faces with challenges and drawbacks.

Feedstock availability is a key issue in determining the economic viability of biomass projects. A poor logistic management plan can negate the financial benefits obtained from available incentives. In countries with advanced bioenergy policies, such as European countries, the bioenergy market is regulated and supported by policy measures, such as national targets or feed-in-tariff (FIT) incentives. In other countries, such as the U.S., improvement of exiting policies and incentive schemes is necessary to make biopower competitive in energy market. Sustainability is becoming an ever more important issue in biopower projects. At coal plants, replacing biomass with coal reduces the emissions due to combustion, however, the total footprint of the associated supply chain still needs to be carefully investigated. Cultivating biomass resources for cofiring can restrict the land-use diversity and reduce the capability for producing food for livestock or human use.

Despite the challenges mentioned above, biomass energy market offers a significant growth potential. In the New Policies Scenario of the IEA World Energy Outlook, global biopower generation is assumed to increase from 424TWh in 2011 to 1,204TWh in 2030 (EIA 2013b). In the following list, we provide a summary of related problems that this dissertation addresses.

- *Supply chain design and integration of logistic decisions and production planning.* Biomass cofiring in coal plants does not require significant infrastructural changes or investment costs. However, the decisions related to the logistics of acquiring biomass resources in conjunction with production processes at coal plants impacts the efficiency and economic benefits of this technology. Biomass has a disperse and often uncertain availability throughout the country. Questions such as which supplier(s) to select, what kind of transportation mode to chose, and what is the best cofiring strategy, need to be addressed in order to have a better picture about complications of this technology.

- *Governmental incentives in support of biomass cofiring.* The importance of governmental incentives to make cofiring an attractive investment option is highlighted in

several studies (O'Mahoney et al. 2013, Wils et al. 2012). In the U.S., the main support program for biomass cofiring is a fixed rate production tax credit (PTC) which is provided per unit of renewable energy generated from biomass resources (in form of $¢/kWh$). Whether the current support mechanism is effective in motivating coal plants to participate in cofiring, and how this mechanism can be improved to provide a fair and efficient scheme are some of the key questions that need to be answered in this context.

- *Trade-offs between economic and environmental impacts of biopower supply chain.* Biomass cofiring has the potential to decrease GHG emission levels at coal plants. However, the extent of environmental impacts of this technology will ultimately depend on emissions during product's life cycle, including biomass supplier activities, feedstock transportation, and processes at power plants. It is also necessary to take into account how biomass utilization affect biodiversity and environmental sustainability in the region (e.g. by deforestation or exploitation of the land which is otherwise used for cultivating human or animal foods). Exploring the trade-offs between related cost/benefits and sustainability issues is crucially important to gain insight on generating electricity using biomass. There is a need for models which optimize the economic and environmental impacts of biopower generation in an uncertain environment.

In this dissertation, we develop optimization models and solution algorithms in order to address the challenges listed above. These models enable coal-fired power plants to identify strategies which allow them to comply with new environmental regulations at the minimum cost. The proposed models also capture the social and environmental impacts of operational and strategic decisions made by coal plants. Additionally, we propose models which enable policy makers identify policies which encourage renewable energy generation. We apply different modeling approaches (such as mixed integer programming, multiobjective optimization, stochastic programming) to capture the multifaceted and often uncertain nature of related information. To solve the proposed models and carry out sensitivity anal-

yses, we develop problem specific solution methods and algorithms based on several OR tools (such as Benders decomposition, Lagrangian relaxation, ϵ-constraint method).

We develop real-world case studies to illustrate the practical use of the proposed models and solution methods. These case studies use data on existing coal-fired power plants and biomass resources in southeastern states of the U.S. This region of the country is known to be rich in biomass resources and appropriate for cofiring projects. Two main case studies are developed and studied in the dissertation. For the case studied in Chapters 2 and 3, we work on the coal plants spread in the nine major states of the Southeast: Alabama, Arkansas, Florida, Georgia, Louisiana, Mississippi, North Carolina, South Carolina, and Tennessee. For the case studied in Chapter 4, we work on a utility company which owns a group of plants in the states of North Carolina and South Carolina.

1.2 Dissertation Structure

The remainder of dissertation is structured as follows:

In Chapter 2, we develop an optimization model to integrate production and transportation planning at power plants that cofire biomass. These models aid the coal-fired power plants with logistics and operational decisions. The goal is to minimize supply chain costs. The developed model is a mixed integer nonlinear program (MINLP). We provide a linear approximations for the MINLP model and use Lagrangian relaxation to calculate upper and lower bounds for the problem.

In Chapter 3, we provide an analysis of current and proposed tax incentive schemes to support biomass utilization at existing coal-fired power plants. The proposed alternative schemes can be used by policy makers to design fair and efficient support mechanisms and increase plants participation in cofiring given a limited budget. We use a resource allocation framework to compare and analyze the efficiency and fairness of different flexible tax schemes.

Finally, in Chapter 4, we provide a stochastic biobjective optimization model to

analyze the economic and environmental impacts of biopower supply chains. The first objective function identifies strategies which maximize the potential profits in supply chain. The second objective function minimizes the GHG emissions throughout the life cycle of biomass feedstock. We propose a chance constraint approach to capture the uncertainties in the model. We develop an exact formulation of chance constraint in form of quadratic constraints. The quadratic constraint makes the model nonlinear. We develop another formulation based on sample average approximation that only involves linear constraints. The Pareto optimal solutions are find via ϵ-constraint algorithm.

For further discussions on the problem structure and analytical aspects of the optimization models refer to appendices 1-4 at the end of the document.

Chapter 2

Optimization Models to Integrate Production and Transportation Planning for Biomass Co-Firing in Coal-Fired Power Plants

2.1 Introduction

Coal-fired power plants in the US consume 1.1 to 1.2×10^9 tons of coal annually in order to generate electricity. The burning of coal in these plants produces many gases (e.g., CO_2, SO_2, NO_x, etc.) and heavy metals (e.g., mercury and arsenic), which adversely affect the environment and human health (US Energy Information Administration (EIA, 2014)). It is estimated that, for each megawatt-hour of electricity generated, a total of 2,249 lbs of CO_2, 13 lbs of SO_2, and 6 lbs of NO_x are emitted. In 2013, coal accounted for 32% of the total energy-related CO_2 emissions in the US (US Environmental Protection Agency (EPA), 2013).

New performance standards and rules proposed by the EPA have placed stringent

limitations on greenhouse gas (GHG) emissions from new and existing power plants. In January 2014, EPA issued a revised performance standard proposal for CO_2 emissions, according to which, new coal fired power plants are required to limit emissions to 1,100 lbs per megawatt-hour. The proposed emissions limit is forcing new coal-fired power plants to identify technologies which will reduce CO_2 emissions by approximately 50%. In June 2014, EPA released proposed rules that are designed to cut CO_2 emissions for existing power plants by 30% from 2005 levels by the year 2030. In March 2013, the agency finalized the Mercury and Air Toxics Standards to reduce emissions of mercury and other air toxics from new and existing coal and oil-fired electric generating units. In July 2011, EPA finalized the Cross-State Air Pollution Rule (CSAPR), which seeks to reduce SO_2 and NO_x emissions from power plants in 28 states.

Researchers agree that co-firing offers a near-term solution to reduce CO_2 emissions from coal-fired power plants since viable and long-term solution alternatives (such as, carbon capture and sequestration (CCS), oxy-firing and carbon loop combustion) still remain in the early to mid stages of development (Basua et al. 2011). Currently, 40 of the 560 coal-fired power plants in the US are co-firing biomass, a renewable energy process that is encouraged by incentives such as the renewable portfolio standards (RPS) at the state level; and the production tax credit (PTC) at the federal level. The federal PTC is a flat rate income tax credit of 1.1 cents per kilowatt-hour which supports biomass-based electricity generation technologies such as full-scale biomass cofiring and closed loop partial cofiring; however, its support for general cofiring (open loop biomass) is not clearly specified (Internal Revenue Code, Section 45). The importance of extending current tax incentive plan to cover partial cofiring is suggested in the literature (Smith and Rousaki (2002)). In this chapter, we evaluate the impact of presenting PTC to support partial cofiring in current coal-fired power plants. At the state level, RPS requires investor-owned utilities, electric service providers, and community choice aggregators to increase procurement from eligible renewable energy resources (EIA 2013a, 2013b, 2013c). Researchers also agree that co-firing biomass with coal in power plants is an option for RPS compliance and a near-term solution

for introducing biomass into today's renewable energy mix (Basua et al. 2011). Based on the renewable fuel standards (RFS), cellulosic biomass is expected to be the largest source of renewable energy comprising 44.4% of the targets set for 2020 (EPA 2007). Biomass used in direct combustion has shown to be dispatchable, i.e., capable of responding to user needs without energy storage unlike wind and solar power which are at the mercy of nature (Tillman et al. 2010). While the technology to produce liquid fuels by using biomass is not yet available, co-firing of biomass is a feasible option worth investigating.

Based upon our review of the literature, we contend that most current research has involved elucidating the technological aspects of co-firing processes (Li et al. 2012, Tumuluru et al. 2012) and the techno-economic and feasibility analysis (Dong et al. 2010, Ruhul-Kabir and Kumar 2012, Steer et al. 2013, Goerndt et al. 2013b, Paudel 2013, Mehmood et al. 2014). Very little research has been undertaken to estimate the transportation costs of delivering biomass to power plants (Roni et al. 2014). To the best of our knowledge, there are no studies which provide models to optimize co-firing decisions at the plant level by integrating plant operations-, with, transportation and other logistics-related decisions. Thus, the main contribution of this chapter is the development of mathematical models to aid co-firing decisions at plant level. The proposed model takes a holistic view of the processes affected by these decisions such as production, storage, and transportation.

Biomass co-firing impacts the performance of the coal plants in several ways. *First*, biomass has less energy density as compared to coal, and therefore, larger quantities of biomass are required to substitute the same amount of coal. Additionally, biomass in the form of agricultural and forest waste has poor flowability properties, and thus, it is bulky, heterogeneous, and unstable. For these reasons, processes such as loading, unloading and transportation of biomass are challenging and expensive. *Second*, existing power plants are typically co-located with coal mines which would typically supply enough coal to satisfy plant's demand. Biomass suppliers are typically small or medium sized farms, which are widely dispersed geographically. Thus, processes such as biomass collection, biomass delivery, and supplier management are expensive (Aden et al. 2002). *Third*, co-firing of biomass

reduces boilers efficiency, and as a consequence, reduces overall system efficiency. *Fourth*, biomass co-firing requires investments to adjust the feeding system, since the same system often cannot be used to feed biomass in burners (Tillman 2000).

Coal plants are aware of the challenges and opportunities related to co-firing. However, decision makers are in need of tools which integrate the additional savings, additional costs, and loss of process efficiencies from co-firing. Such tools would enable decision makers identify the level of co-firing that maximizes profits while complying with existing GHG emission regulations. To support these decisions we propose an optimization model which encompasses the (a) additional investments necessary to adopt co-firing at power plants; (b) reduction in process and equipment (e.g., boiler) efficiency from this coal substitution; (c) additional transportation-related costs necessary for biomass delivery; (d) savings from incentives such as PTC. This model is useful in evaluating the existing trade-offs between profits and the environmental impacts associated with co-firing. We propose solution approaches to solve these large scale, nonlinear optimization problems. These approaches are novel and rely on the properties of the models presented.

Another important contribution of this study is that we use real world data to build a case study. Thus, through our numerical analysis we make a few important observations about the impact of incentives such as PTC on renewable electricity production. These findings can help policy makers at the federal or state level to evaluate the economic feasibility of producing renewable electricity, and design policies in support of co-firing.

2.2 Review of Related Literature

The work presented in this chapter contributes to the literature on biomass supply chain optimization as well as technological and economical feasibility of co-firing.

2.2.1 Biomass supply chain optimization

The literature on biomass supply chain has grown in the recent years. Early studies in the area of biomass supply chain management focused mainly on cost-benefit analysis, such as estimating the cost of collecting, handling, and hauling biomass (Perlack and Turhollow 2002, Petrolia 2008) and comparing different modes of transportation to deliver biomass (Kumar et al. 2005, Mahmudi and Flynn 2006). This literature pays attention to mainly operational-level supply chain decisions. More recently, a number of models have been proposed to optimize the performance of the supply chain by incorporating strategic and tactical decisions. Models proposed by Eksioglu et al. (2009), Zamboni et al. (2009), Huang et al. (2010), An et al. (2011) integrate plant location, production, and transportation decisions in the biomass supply chain. For a comprehensive review of modeling frameworks, challenges faced, and the future of biomass supply chains we refer the readers to Sharma et al. (2013).

Related to this research are works by Aguilar et al. (2012) and Roni et al. (2014). Aguilar et al. (2012) propose a supply chain model to evaluate the likelihood of using biomass for co-firing. The model evaluates the impact of the locations of biomass suppliers and the location of coal-fired power plant on co-firing decisions. Roni et al. (2014) propose a framework to design biomass supply chains to support co-firing of biomass at the national level. Based on this framework, small-sized plants are better off receiving biomass shipments from local suppliers. Large-sized plants are better-off using hub-and-spoke in-bound networks that rely both on truck and rail transportation for biomass delivery. Hub-and-spoke networks are typically used for long-haul delivery of bulky products. These models either focus on optimizing transportation decisions for a given biomass co-firing strategy or focus on optimizing co-firing decisions within a plant given the amount of biomass available in the region. The model we propose integrates transportation and co-firing decisions with the goal of optimizing system-wide profits.

2.2.2 Technological and economical feasibility of co-firing

Most of the literature about co-firing is mainly focused on analyzing its technological and economical feasibility. Work by Goerndt et al. (2013a) identifies the necessary drivers for successful implementation of co-firing. The drivers identified are the adequate biomass supply and competitive biomass purchase and transportation costs. The work of Baxter (2005) indicates that biomass-coal co-combustion is an affordable renewable energy option that promises reductions in GHG emissions. Works of Hansson et al. (2009) and Al-Mansour and Zuwala (2010) indicate that biomass co-firing is a technologically sound and near-term solution to comply with GHG emission regulations in the European Union (EU). They support their findings by discussing some successful implementations of the technology in EU. A study by Basua et al. (2011) indicates that nearly all coal-fired power plants can achieve an incremental gain in GHG reductions with minimum modifications and moderate investments. Hansson et al. (2009) predict that biomass co-firing will become a major contributor to meeting the renewable energy production goals in near future. Works by Li et al. (2012), Shao et al. (2012), Tumuluru et al. (2012), Steer et al. (2013), Tchapda and Pisupati (2014) investigate the technological challenges and process inefficiencies associated with biomass co-firing.

Baxter (2005), De and Assadi (2009), Wils et al. (2012), O'Mahoney et al. (2013), Paudel (2013) study the economic feasibility of co-firing. Ruhul-Kabir and Kumar (2012) conduct a life cycle energy and environmental performance analysis of co-firing different types of biomass since the efficiency of co-firing process depends on the specific chemical content and properties of the biomass used in co-combustion (Mehmood et al. 2014). O'Mahoney et al. (2013) and Wils et al. (2012) use a cost-benefit analysis to show that governmental incentives are necessary for making co-firing an attractive investment option. Similarly, McIlveen-Wright et al. (2011) and De and Assadi (2009) conduct comprehensive techno-economic analysis of co-firing. They evaluated the technological and economical feasibilities of existing pilot plants, and suggest that there is a need for additional governmental incentive schemes. The effect of subsidizing biomass co-firing is also discussed by Lintunen

and Kangas (2010). Their numerical results show that subsidizing biomass combustion in a coal-fired power plant provides great results with minimum investments in renewable technology. Tharakan et al. (2005) evaluate the impacts of three co-firing incentive programs in the US. One of the incentives analyzed is the PTC.

2.3 Problem Description

There are two main co-firing methods used in coal plants, which are direct and indirect co-firing. Direct biomass co-firing systems include solutions such as: co-milling, co-feeding, combined burner and new burners. In these systems, biomass is milled and then fed to coal burners for combustion. This method is the simplest, cheapest and most-widely used (see Touš et al. (2011), Piriou et al. (2013)). However, direct co-firing is sensitive to the biomass quality, and, in the long run, direct co-firing shortens the lifespan of equipment used. Indirect biomass co-firing systems include solutions such as: separated burning, coupled plant, gasification systems, and pyrolysis. In these systems, biomass is either burned separately using specially designed boilers; or, it is transformed into a gas using a gasifier; or it is transformed into a mixture of gas, bio-oils and char through pyrolysis (see Dong et al. (2010), Caputo et al. (2005), Dasappa et al. (2004)). These systems are more complex and expensive. However, these systems reduce equipment degradation problems, such as, corrosion, fouling, and slagging. Such systems allow for larger co-firing rates as compared to direct co-firing.

The focus of this study is direct co-firing since this method is easy to implement, requires less capital investments, thus, easier to adopt by existing coal fired power plants. In this case, the percentage of coal substituted varies between 0-50%.

2.3.1 Biomass Co-Firing: Modeling Plant Efficiency

Biomass has a lower heating value as compared to coal. Additionally, using biomass negatively impacts the efficiency of the burners used in a coal plant. Thus, co-firing as

much biomass (by mass) as the amount of coal displaced would reduce the amount of energy generated. The objective of this section is to determine the relationship that exists between the amount of coal displaced and the amount of biomass co-fired to maintain the same energy output at a coal plant.

Let Q_j^0 (in MW) be the initial (before co-firing) annual heat input rate of a coal plant j. The heat input is a function of plant's nameplate capacity (TC_j in MW), capacity factor f_j (or utilization rate), and initial plant efficiency rate (ρ_j^0). The annual heat input is equal to $Q_j^0 = \frac{TC_j * f_j}{\rho_j^0}$.

A coal plant would typically use coal in order to generate electricity. The mass of coal used is a function of the lower heating value for coal (LHV_j^{coal} in BTU/ton) and the total number of operating hours (OH_j in hours/year). The amount of coal used (M_j^{coal} in tons) is equal to:

$$M_j^{coal} = \frac{Q_j^0 * OH_j * C^{wb}}{LHV_j^{coal}}, \tag{2.1}$$

where, C^{wb} is the conversion factor from 1 MW to BTU/hr.

Suppose that ∇M_j^{coal} tons of coal will be displaced in the coal plant. We estimate the amount of biomass required (M_j^{bm} in tons) to maintain the same energy output using the following energy equilibrium equation

$$M_j^{bm} * LHV_j^{bm} = \nabla M_j^{coal} * LHV_j^{coal}.$$

Thus, the amount of biomass required to displace ∇M_j^{coal} tons of coal is equal to

$$M_j^{bm} = \nabla M_j^{coal} * \left(\frac{LHV_j^{coal}}{LHV_j^{bm}} \right).$$

We now can calculate β_j, the percentage of biomass co-fired in facility j, as follows:

$$\beta_j = \frac{M_j^{bm}}{(M_j^{coal} - \nabla M_j^{coal}) + M_j^{bm}} = \frac{1}{\frac{M_j^{coal}}{M_j^{bm}} + (1 - \frac{LHV_j^{bm}}{LHV_j^{coal}})} = \frac{1}{\frac{M_j^{coal}}{M_j^{bm}} + \alpha_j}, \tag{2.2}$$

where $\alpha_j = 1 - \frac{LHV_j^{bm}}{LHV_j^{coal}}$. Thus, for a fixed value of β_j, the amount of biomass required to displace coal should be:

$$M_j^{bm} = \frac{M_j^{coal}}{1/\beta_j - \alpha_j} = \left(\frac{1}{1/\beta_j - \alpha_j}\right) * \left(\frac{Q_j^0 * OH_j * C^{wb}}{LHV_j^{coal}}\right). \tag{2.3}$$

Equation (2.3) calculates the amount of biomass required to displace $\beta\%$ of coal under the assumption that there would be no equipment efficiency loss due to co-firing. However, equipment efficiency is indeed affected. Let ρ_j denote plant efficiency, which is a function of the efficiency of all processes involved. Initially, $\rho_j^0 = \rho_j^b * \rho_j^{rp}$, where, ρ_j^b represents boiler efficiency and ρ_j^{rp} represents the efficiency of rest of the plant. The efficiency loss of boilers (EL_j) due to displacing $\beta_j\%$ of coal, is calculated as follows: $EL_j = 0.0044\beta_j^2 + 0.0055$ (Tillman 2000). Due to this efficiency loss, plant efficiency decreases from ρ_j^0 to $\rho_j = (\rho_j^b - EL_j) * \rho_j^{rp}$.

The efficiency loss impacts the annual heat input of the coal plant. Thus, the heat input required to maintain the same energy output increases to:

$$Q_j = \frac{TC_j * f_j}{\rho_j} = \left(\frac{\rho_j^0}{\rho_j}\right) * Q_j^0 = \left(\frac{\rho_j^b}{\rho_j^b - EL_j}\right) * Q_j^0.$$

Consequently, the corresponding amount of biomass required for co-firing increases to:

$$M_j^{bm} = \left(\frac{1}{1/\beta_j - \alpha_j}\right) * \left(\frac{Q_j^0 * OH_j * C^{wb}}{LHV_j^{coal}}\right) * \left(\frac{\rho_j^b}{\rho_j^b - EL_j}\right) =$$

$$= \left(\frac{1}{1/\beta_j - \alpha_j}\right) * \left(\frac{\rho_j^b}{\rho_j^b - EL_j}\right) * M_j^{coal}. \tag{2.4}$$

Equation (2.4) indicates that the amount of biomass requirement to displace $\beta_j\%$ of the coal is a function of plant nameplate capacity, plant efficiency, lower heating values of coal, lower heating values of biomass, and plant operating hours.

2.3.2 Biomass Co-Firing: Modeling Costs and Savings

This section estimates the additional costs and savings due to biomass co-firing.

Plant Investment Costs:

Investments on building a new feeding system, purchasing compressors and dryers, purchasing biomass handling equipment, and investments on additional storage space are typically required to facilitate direct co-firing. Studies such as, Sondreal et al. (2001), Caputo et al. (2005) indicate that when less than 4% of coal is displaced in a plant, the existing fuel feeding system can be used for both products. In this case, the annual investments (I_j^{CAP}) of plant j are expected to be \$50 per KW of power generated from biomass, assuming 20 years investment lifetime and 9% discount rate.

In order to calculate the annual investment costs, we first need to calculate how much power (in MW) could be generated from biomass at a plant of capacity TC_j when $\beta_j\%$ of coal ($\beta_j\% < 4\%$) is being displace. Next, we multiply this amount with the \$50/KW (or \$50,000/MW) to calculate the annual investment costs as follows:

$$I_j^{CAP} = 50,000 * \left(\frac{M_j^{bm}}{M_j^{coal} - \nabla M_j^{coal}} \right) * \left(TC_j * f_j * \frac{LHV_j^{bm}}{LHV_j^{coal}} \right) = 50,000 * \left(TC_j * f_j * \frac{LHV_j^{bm}}{LHV_j^{coal}} \right) * \left(\frac{\beta_j}{1-\beta_j} \right).$$

Let, $I_j^{cap} = 50,000 * \left(TC_j * f_j * \frac{LHV_j^{bm}}{LHV_j^{coal}} \right)$, then,

$$I_j^{CAP} = I_j^{cap} * \left(\frac{\beta_j}{1-\beta_j} \right). \tag{2.5}$$

In the case when $\beta_j > 4\%$, the annual investment costs are higher since large amounts of biomass would be used by the plant. In this case, the plant would be investing

in extra storage space, material handling equipments, and compressors and dryers necessary to process biomass prior to co-firing. The annual investment costs necessary for biomass storage (I_j^S), biomass handling (I_j^H), and investments on compressors and dryers (I_j^{CD}) are presented next. The annual storage costs are estimated to be \$136,578 per MW of power generated from biomass; the annual handling costs are estimated to be \$55,780 and the annual compressors and dryers costs are \$13,646 per MW of power generated from biomass (Caputo et al. 2005).

The annual cost of biomass storage as follows:

$$I_j^S = 136,578 * \left(\frac{M_j^{bm}}{M_j^{coal} - \nabla M_j^{coal}} * TC_j * f_j * \frac{LHV_j^{bm}}{LHV_j^{coal}} \right)^{0.5575} =$$

$$136578 * \left(TC_j * f_j * \frac{LHV_j^{bm}}{LHV_j^{coal}} * \frac{\beta_j}{1-\beta_j} \right)^{0.5575}.$$

The annual cost of biomass handling is estimated as follows:

$$I_j^H = 55780 * \left(\frac{M_j^{bm}}{M_j^{coal} - \nabla M_j^{coal}} * TC_j * f_j * \frac{LHV_j^{bm}}{LHV_j^{coal}} \right)^{0.9554} =$$

$$55780 * \left(TC_j * f_j * \frac{LHV_j^{bm}}{LHV_j^{coal}} * \frac{\beta_j}{1-\beta_j} \right)^{0.9554}.$$

The annual cost of compressors and dryers is estimated as follows:

$$I_j^{CD} = 13646 * \left(\frac{M_j^{bm}}{M_j^{coal} - \nabla M_j^{coal}} * TC_j * f_j * \frac{LHV_j^{bm}}{LHV_j^{coal}} \right)^{0.5575} =$$

$$13646 * \left(TC_j * f_j * \frac{LHV_j^{bm}}{LHV_j^{coal}} * \frac{\beta_j}{1-\beta_j} \right)^{0.5575}.$$

Let, $I_j^s = 136578 * \left(TC_j * f_j * \frac{LHV_j^{bm}}{LHV_j^{coal}} \right)^{0.9554}$, $I_j^h = 55780 * \left(TC_j * f_j * \frac{LHV_j^{bm}}{LHV_j^{coal}} \right)^{0.9554}$, and $I_j^{cd} = 13646 * \left(TC_j * f_j * \frac{LHV_j^{bm}}{LHV_j^{coal}} \right)^{0.5575}$.

The total capital investment costs in plant j when $\beta_j \geq 4\%$ are:

$$I_j^{CAP} = I_j^S + I_j^H + I_j^{CD} = I_j^s \left(\frac{\beta_j}{1-\beta_j}\right)^{0.5575} + I_j^h \left(\frac{\beta_j}{1-\beta_j}\right)^{0.9554} + I_j^{cd} \left(\frac{\beta_j}{1-\beta_j}\right)^{0.5575}. \quad (2.6)$$

Operating Costs:

Operating costs consist of the cost of purchasing and transporting biomass. Let c_i^{bm} denote the unit purchase cost of biomass (in \$/ton) from supplier i, and, let S denote the set of biomass suppliers. Then, the total biomass purchasing cost at plant j is equal to $\sum_{i \in S} c_i^{bm} * M_j^{bm}$.

Transportation costs consist of the trucking costs necessary to deliver biomass to coal plants. We assume that truck shipments of biomass are delivered by third party service providers who charge a fixed \$ amount per ton of biomass shipped. The unit delivery cost from supplier i to plant j is denoted by c_{ij}. The total biomass transportation costs of plant j are equal to $\sum_{i \in S} c_{ij} M_j^{bm}$.

Savings:

Savings resulted from the PTC of 1.1¢ per KWh of renewable electricity, and from the displacement of ∇M_j^{coal} tons of coal.

Savings due to the PTC are calculated as follows:

$$S_j^{tax} = \sigma_j^t * M_j^{bm}, \quad (2.7)$$

where, $\sigma_j^t = 11 * \frac{LHV_j^{bm}}{C^{wb}}$.

Savings due to coal displacement are calculated as follows:

$$S_j^p = c_j^{coal} * (\nabla M_j^{coal}) = c_j^{coal} * \left(M_j^{bm} * \frac{LHV_j^{bm}}{LHV_j^{coal}}\right) = \sigma_j^p * M_j^{bm}, \quad (2.8)$$

where, $\sigma_j^p = c_j^{coal} * \frac{LHV_j^{bm}}{LHV_j^{coal}}$. Here c_j^{coal} is the door price of coal (in \$/ton). This cost includes purchasing and transportation costs.

2.4 A Mixed Integer Nonlinear Programming Formulation

This section presents a nonlinear problem formulation which identifies co-firing strategies that optimize the total profits of coal-fired power plants which share the same regional biomass resources. The model presented is a nonlinear mixed-integer program. In the following sections we present a Lagrangean relaxation algorithm that generates upper bounds for the non-linear model; as well as two linear approximation that provide feasible solutions to the nonlinear model.

Let X_{ij} be a decision variable which represents the amount of biomass (in tons) delivered annually from supplier i to coal plant j. Let B_j be a decision variable which represents the percentage of coal displaced in plant j. Let C denote the set of coal plants, and S denote the set of suppliers in the supply chain. Then, the amount of biomass used in plant j can be represented as

$$M_j^{bm} = \sum_{i \in S} X_{ij}.$$

We use Equation (2.4) to derive the following expression which represents the amount of biomass used as a function of the decision variables declared.

$$\sum_{i \in S} X_{ij} = \left(\frac{1}{1/B_j - \alpha_j} \right) * \left(\frac{\rho_j^b}{\rho_j^b - 0.0044 B_j^2 - 0.0055} \right) * M_j^{coal}. \tag{2.9}$$

We express the savings from biomass co-fire at plant j as a function of these decision variables as follows:

$$\sum_{i \in S} (\sigma_j^p + \sigma_j^t) X_{ij}.$$

Biomass purchasing costs at plant j are equal to

$$\sum_{i \in S} c_i^{bm} X_{ij}.$$

Truck transportation costs at plant j are equal to

$$\sum_{i \in S} c_{ij} X_{ij}.$$

As described in Section 2.3.2, the functions used to estimate investment costs for $B_j\% < 4\%$ are different from the functions used when $B_j\% \geq 4\%$. In order to capture these differences in our model, we introduce the binary decision variables Y_j, and define them as follows:

$$Y_j = \begin{cases} 1 & \text{if } B_j \leq 0.04 \\ 0 & \text{if } B_j > 0.04 \end{cases}$$

We linearize the relationship between Y_j and B_j using the following equations.

$$\begin{aligned} B_j &\leq 0.04 + M(1 - Y_j) \\ B_j &> 0.04 * (1 - Y_j) \end{aligned}$$

We can now express the investment costs of plant j as:

$$I_j^{cap} * \left(\frac{B_j}{1 - B_j}\right) Y_j + \left(I_j^s + I_j^{cd}\right) \left(\frac{B_j}{1 - B_j}\right)^{0.5575} (1 - Y_j) + I_j^h * \left(\frac{B_j}{1 - B_j}\right)^{0.9554} (1 - Y_j).$$

The following is the nonlinear mixed-integer programming formulation for this problem which we will be referring to as formulation (**P**).

$$Maximize : \mathcal{Z}^P(X, Y, B) = \sum_{j \in C} \left(\sigma_j^p + \sigma_j^t\right) \left(\sum_{i \in S} X_{ij}\right) - \sum_{i \in S} \sum_{j \in C} (c_{ij} + c_i^{bm}) X_{ij} -$$

$$- \sum_{j \in C} I_j^{cap} \left(\frac{B_j}{1 - B_j}\right) Y_j - \sum_{j \in C} I_j^h \left(\frac{B_j}{1 - B_j}\right)^{0.9554} (1 - Y_j) -$$

$$- \sum_{j \in C} \left(I_j^s + I_j^{cd}\right) \left(\frac{B_j}{1 - B_j}\right)^{0.5575} (1 - Y_j)$$

Subject to:

$$\sum_{j \in C} X_{ij} \leq s_i \qquad \forall i \in S, \tag{2.10}$$

$$\sum_{i \in S} X_{ij} \leq \frac{(M_j^{coal} * \rho_j^b)}{(1/B_j - \alpha_j)(\rho_j^b - 0.0044B_j^2 - 0.0055)} \qquad \forall j \in C, \tag{2.11}$$

$$B_j \leq 0.04 + M(1 - Y_j) \qquad \forall j \in C, \tag{2.12}$$

$$B_j > 0.04(1 - Y_j) \qquad \forall j \in C, \tag{2.13}$$

$$X_{ij} \in R^+ \qquad \forall i \in S, j \in C \tag{2.14}$$

$$B_j \in [0, 1] \qquad \forall j \in C. \tag{2.15}$$

$$Y_j \in \{0, 1\} \qquad \forall j \in C. \tag{2.16}$$

The objective function maximizes the benefits of co-firing across all $j \in C$. Constraints (4.1) indicate that the biomass delivered by supplier i is limited by its availability (s_i). Constraints (4.3) represent the amount of biomass required in a plant as a function of plant capacity, plant efficiency and as a function of the percentage of biomass co-fired. Constraints (2.12) and (2.13) provide a linear representation of the relationship between the decision variables B_j and Y_j. Constraints (2.14) are the non-negativity constrains, (2.15) are the boundary constraints, and (2.16) are the binary constraints.

2.5 Generating Upper Bounds via a Lagrangean Relaxation Algorithm

In this section we present a Lagrangean relaxation algorithm that generates upper bounds for model (**P**). This algorithm relaxes constraints (4.1). The Lagrangean relaxation model is:

$$Maximize: \mathcal{Z}^P(\lambda) = \sum_{i \in S} \sum_{j \in C} (\overline{c}_{ij} - \lambda_i) X_{ij} + \sum_{i \in S} s_i \lambda_i - \sum_{j \in C} I_j^{cap} \left(\frac{B_j}{1 - B_j} \right) Y_j$$

$$-\sum_{j\in C} I_j^h \left(\frac{B_j}{1-B_j}\right)^{0.9554}(1-Y_j) - \sum_{j\in C}\left(I_j^s + I_j^{cd}\right)\left(\frac{B_j}{1-B_j}\right)^{0.5575}(1-Y_j)$$

Subject to: (4.3) to (2.16)

Where, $\bar{c}_{ij} = \sigma_j^p + \sigma_j^t - c_i^{bm} - c_{ij}$. The Lagrangean dual (**LD**) problem is: $\min_{\lambda\geq 0} \mathcal{Z}^P(\lambda)$.

The Lagrangean relaxation model $\mathcal{Z}^P(\lambda)$ can be decomposed into $|C|$ single plant problems. We refer to the single plant problems as subproblems $(\mathbf{SP})_j$. The following is the corresponding problem formulation.

$$Maximize: \mathcal{Z}^{SP_j}(X,Y,B) = \sum_{i\in S}\overline{c}_i X_i - I^{cap}\left(\frac{B}{1-B}\right)Y$$

$$-I^h\left(\frac{B}{1-B}\right)^{0.9554}(1-Y) - \left(I^s + I^{cd}\right)\left(\frac{B}{1-B}\right)^{0.5575}(1-Y)$$

Subject to:

$$X_i \leq s_i \qquad \forall i \in S \tag{2.17}$$

$$\sum_{i\in S} X_{ij} \leq \frac{(M_j^{coal} * \rho_j^b)}{(1/B_j - \alpha_j)(\rho_j^b - 0.0044B_j^2 - 0.0055)} \tag{2.18}$$

$$B \leq 0.04 + M(1-Y) \tag{2.19}$$

$$B > 0.04(1-Y) \tag{2.20}$$

$$X_i \in R^+ \qquad \forall i \in S \tag{2.21}$$

$$B \in [0,1] \tag{2.22}$$

$$Y \in \{0,1\} \tag{2.23}$$

Constraints (2.17) are valid inequalities since each feasible solution to the single plant problem $(\mathbf{SP})_j$ meets these supply limitation constraints. The single plant problem can further be decomposed into three sub-problems. Subproblem 1 assumes $B^* \in [0, 0.04]$, subproblem 2 assumes $B^* \in (0.04, 0.221]$, and subproblem 3 assumes $B^* \in (0.221, 0.5]$.

Subproblem 1:

$$Maximize: \mathcal{Z}(X,B) = \sum_{i\in S}\overline{c}_i X_i - I^{cap}\left(\frac{B}{1-B}\right)$$

Subject to: (2.17), (2.18), (2.21)

$$B \in [0, 0.04]$$

Subprobleme 2:

$$Maximize : \mathcal{Z}(X, B) = \sum_{i \in S} \overline{c}_i X_i - I^h \left(\frac{B}{1-B}\right)^{0.9554} - \left(I^s + I^{cd}\right) \left(\frac{B}{1-B}\right)^{0.5575}$$

Subject to: (2.17), (2.18), (2.21)

$$B \in (0.040.221]$$

Subproblem 3:

$$Maximize : \mathcal{Z}(X, B) = \sum_{i \in S} \overline{c}_i X_i - I^h \left(\frac{B}{1-B}\right)^{0.9554} - \left(I^s + I^{cd}\right) \left(\frac{B}{1-B}\right)^{0.5575}$$

Subject to: (2.17), (2.18), (2.21)

$$B \in (0.2210.5]$$

These subproblems are easy and can be solved by inspection in polynomial time. The corresponding algorithm is presented in Table 4.

Theorem 1 *In an optimal solution $X^* = \{X_1^*, X_2^*, \ldots, X_l^*\}$ to the single plant problem, at most one of the suppliers' is used partially. That means, $X_i^* = s_i$, $\forall i \in S^*/k$; $X_k^* = \gamma$; and $X_i^* = 0$ for $i \notin S^*$. Where, S^* is the set of suppliers selected in the optimal solution. (See the proof in Appendix A.)*

Theorem 2 *The special case of problem (**P**) -when there is a single plant in the supply chain- can be solved to optimality via an $O(|S|log(|S|))$ algorithm, where $|S|$ represents the number of suppliers in the supply chain. (See the proof in Appendix A.)*

The algorithm that solves the single plant problem starts by sorting the suppliers in a decreasing order of $\overline{c}_i$. Without loss of generality, we assume that $\overline{c}_i > 0$ for $i \in S$. Let S^* denote the set of suppliers selected in an optimal solution. Initially S^* is empty. We start by finding the B_1^* that maximizes $\mathcal{Z}(X, B)$ for $B \in [0, 0.04]$. Next, we find B_2^* that maximizes $\mathcal{Z}(X, B)$ for $B \in (0.04, 0.221]$, and B_3^* that maximizes $\mathcal{Z}(X, B)$ for $B \in (0.221, 0.5]$. Therefore, the optimal solution to this problem is $B^* = \arg\max\{\mathcal{Z}(B_1^*), \mathcal{Z}(B_2^*), \mathcal{Z}(B_3^*)\}$. Recall that, in an optimal solution constraints (2.18) are binding. Thus, we can express the optimal objective function value as a function of B only.

Let's show how we find B_1^*. We start with supplier 1 and calculate $\mathcal{Z}(B_1)$. If $\mathcal{Z}(B_1) > 0$, then $S^* = S^* \bigcup 1$. We add supplier i to S^* as long as the following holds true $Z\mathcal{Z}(B_{i-1}) < \mathcal{Z}(B_i) > 0$. Let supplier j be such that $\mathcal{Z}(B_{j-2}) < \mathcal{Z}(B_{j-1}) > \mathcal{Z}(B_j)$. This implies that at some $B^* \in [B_{j-1}, B_j]$ function $\mathcal{Z}(B)$ reached its maximum. Since the slope of $\mathcal{Z}(B)$ could change its sign at most twice in the interval $[B_{j-1}, B_j]$, and $\mathcal{Z}(B_{j-1}) > \mathcal{Z}(B_j)$, that means, within this interval, the slope increased from B_{j-1} to $\overline{B} \leq B_j$, and then, decreased from $\overline{B}$ to B_j. This implies that there is at most one maximum within this interval. We use the Golden Search algorithm to identify B^* which maximized $\mathcal{Z}(B)$ (Luenberger and Ye 2008). The Golden Search algorithm will be used at most three times, ones for each interval $[0, 0.04], [0.04, 0.221), (0.221, 0.5]$.

Figure 12 outlines the Lagrangean relaxation algorithm. In each iteration of this algorithm $|C|$ single plant problems are solved. These solutions are used to update the upper bound (UB). The lower bound is found by solving model (**Q**) (see Section 2.6.1). We employ the subgradient optimization method to solve the Lagrangean dual problem (**LD**) (Nemhauser and Wolsey 1988) and update the Lagrangean multipliers λ_i. We use the following equation:

$$\lambda_i^n = \lambda_i^{n-1} + u^n(s_i - \sum_j X_{ij}^n),$$

where $u^n = \frac{\xi^n(UB-LB)}{\sum_{i\in S}(s_i - \sum_j X_{ij})}$. The parameter $\xi \in (0; 2]$ is reduced if the upper bound fails to improve after a fixed number of iterations. The algorithm stops if one of the following

conditions is satisfied: (i) the error gap ($\epsilon = \left(\frac{UB-LB}{LB}\right) * 100$) is less than 1%, or (ii) the number of iterations reaches a pre-specified bound.

2.6 Generating Lower Bounds via Linear Approximation Algorithms

2.6.1 A Linear Mixed Integer Problem Formulation

Let's assume that plant j decides to use biomass to displace coal at a fix rate of $\beta_j = 1\%, 2\%, 3\%$ etc. Without loss of generality, we assume that this plant would pursue a single coal displacement strategy, and therefore, would select a single value of β_j. We denote the finite set of all the values that β_j can potentially take by L. Let $l = 1, \ldots, |L|$ index this set, and let L_l denote the $l-$the element of this set. We declare Y_{lj} to be a binary variable which takes the value 1 if facility j displaces $L_l = \beta_j\%$ coal, and takes the value 0 otherwise.

For a given value of β_j, the amount of biomass needed at plant j is constant and is calculated using equation (2.4). We denote this amount by M_{lj}^{bm}. The total amount of biomass required at plant j is equal to:

$$M_j^{bm} = \sum_{l \in L} M_{lj}^{bm} Y_{lj}. \tag{2.24}$$

Investment costs also depend on the value of β_j. For a given value of β_j these costs are fixed. Thus, we use equation (2.5) to calculate investment costs when $\beta_j \leq 0.04$. For $\beta_j > 0.04$, we calculate investment costs using equation (2.6). Let I_{lj} denote investment costs at plant j for a given value of β_j. The total investment costs are equal to

$$\sum_{l \in L} \sum_{j \in C} I_{lj} Y_{lj}. \tag{2.25}$$

The following is a linear mixed integer programming formulation for problem (**P**)

which we will be referring to as formulation (**Q**).

$$Maximize: \mathcal{Z}^Q(X,Y) = \sum_{i\in S}\sum_{j\in C}\bar{c}_{ij}X_{ij} - \sum_{l\in L}\sum_{j\in C} I_{lj}Y_{lj}$$

Subject to:

$$\begin{aligned}
\sum_{j\in C} X_{ij} &\leq s_i && \forall i \in S, && (2.26)\\
\sum_{l\in L} Y_{lj} &\leq 1 && \forall j \in C, && (2.27)\\
\sum_{i\in S} X_{ij} &\leq \sum_{l\in L} M_{lj}^{bm} Y_{lj} && j \in C, && (2.28)\\
X_{ij} &\in R^+ && \forall i \in S, j \in C && (2.29)\\
Y_{lj} &\in \{0,1\} && \forall l \in L, \forall j \in C && (2.30)
\end{aligned}$$

The objective function maximizes the benefits of co-firing across all $j \in C$. Constraint (2.27) limits the number of co-firing strategies adopted by a coal plant to one. Constraints (2.28) set the upper bound on the amount of biomass requirements based on the co-firing strategy selected. (2.29) and (2.30) are the non-negativity and binary constraints.

Proposition 1: *A feasible solution to problem (***Q***) is feasible to the non-linear problem (***P***); and the objective function value of (***Q***) is a lower bound for problem (***P***). (See the proof in Appendix A.)*

Theorem 3 *As $|L|$ approaches infinity, an optimal solution to (***Q***) is optimal to (***P***) with probability 1. (See proof in Appendix A.)*

2.6.2 A Linear Approximation of Model (P)

Linearizing constraints (4.3):

The right hand side of constraints (4.3) are nonlinear functions. Let $f_j = \frac{(\rho_j^b * B_j)}{(1-\alpha_j * B_j)(\rho_j^b - 0.0044B_j^2 - 0.0055)}$.

Thus, these constraints can be expressed as:

$$\sum_{i \in S} X_{ij} \leq M_j^{coal} * f_j \qquad \forall j \in C.$$

Proposition 2:

$$B_j \leq \frac{1}{M_j^{coal}} \sum_{i \in S} X_{ij} \leq f_j \leq (B_j + \overline{a}_j) \qquad \forall j \in C.$$

Where, $\overline{a}_j = \frac{0.5\left(\rho_j^b - (1-0.5\alpha_j)(\rho_j^b - 0.0066)\right)}{(1-0.5\alpha_j)(\rho_j^b - 0.0066)}$ (See proof in Appendix A).

Corollary 1: *Let (***LR***) be the following linear approximation of problem (***P***).*

$$\begin{aligned} &Maximize: && \mathcal{Z}^P(X, Y, B) \\ &\text{Subject to:} && (4.1), (2.12) \text{ to } (2.16) \\ &M_j^{coal} * B_j && \leq \textstyle\sum_{i \in S} X_{ij} \leq && M_j^{coal} * (B_j + \overline{a}_j) && \forall j \in C. \end{aligned} \tag{2.31}$$

*Problem (***LR***) is a relaxation of (***P***). The objective function value of (***LR***) is an upper bound for (***P***).*

On addition to constraints (2.31), we develop the linear function $\overline{f}_j = a_j * B_j + b_j$ which is such that:

$$\sum_{i \in S} X_{ij} \leq M_j^{coal} * \overline{f}_j \leq M_j^{coal} * f_j \qquad \forall j \in C.$$

Corollary 2: *Let (***LA***) be the following linear approximation of problem (***P***).*

$$\begin{aligned} &Maximize: && \mathcal{Z}^P(X, Y, B) \\ &\text{Subject to:} && (4.1), (2.12) \text{ to } (2.16) \\ &\sum_{i \in S} X_{ij} && \leq M_j^{coal} * \overline{f}_j && \forall j \in C. \end{aligned} \tag{2.32}$$

*Constraints (2.32) are an inner approximation of (4.3). A solution to problem (***LA***) is*

*feasible for (***P***). The objective function value of (***LA***) is a lower bound for (***P***).*

Linearizing the objective function:

For $B_j \in [0, 0.5]$, the following nonlinear terms in the objective function, $f_j^1 = \left(\frac{B_j}{1-B_j}\right)$ is convex for $B_j \in [0, 0.5]$, and $f_j^2 = \left(\frac{B_j}{1-B_j}\right)^{9554}$ is convex for $B_j \in [0.04, 0.5]$ (see Propositions **6** and **7**). The nonlinear term $f_j^3 = \left(\frac{B_j}{1-B_j}\right)^{0.5575}$ is concave for $B_j \in [0, 0.22]$ and convex for $B_j \in (0.22, 0.5]$ (see Proposition **8**). For each of these three terms, we develop three linear approximations, one that overestimates the function (an outer approximation), one that underestimates the function (an inner approximation), and one that minimizes the squared error (fit line). Let $\overline{f}_j^{oi} = a_j^{oi} * B_j + b_j^{oi}$ be the outer approximation line of the i-th term (i = 1,2,3) for each $j \in C$. Let $\overline{f}_j^{ui} = a_j^{ui} * B_j + b_j^{ui}$ be the inner approximation line and $\overline{f}_j^{fi} = a_j^{fi} * B_j + b_j^{fi}$ the fit line. By substituting the non-linear terms in the objective function of (**P**), with the outer approximation lines we get the following, partial linearization of the objective function of (**P**).

$$Maximize: \sum_{i\in S}\sum_{j\in C} \overline{c}_{ij} X_{ij} - \sum_{j\in C} I_j^{cap}\left(a_j^{o1} B_j + b_j^{o1}\right) Y_j - \sum_{j\in C} I_j^h \left(a_j^{o2} B_j + b_j^{o2}\right)(1 - Y_j) -$$

$$- \sum_{j\in C} \left(I_j^s + I_j^{cd}\right)\left(a_j^{o3} B_j + b_j^{o3}\right)(1 - Y_j)$$

Rearranging the terms in the objective function we have:

$$Maximize: \sum_{j\in C}\left(\sum_{i\in S} \overline{c}_{ij} X_{ij} - \overline{a}_j^o B_j - \overline{b}_j^o B_j Y_j - \overline{d}_j^o Y_j - \overline{e}_j^o\right).$$

Where, $\overline{a}_j^o = I_j^h a_j^{o2} + \left(I_j^s + I_j^{cd}\right) a_j^{o3}$; $\overline{b}_j^o = I_j^{cap} a_j^{o1} - I_j^h a_j^{o2} - \left(I_j^s + I_j^{cd}\right) a_j^{o3}$; $\overline{d}_j^o = I_j^{cap} b_j^{o1} - I_j^h b_j^{o2} - \left(I_j^s + I_j^{cd}\right) b_j^{o3}$; and $\overline{e}_j^o = I_j^h b_j^{o2} + \left(I_j^s + I_j^{cd}\right) b_j^{o3}$. Figure 2.1 presents the liner approximations of the objective function and constraints (4.3).

To get a fully linear objective function we introduce $Z_j = B_j Y_j$. Thus,

$$Z_j = \begin{cases} B_j & \text{if } Y_j = 1 \\ 0 & \text{if } Y_j = 0 \end{cases} \tag{2.33}$$

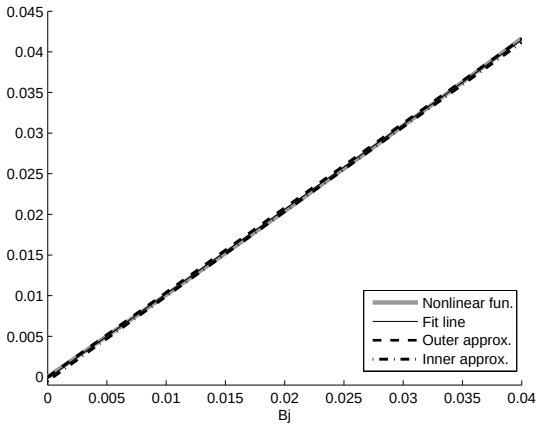

(a) Linear approximations of $\left(\frac{B_j}{1-B_j}\right)$

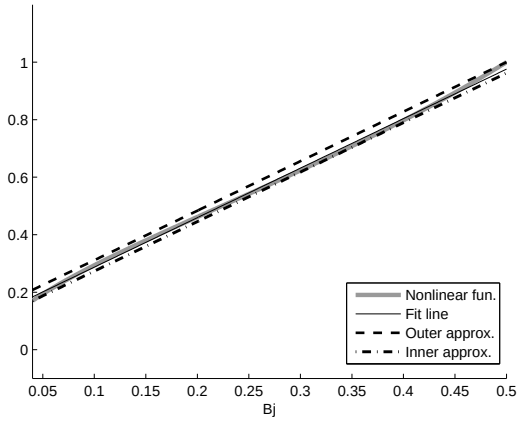

(b) Linear approximations of $\left(\frac{B_j}{1-B_j}\right)^{0.5575}$

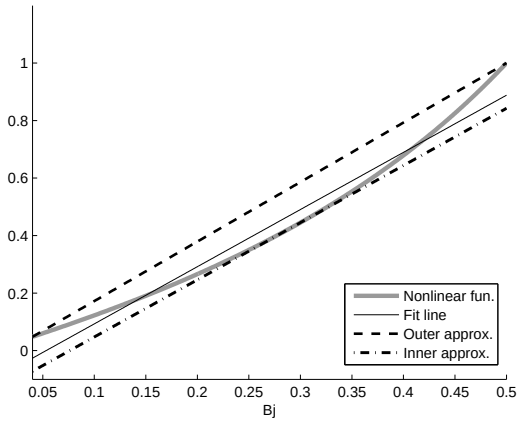

(c) Linear approximations of $\left(\frac{B_j}{1-B_j}\right)^{0.9554}$

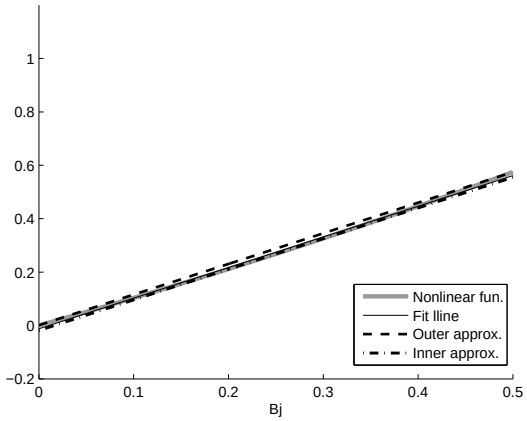

(d) Linear approximations of constraints (4.3)

Figure 2.1: Linear Approximation Schemes

To represent this relationship using linear functions, we introduce additional variables. Let $\mathcal{Y}_j^1$ and $\mathcal{Y}_j^2$ be binary variables, and let w_j^1, w_j^2, w_j^3 be continuous variables in $[0, 1]$. Let $(\mathbf{LA^u})$ be the following linear approximation of problem $(\mathbf{P})$. Equations (2.38) to (2.45) linearize the relationship between Z_j nd B_j.

$$Maximize : \mathcal{Z}^{LA^u} = \sum_{j \in C} \left(\sum_{i \in S} \overline{c}_{ij} X_{ij} - \overline{a}_j^u B_j - \overline{b}_j^u Z_j - \overline{d}_j^u Y_j - \overline{e}_j^u \right).$$

$$\sum_{j\in C} X_{ij} \leq s_i \qquad \forall i \in S \qquad (2.34)$$

$$\sum_{i\in S} X_{ij} \leq M_j^{coal} * \overline{f}_j \qquad \forall j \in C \qquad (2.35)$$

$$B_j \leq 0.04 + M(1 - Y_j) \qquad \forall j \in C \qquad (2.36)$$

$$B_j > 0.04(1 - Y_j) \qquad \forall j \in C \qquad (2.37)$$

$$\mathcal{Y}_j^1 + \mathcal{Y}_j^2 = 1 \qquad \forall j \in C \qquad (2.38)$$

$$w_j^1 \leq \mathcal{Y}_j^1 \qquad \forall j \in C \qquad (2.39)$$

$$w_j^2 + w_j^3 = \mathcal{Y}_j^2 \qquad \forall j \in C \qquad (2.40)$$

$$0.04w_j^1 = Z_j \qquad \forall j \in C \qquad (2.41)$$

$$0.04w_j^1 + 0.04w_j^2 + 0.5w_j^3 = B_j \qquad \forall j \in C \qquad (2.42)$$

$$w_j^1, w_j^2, w_j^3, B_j \in [0, 1] \qquad \forall j \in C \qquad (2.43)$$

$$\mathcal{Y}_j^1, \mathcal{Y}_j^2, Y_j \in \{0, 1\} \qquad \forall j \in C \qquad (2.44)$$

$$X_{ij} \in R^+ \qquad \forall i \in S, j \in C \qquad (2.45)$$

Let ($\mathbf{LA^o}$) be the following liner approximation of problem ($\mathbf{P}$).

$$Maximize : \mathcal{Z}^{LA^o} = \sum_{j\in C} \left(\sum_{i\in S} \overline{c}_{ij} X_{ij} - \overline{a}_j^o B_j - \overline{b}_j^o Z_j - \overline{d}_j^o Y_j - \overline{e}_j^o \right).$$

Subject to: (2.34) to (2.45).

Let ($\mathbf{LA^f}$) be the following liner approximation of problem ($\mathbf{P}$).

$$Maximize : \mathcal{Z}^{LA^f} = \sum_{j\in C} \left(\sum_{i\in S} \overline{c}_{ij} X_{ij} - \overline{a}_j^f B_j - \overline{b}_j^f Z_j - \overline{d}_j^f Y_j - \overline{e}_j^f \right).$$

Subject to: (2.34) to (2.45).

Corollary 3: *A solution of problem (*$\mathbf{LA^u}$*) is feasible for problem (*$\mathbf{P}$*).*

Corollary 4: *A solution of problem (*$\mathbf{LA^o}$*) is feasible for problem (*$\mathbf{P}$*).*

Corollary 5: *A solution of problem (*$\mathbf{LA^f}$*) is feasible for problem (*$\mathbf{P}$*).*

Let ($\mathbf{LR^u}$) be the following liner approximation of problem ($\mathbf{P}$).

$$Maximize: \mathcal{Z}^{LR^u} = \sum_{j \in C} \left(\sum_{i \in S} \overline{c}_{ij} X_{ij} - \overline{a}_j^u B_j - \overline{b}_j^u Z_j - \overline{d}_j^u Y_j - \overline{e}_j^u \right).$$

Subject to: (2.34), (2.31), (2.36) to (2.45).

Proposition 3: Problem ($\mathbf{LR^u}$) is a relaxation of problem ($\mathbf{P}$), thus its objective function value is an upper bound for ($\mathbf{P}$).

Proof: Problem ($\mathbf{LR^u}$) is a relaxation of ($\mathbf{P}$) since the feasible region of ($\mathbf{LR^u}$) contains the feasible region of ($\mathbf{P}$). This is due to replacing constraints (2.35) with their corresponding outer approximation, constraints (2.31).

2.7 Numerical Analysis

We develop a case study in order to evaluate the impact of biomass co-firing on the production of renewable electricity. The case study is focused on the following 9 states located in the southeast: Alabama, Arkansas, Florida, Georgia, Louisiana, Mississippi, North Carolina, South Carolina and Tennessee. We focus on this region since it is rich with biomass. Numerical analysis is also used to evaluate the performance of the algorithms proposed.

2.7.1 Data Description

2.7.1.1 Biomass supply:

Biomass availability data by state and county is extracted from the Knowledge Discovery Framework (KDF) database, an outcome of the US Billion Ton Study led by the Oak Ridge National Laboratory (KDF Accessed 12.10.2013). This database provides the amount of biomass available at the county level in the form of forest products, forest residues, agricultural products, agricultural residues, energy plants, etc. The database provides the amount of biomass available at different market prices for the 2012 to 2030

period.

From this data set we extracted and used data about forest products and residues. We focus the analysis on these products only, because, research has shown that these products are low in sulfur, as well as, chemicals such as, chlorine, potassium and nitrogen. These chemicals when burned cause corrosion and consequently impact the lifetime of burners. Thus, the chances are these will be the types of biomass used by coal plants.

2.7.1.2 Coal plants:

The data about coal-fired power plant locations, nameplate capacities, types of coal used, utilization rates, and annual heat input rates, is collected from the US Energy Information Administration (2011). This database presents a total of 1,400 coal-fired power plants across the USA, with an overall nameplate capacity of 343,757 MW.

Table 2.1 summarizes the data about biomass available and coal plants in Southeast USA. The amounts of biomass listed represent the available biomass at $200/ton in 2014 based on KDF (Accessed 12.10.2013).

Table 2.1: Distribution of biomass and coal plants in Southeast USA

State	Biomass available (in tons)	Number of coal plants
AL	5,004,000	11
AR	4,505,800	4
FL	2,878,500	15
GA	6,892,500	14
LA	5,044,100	4
MS	5,772,200	5
NC	5,755,400	25
SC	3,666,300	16
TN	2,872,500	10

2.7.1.3 Truck transportation costs:

In order to estimate costs for truck transportation of biomass, we use the data provided by Searcy et al. (2007). They provide two cost components which are the distance variable cost (DVC) and distance fixed cost (DFC). The distance variable cost includes the fuel and labor costs. The distance fixed cost includes the cost of loading and unloading a truck. These costs were provided for different types of biomass, such as, woodchips, straw and stover. We used the data provided for woodchips. The DVC of woodchips is estimated \$0.112/(tons mile) and DFC is estimated \$3.01/(tons). Woodchips are shipped using truck with a capacity of 40 tons. This data is used as follows in order to calculate $c_{ij}(\$/ton) = DFC + DVC * d_{ij}$, where d_{ij} represents the distance between supplier i and plant j.

2.7.2 Experimental Results

The nonlinear model (**P**) is solved using GAMS/BONMIN solver. The linear approximation models are solved using Version 20141128 of AMPL an GUROBI 6.0.0. solver. The experiments are completed using a Dell personal computer with Intel(R) Core(TM) i5-4300U CPU @ 1.90GHz 2.50 GHz; and 8.00 GB of RAM. The following summarizes our experimental results.

2.7.2.1 Evaluating the quality of the upper and lower bounds:

In order to test the performance of the upper and lower bounds proposed we randomly generate a number of problems. We tried solving model (**P**) using the overall dataset. However, BONMIN ran out of memory without finding a feasible solution due to the problem size. Thus, we solved model (**P**) using the data from Alabama. Next, we changed one problem parameter at a time and generated 8 different problems. For example, in Problems 1 and 2, biomass supply for each county in Alabama is generated randomly based on the intervals presented in the Table 2.2. For each problem we generated 5 random instances, and the results presented are the averages overall problem instances. The rest of problem

parameters remain the same as the ones described in Section 2.7.1.

Table 2.2: Summary of problem parameters

Problem Nr.	**Parameter**	**Random interval**
1	Biomass supply (s_i): low	[0,10000]
2	Biomass supply (s_i): high	[0,40000]
3	Biomass cost (c_i^{bm}): low	[0,100]
4	Biomass cost (c_i^{bm}): high	[0,500]
5	Coal price (σ_j^p): low	[10,50]
6	Coal price (σ_j^p): high	[50,200]
7	Transportation cost (c_{ij}): low	[0,80]
8	Transportation cost (c_{ij}): high	[30,100]

Table 2.3 summarizes the results of the Lagrangean relaxation algorithm. The error gap $= \left(\frac{UB-LB}{LB}\right) * 100$. The quality of the upper bounds is very good. The maximum error bound is less than 4%.

Table 2.3: Upper bounds via Lagrangean relaxation

Problem Nr.	**Error** (%)	**Lagr. Relaxation CPU** (sec)	**BONMIN CPU** (sec)
1	0.78	671	368
2	0.01	49	410
3	1.28	813	578
4	3.69	911	128
5	0.00	70	170
6	0.00	33	96
7	0.00	79	439
8	0.36	109	502

We solved model (**P**) and its linear approximation model (**Q**) in order to evaluate the quality of the solutions provided by the linear approximation as a function of problem size ($|L|$). This analysis gave us an indication of what would be a good size for set L. We tried solving model (**P**) using the overall dataset. Initially, we solved model (**P**) using the data from Alabama. Next, we solved model (**Q**) several times using the same dataset. Each time we changed $|L|$. We focus on strategies for which the value of B_j is between

1% and 50% which are appropriate strategies for direct co-firing. As we increase $|L|$, we explore additional co-firing strategies within this range. For example, when $\mid L \mid = 3$, the only strategies considered are $B_j = 0\%, 25\%$, and 50%. When $\mid L \mid = 51$, then strategies considered are $B_j = 0\%, 1\%, 2\%, \ldots, 49\%, 50\%$.

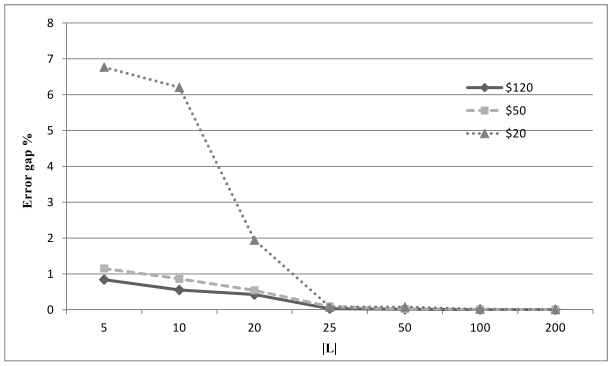

Figure 2.2: The error gap between $\mathcal{Z}^P$ and $\mathcal{Z}^Q$ as a function of $|L|$

Figure 2.2 presents the relationship between the size of $|L|$ and the relative error gap between the optimal solution to models (**Q**) and (**P**) when biomass market price is fixed at \$20/ton, \$50/ton and \$120/ton. The error gap is calculated as follows:

$$\text{Error gap} = \frac{(\mathcal{Z}^P - \mathcal{Z}^Q)}{\mathcal{Z}^P} * 100.$$

As expected, the relative error gap approaches zero as we increase the size of L. The results of this graph indicate that the error gap is smaller than 0.1 when the size of L is smaller than 25. In our numerical analysis we use $|L| = 200$ to ensure high quality solutions from the approximation.

Table 2.4 summarizes the running time of GUROBI when solving model (**Q**) and BONMIN when solving model (**P**). The running time of GUROBI increases only slightly due to the increase in problem size.

Table 2.5 summarizes the results from solving the linear approximation models presented in Sections 2.6.1 and 2.6.2. As indicated by Proposition **1** and Corollaries 2 to 5, by

Table 2.4: Solution times in cpu seconds.

	Solution time	
$\|L\|$	**P**	**Q**
	297	
5		4.2
10		3.9
20		4.7
25		4.3
50		4.8
100		5.2
200		7.2

solving problems (**Q**), (**LA**), ($\mathbf{LA^o}$), ($\mathbf{LA^u}$) and ($\mathbf{LA^f}$) we generate feasible solutions for problem (**P**). We use these solutions to calculate lower bounds for (**P**). Based on these numerical results, the time it took to solve problem (**P**) using BONMIN is order of magnitude higher than the time required to solve problem (**Q**). The time required to solve problems ($\mathbf{LA^o}$), ($\mathbf{LA^u}$) and ($\mathbf{LA^f}$) is clearly the best, however, the quality of the corresponding solutions is poor.

Table 2.5: Comparing the performance of the lower bounds for problem (**P**).

Prob.	**BONMIN**	(**Q**)		(**LA**)		($\mathbf{LA^u}$)		($\mathbf{LA^o}$)		($\mathbf{LA^f}$)	
Nr.	**CPU**	**Error**	**CPU**	**Error**	**CPU**	**Error**	**CPU**	**Error**	**CPU**	**Error**	**CPU**
	(sec)	(%)	(sec)	(%)	(sec)	(%)	(sec)	(%)	(sec)	(%)	(sec)
1	368.00	0.00*	7.96	10.40	454.60	13.69	0.61	11.35	0.45	30.79	0.17
2	410.40	0.00	6.64	1.09	255.80	5.08	0.54	5.08	0.22	7.41	0.16
3	578.60	0.00	8.00	2.93	325.80	8.48	0.83	3.45	0.63	8.77	0.21
4	128.20	0.00	6.40	22.71	147.00	23.77	0.23	25.13	0.19	107.51	0.07
5	170.60	0.00	7.44	2.04	112.00	8.45	0.25	4.20	0.18	7.62	0.10
6	95.80	0.00	6.92	1.11	115.80	1.49	0.34	1.39	0.28	2.80	0.17
7	439.00	0.09*	8.23	1.05	220.00	2.12	0.29	1.58	0.14	3.91	0.14
8	502.33	0.00*	9.00	3.14	295.00	6.70	0.22	5.36	0.17	12.58	0.08

*The quality of solutions from solving model (Q) are slightly better than solutions found from BONMIN, although BONMIN reports 0% error gap for these solutions.

2.7.2.2 Sensitivity analysis:

Table 2.6 presents the total amount of biomass used by state as biomass price increases. Table 2.7 presents the total profits by state as biomass price increases. In order to generate these results we solved model (**Q**) for different values of biomass market price. Note that, not all of the available biomass is sold at the highest price, only the additional amount that becomes available at that price. Increasing the price positively impacts the amount of biomass that can be used for production of renewable energy. This is mainly because the amount of biomass made available to and used by power plants increases as plants are willing to pay a higher price.

Table 2.6: The total biomass used at different levels of biomass market price

Biomass price	Total biomass used (in mill tons)								
(in $/ton)	AL	AR	FL	GA	LA	MS	NC	SC	TN
20	1.40	0.04	1.15	1.75	0.44	1.62	1.81	0.73	1.45
40	4.27	0.85	4.40	5.22	1.16	3.32	4.87	3.30	3.97
60	4.48	0.90	4.69	5.43	1.17	3.36	5.29	3.29	4.10
80	4.60	0.90	4.73	5.51	1.17	3.36	5.35	3.33	4.13
100	4.82	0.90	4.73	5.51	1.17	3.36	5.35	3.33	4.13
140	4.82	0.90	4.73	5.51	1.17	3.36	5.35	3.33	4.13
200	4.82	0.90	4.73	5.51	1.17	3.36	5.35	3.33	4.13

The results of Figures 2.6 and 2.7 indicate that, the amount of biomass used depends on the number of coal plants, rather than biomass availability within the state. For example, North Carolina, South Carolina, Florida, Georgia and Tennessee use most of the biomass available in the region. This is because the number of coal plants in these states varies between 10 and 25. The number of coal plants in the remaining states in Southeast is smaller (see Table 2.1). Therefore, these states become biomass suppliers to states that have more coal plants.

Let consider the case of Florida. Biomass availability in Florida (at the highest market price of $200/ton) is close to 2.88 million tons. However, the amount of biomass used in Florida, based on our numerical results, is 4.73 million tons at a market price of

$80/ton. The corresponding system wide profits are $213 million. In this case, although biomass is produced in other states within the region, the benefits of the PTC will be collected by Florida. Similarly, Tennessee produces only 2.87 million tons of biomass. Based on our model, Tennessee would use up to 4.13 million tons of biomass and generate up to $152 million in profits mainly due to PTC. On the other side, states such as Arkansas and Louisiana that are rich in biomass (over 5 million tons of biomass available each) would make a small profit of $0.9 million and $1.17 million correspondingly.

Table 2.7: Total profits at different levels of biomass market price

Biomass price	Total profits (in mill $)								
in ($/ton)	AL	AR	FL	GA	LA	MS	NC	SC	TN
20	172.93	0.98	65.94	100.28	12.68	67.64	104.58	45.69	67.36
40	376.20	8.90	206.48	247.77	22.57	108.54	235.01	160.27	150.62
60	378.73	9.16	212.80	251.60	23.30	108.57	247.54	155.99	152.65
80	378.67	9.22	213.21	252.27	23.54	108.53	247.07	156.86	152.41
100	378.81	9.16	213.21	252.27	23.51	108.85	247.21	156.86	151.90
140	378.74	9.23	213.08	252.41	23.50	108.90	247.32	156.49	152.12
200	379.35	9.16	213.06	252.42	23.81	108.04	247.48	156.33	152.12

The results of Table 2.7 indicate that biomass usage and total profits remain the same as the market price increases beyond $80/ton. Using the additional biomass which becomes available at the higher market price decreases profits. This is because the additional tax savings are smaller than the additional purchase, transportation and investment costs necessary to use the additional biomass.

Figure 2.3 presents the relationship that exists between biomass market price and total profits, tax savings, biomass used, and investment and logistics costs. The PTC is fixed at 1.1 cents per kilowatt-hour. As the market price of biomass increases from $20/ton to $80/ton, the amount of biomass available and overall system profits increase. The rate of increase of profits is higher when the market price increases from $20 to $40/ton. The amount of biomass used and corresponding profits do not change at market prices higher

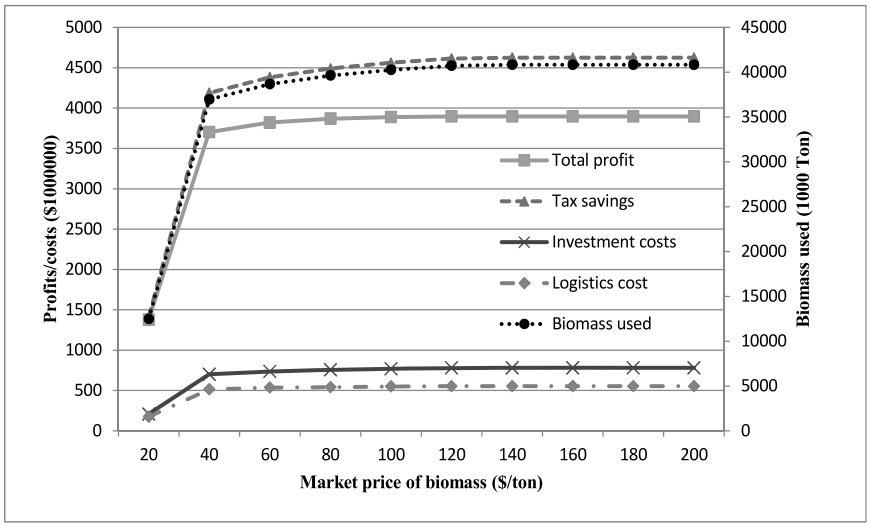

Figure 2.3: Analyzing the impact of biomass market price on average profits, costs and biomass usage in Southeast USA

that \$80/ton since the additional tax savings are smaller than the additional purchase, transportation and investment costs.

Figure 2.4 depicts the relationship between PTC and total profits, tax savings, biomass used, and investment and logistics costs in Southeast US as well as, in Arkansas, Mississippi and South Carolina. The market price of biomass here is fixed at \$100/ton. Results indicate that, when PTC is equal to zero, the average benefits from co-firing biomass - although small- are positive. Plants find co-firing to be beneficial when PTC is zero, with the exception of plants located in Arkansas and Louisiana. In Arkansas, coal plants would use biomass for co-fire when PTC is greater than 0.7 cents per kilowatt-hour (Figure 2.4(b)); and in Louisiana when PTC is greater than 0.2 cents per kilowatt-hour.

The results of Figure 2.4(a) indicate that an increase of PTC from 0 to 1 cent per kilowatt-hour has a dramatic impact on biomass usage in Southeast. The amount of biomass used increases 4.8 times. Increasing the PTC from 1 to 2 cents per kilowatt-hour increases biomass usage by 6%; and increasing PTC from 2 to 3 cents per kilowatt-hour increases biomass usage by 0.5%. These results indicate that the impact of increasing PTC beyond 2 cents per kilowatt-hour on the total amount of renewable electricity produced in Southeast

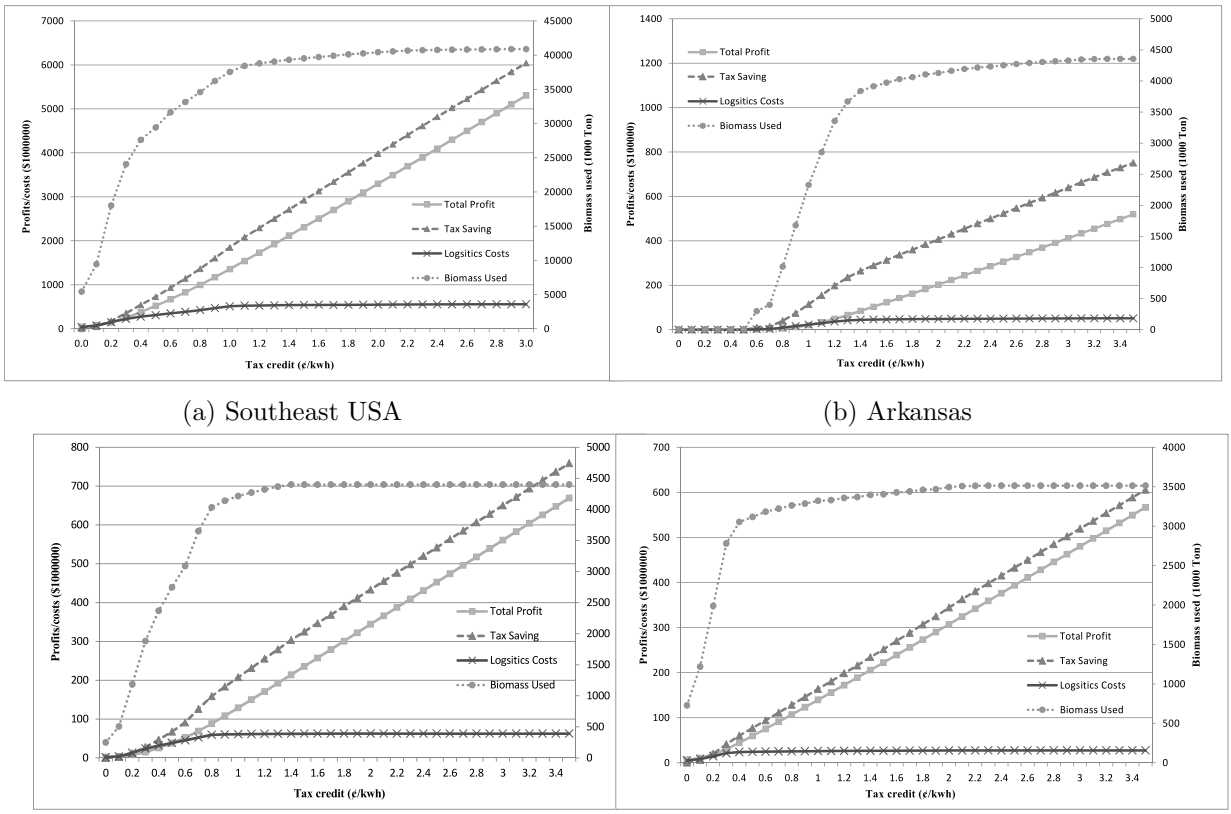

(a) Southeast USA

(b) Arkansas

(c) Mississippi

(d) South Carolina

Figure 2.4: The relationship between total profits and tax credits

is only marginal. The corresponding increase in total profits is just due to the higher PTC, and it is not due to increase use of biomass used.

2.8 Summary and Conclusions

Co-firing biomass in coal-fired power plants is a strategy that leads to reduced greenhouse gas emissions. This chapter presents a mathematical model to evaluate the impact of biomass co-firing in generating renewable electricity. The model captures the additional biomass purchasing and transportation costs, plant investment costs, savings due to PTC, and savings from reducing the amount of coal purchased. The model also captures the loss in process efficiencies due to using biomass, a product which has lower heating value as compared to coal. The model proposed is a MINLP, thus, we present a

linear approximation which is easier to solve. We use numerical analysis to evaluate the quality of solutions from the linear approximation model.

We develop a case study using data from nine states located in the southeast region of the US. The data source used are the Knowledge Discovery Framework KDF (Accessed 12.10.2013) and the US Energy Information Administration (2011). These databases provide information about the available amount of biomass for production of renewable energy by county and state, at different market prices, during the period 2012 to 2020. The databases also provide detailed information about the coal-fired power plants in the US. We used this data and conducted an extensive number of experiments. The following summarizes our main observations:

Observation 1: *Tax credits are necessary in order to increase production of renewable energy.* The results of Figure 2.4 indicate that increasing the PTC impacts greatly the production of renewable electricity. Our numerical results indicate that increasing PTC beyond 2 cents/kilowhat hour has only marginal impacts in increasing renewable energy generation.

Observation 2: *Tax credit should not be "one size fits all".* Instead, tax credits could be a function of the amount of renewable electricity produced, or plant capacity.

The results of Figure 2.3 indicate that the amount of biomass used increases only slightly with the increase of biomass market price beyond \$80/ton given that PTC is fixed at 1.1 cents per kilowatt-hour. Since biomass is a bulk product with low energy density and widely dispersed geographically, collection and transportation costs are high. For every 1% increase in biomass usage, the corresponding increase of transportation and collection costs is higher. In order to encourage the production of renewable energy, it makes sense to design a PTC which is a function of the amount of biomass used, and consequently, a function of the amount of renewable energy produced.

Production tax credits based on coal plant capacity are being currently implemented in

European countries (IEA-ETSAP and IRENA 2013, Boekhoudt and Behrendt 2015). Typically, the tax credit (such as, the "feed-in tariff" implemented in Austria) is higher for smaller sized plants. Higher credits allow smaller plants to overcome the burdens of implementing biomass co-firing.

Observation 3: *There is a need for comprehensive tax credit schemes to encourage renewable electricity production and reduce GHG emissions.* Biomass distribution in the US differs by region, and it does not match the distribution of coal-fired power plants (Figure 2.1). Therefore, in our case study, some states of Southeast became biomass suppliers to other states that do currently have a larger number of power plants. Consequently, states that have the resources to transform biomass to renewable electricity rip the gains from PTC. Recall that, one of the main reasons of producing renewable energy is to reduce GHG emissions due to burning of coal. Clearly, when biomass is transported over state borders, the transportation distances and corresponding GHG emissions do increase. Further increases of PTC would allow power plants to remain profitable even if biomass is delivered from suppliers located far away. Thus, decisions related to PTC size and scheme should be mindful of of the impacts of PTC to GHG emissions due to co-firing and transportation in the supply chain.

Notations

Table 2.8: Set Notations

Sets	
C	the set of coal plants
S	the set of biomass suppliers
L	the set of potential values of β

Table 2.9: Notations: Decision Variables

Decision Variables	
B_j	represents the percentage of coal (mass basis) displaced in plant $j \in C$ (in %)
X_{ij}	represents the amount of biomass transported from supplier i to plant j (in tons)
Y_j	binary variable that takes the value 1 if $\beta \leq 4$ in plant $j \in C$, and takes the value 0 otherwise
Y_{lj}	binary variable that takes the value 1 if facility $j \in C$ displaced $L_l = \beta\%$ coal, and takes the value 0 otherwise
Z_j	semi-continuous variable that takes the same value as B_j if $Y_j = 1$ and takes the value 0 if $Y_j = 0$

Table 2.10: Other Notations

Other Notations	
α_j	is equal to $1-(LHV_j^{coal}/LHV_j^{bm})$
β	the percentage of biomass (mass basis) used for cofiring (in %)
β_j	the percentage of biomass co-fired in plant $j \in C$ (in %)
C^{wb}	the conversion factor from MW to BTU/hr (in BTU/(hr*MW)
c_j^{coal}	the unit door price of coal (in %/ton)
c_i^{bm}	the unit purchase cost of biomass from supplier $i \in S$ (in $/ton)
c_{ij}	the unit transportation cost along arc (i,j) inA (in $/ton)
∇M_j^{coal}	the change in the value of M_j^{coal} (in tons)
EL_j	the efficiency loss of boilers due to co-firing in plant $j \in C$ (in %)
f_j	the utilization rate / capacity factor of plant $j \in C$ (in %)
I_j^{cap}	is equal to $(50,000 * TC_j * f_j * LHV_j^{bm})/LHV_j^{coal}$
I_j^{CAP}	the investment costs in plant $j \in C$ (in $)
I_j^s	is equal to $I_j^s = 136578 * \left(TC_j * f_j * \frac{LHV_j^{bm}}{LHV_j^{coal}}\right)^{0.9554}$,
I_j^S	the investment necessary for biomass storage in plant $j \in C$ (in $)
I_j^h	is equal to $I_j^h = 55780 * \left(TC_j * f_j * \frac{LHV_j^{bm}}{LHV_j^{coal}}\right)^{0.9554}$,
I_j^H	the investment necessary for biomass handling in plant $j \in C$ (in $)
I_j^{cd}	is equal to $I_j^{cd} = 13646 * \left(TC_j * f_j * \frac{LHV_j^{bm}}{LHV_j^{coal}}\right)^{0.5575}$
I_j^{CD}	the investment necessary for compressors and dryers in plant $j \in C$ (in $)
LHV_j^{coal}	the lower heating value of coal used in plant $j \in C$ (in BTU/ton)
LHV_j^{bm}	the lower heating value of biomass used in plant $j \in C$ (in BTU/ton)
M_j^{coal}	the amount of coal used in plant $j \in C$ (in tons/year)
M_j^{bm}	the amount of biomass used in plant $j \in C$ (in tons/year)
M	a very large number
m_{lj}^{mb}	the amount of biomass necessary to displace $l(\in L)$% of coal in plant $j \in C$ (in tons)
OH_j	the number of operating hours in plant $j \in C$ (in hours/year)
Q_j^0	the initial (before co-firing) annual heating input of plant $j \in C$ (in MW)
Q_j	the annual heating input after co-firing of plant $j \in C$ (in MW)
ρ_j^0	the initial (before co-firing) efficiency rate of plant $j \in C$ (in %)
ρ_j	the efficiency rate after co-firing of plant $j \in C$ (in %)
ρ_j^b	the efficiency rate of boilers in plant $j \in C$ (in %)
ρ_j^{rp}	the efficiency rate of the rest (without boilers) of plant $j \in C$ (in %)
σ_j^p	is equal to $(c_j^{coal} * \frac{LHV_j^{bm}}{LHV_j^{coal}})$
S_j^p	the total savings due to reducing the amount of coal purchased in plant $j \in C$, (in $/year)
σ_j^t	is equal to $(11 * LHV_j^{bm})/(C^{wb})$
S_j^{tax}	the total savings due to production tax savings in plant $j \in C$, (in $/(ton*year))
TC_j	coal plant $j \in C$ nameplate capacity (in MW)

Chapter 3

Analyzing Tax Incentives for Producing Renewable Energy by Biomass Cofiring

3.1 Introduction

Concerns about the impacts of Greenhouse Gas (GHG) emissions on the environment, human health, and the worldwide economy brought many nations leaders together during the 2015 United Nations (UN) Climate Change Conference in Paris (2015). UN members reached an agreement, committing to control GHG emissions. In the U.S., coal is the single largest contributor to GHG emissions, totaling as much as 28% of the GHG released into the environment (U.S. Environmental Protection Agency (EPA), 2017). This chapter focuses on tax incentives for biomass cofiring, the direct co-combustion of biomass with coal in plants using coal to generate heat and electricity. In the U.S., coal contributes to 71% of the total carbon dioxide (CO_2) emissions from the energy sector (U.S. Energy Information Administration (EIA), 2015). Among all the GHG-reduction technologies, biomass cofiring has been shown to be one of the least expensive and relatively easy to implement (Basua et al. 2011).

The Clean Power Plan, finalized by the U.S. Environmental Protection Agency in 2015, established CO_2 pollution standards for new and existing coal-fired power plants. As a result, researchers estimated that 17% of coal-fired power plants that fail to comply with existing regulations may close over the next few years (Bloomberg New Energy Finance 2015). These plant closings would result in job losses and higher electricity prices. While governmental support mechanisms in European Union (EU) countries offer many incentives for biomass cofiring, the U.S. is different. At the federal level, the PTC is the only tax incentive offered to support biomass cofiring. At the state level, regulations such as Renewable Portfolio Standards (RPS), mandate that power plants generate more renewable energy by using sources like biomass.

While many researchers agree that cofiring biomass with coal in power plants is an option for RPS compliance and a near-term solution for introducing biomass into today's renewable energy market, only 40 of the 560 power plants in the U.S. currently do so (Basua et al. 2011). These installations are typically in the range of 50 MW to 700 MW (a few units are between 5 and 50 MW) and spread around the Contiguous U.S. (IEA Bioenergy Task 32, 2017). At least two reasons disincentivize the use of cofiring in power plants: First, cofiring is not cost effective because the cost of collecting, transporting, and storing biomass is high, and burning biomass increases slagging and boiler corrosion. Therefore, overall plant efficiency drops. Second, there are only limited state and federal support for cofiring. These facts impact the likelihood of power plants to cofire biomass. This is the reason why many researchers suggest that a comprehensive governmental support system is needed to make biomass cofiring economically attractive (Smith and Rousaki 2002, Kangas et al. 2009, McIlveen-Wright et al. 2011, Moiseyev et al. 2014, Montgomery May 2015, Ekşioğlu et al. 2016).

Indeed, there are other climate policies that lead to GHG emission reductions, such as, carbon cap, carbon tax, RPS, etc. (Fischer and Newell 2008, Goulder and Schein 2013). A number of studies indicate that policies such as PTC and RPS, in contrary to a carbon tax or carbon cap, do not incentivize potentially cheaper GHG emission reductions that could

be achieved via the use of energy efficient equipment and vehicles, use of cleaner fossil fuels, and investments in carbon capture and storage. However, by incentivizing biomass usage, PTC contributes to renewable energy generation, contributes to reductions in agricultural and forest waste (which would otherwise be landfilled) and contributes in creating economic value for farmers.

This study develops models that (a) support federal- or state-level design of efficient tax incentives for biomass cofiring, and (b) optimize the performance of individual plants corresponding supply chains. These models suggest approaches that policymakers may use to make the best use of their limited budgets. The optimization models presented are extensions of resource allocation problems, which provide insights into how to allocate scarce resources among competing players and achieve the best possible overall system performance (Katoh et al. 2013). This research identifies federal or state funding as the scarce resource to be distributed among coal-fired power plants via renewable energy subsidies similar to the PTC. Depending on the definition of performance used and the conditions under which optimal performance is achieved, different types of resource allocation models can be developed. A *profit maximization* model (max-profit) distributes the resources in such a way that the total profits of the supply chain is maximized (in the context of welfare economics, this approach is similar to the utilitarian solution, an allocation of resources that seeks to maximize the total utility of all individuals (Bertsimas et al. 2011)). Considering the systems total profit as the efficiency measure, this resource allocation model provides the solution for a fully efficient system. Such an approach, however, may favor large-capacity plants, which typically have higher profit margins than their smaller counterparts. A fair distribution of financial resources among non-cooperative entities is desirable because of political and social reasons (Crawford 1998). In designing environmental policies, the distributive justice is particularly important for reducing conflicts and retaining equity (Caney 2009). The literature reviews reveal that researchers have not agreed upon criteria for defining fairness (Kumar and Kleinberg 2006, Bertsimas et al. 2011). Some models detailed in the literature include the max-min fairness (Radunović and le Boudec 2007), the proportional fairness

(Kelly et al. 1998), and the total equity models (Luss 1999). Attaining fairness often comes at the price of losing system efficiencies. This efficiency loss can be evaluated by comparing with the optimal solution of profit maximization model (Section 3.3).

The work in this chapter makes two major contributions to the literature: First, this research introduces a novel framework to aid the design of governmental tax incentives, such as the PTC. The resource allocation model proposed identifies how a government might distribute its budget among power plants that cofire biomass. The max-profit approach only focuses on maximizing the total profits, but, to balance equity and fairness in the system, this study proposes policies that can distribute monetary funds to the advantage of small-capacity plants or plants that generate the most renewable energy. This research also investigates a budget distribution that maximizes the minimum attainable profit in the system through a max-min fairness model. Such a scheme is considered to result in the worst-case degradation of the max-profit objective (Bertsimas et al. 2012). Thus, the max-profit and max-min schemes provide the efficiency and fairness bounds within which lay the novel schemes proposed by this research. The resulting resource allocation models are mixed integer bilinear programs (MIBLP) which are reformulated using McCormick relaxation to provide efficient solution methods. The second major contribution this chapter presents is the case study, based on data gathered from the southeastern U.S. The analysis provides novel insights on the efficiency and fairness of various allocation schemes. For example, the existing flat PTC maximizes a systems profitability; however, the model results in the fewest kWh of renewable energy generated. Capacity-based schemes maximize the number of plants that cofire, and they generate the most kWh of renewable energy. Ratio-based schemes provide balanced outcomes in terms of profitability and renewable energy generation. These observations provide helpful insights to policymakers in designing effective incentive schemes that promote biomass cofiring.

3.2 Related Work

Our study in this chapter relates to three main streams of literature: techno-economic studies on biomass cofiring, incentive mechanisms and regulations in renewable energy, and fairness studies in resource allocation problems.

Previous literature establishes the technical feasibility of biomass and coal co-combustion in coal-fired power plants (Baxter 2005, Goerndt et al. 2013a, Koppejan and Van Loo 2012). While most of this research focuses on the techno-economic analysis of cofiring at certain power plants, a few studies extend the scope by considering biomass supply chain costs (Roni et al. 2014, Sharma et al. 2013, Ekşioğlu et al. 2015). Studies by Hansson et al. (2009) and Al-Mansour and Zuwala (2010) demonstrate the potential of biomass cofiring as an affordable near-term solution to comply with GHG regulations in the EU. Most of the techno-economic assessments of biomass cofiring suggest that financial support is essential to encourage existing plants to utilize biomass power (Tharakan et al. 2005, De and Assadi 2009, McIlveen-Wright et al. 2011, Cuellar 2012). Dong (2012) details environmental concerns that providing plants financial incentives for biomass cofiring may lead to increased use of coal to generate power. However, Lintunen and Kangas (2010) show that cofiring does not result in significant increase of fossil fuel use, despite the fact that subsidizing biomass cofiring does use funds that could otherwise be invested in pure renewable technology. In Chapter 2. we propose an integrated transportation and production planning model that captures the impacts of biomass cofiring decisions on supply chain costs. In that chapter, by developing a case study using southeastern U.S. coal plants, we showed that biomass cofiring in some states is not profitable. Therefore, providing a PTC as low as 0.7¢/kWh could increase power plants efforts to generate renewable energy in their respective regions. In this chapter we propose a variety of governmental incentives that may increase companies generating renewable energy via biomass cofiring. The performance of the presented incentives are evaluated via an extensive numerical analysis based on a fact-based case study.

Some papers in sustainable operations management literature address the impacts of environmental policies and tax incentives on production and operational decisions (Drake et al. 2016, Krass et al. 2013, Kroes et al. 2012). Works by Garcia et al. (2012), Shrimali and Baker (2012), Alizamir et al. (2016), Zhou et al. (2011) focus on the design and assessment of incentive mechanisms that promote renewable energy generation. Kim and L. (2012) propose an optimization model that helps policymakers identify feed-in tariffs (FIT), which maximize the incorporation of renewable energy into the regions overall energy supply. Because of the wide-spread usage and proven effectiveness of FIT (Fouquet and Johansson 2008), this support mechanism has received the most attention in the literature. Wiser et al. (2007) analyze the efficiency of the PTC applied to companies generating renewable electricity from wind. A few studies focus on the design and analysis of incentives for biomass cofiring technolog (Lintunen and Kangas 2010, Kangas et al. 2009, Moiseyev et al. 2014, Aguilar et al. 2012). For example, Moiseyev et al. (2014) analyze the impact of subsidies and carbon pricing on woody biomass cofiring in EU markets. Luo and Miller (2013) use a game theoretic approach to design and manage a biofuel supply chain. Their study develops an optimization model that captures the impact of monetary incentives that support biofuel producers. In Aguilar et al. (2012), the economic factors influencing the likelihood of biomass cofiring in the U.S. northern region is investigated. Their study suggests that state-level renewable energy portfolio standards do not show significant effect on the adoption of biomass cofiring at coal plants.

Similar to those studies, this work proposes models that help policymakers identify PTCs that maximize plants efforts to generate renewable energy. In addition, the models proposed in this work ensure a fair allocation of the PTC among participating plants and compare these models performance, using an extensive numerical analysis, to determine their profitability and fairness.

Finally, this research uses a resource allocation modeling framework to design PTC allocation schemes (Katoh et al. 2013). Very few studies in the literature use resource allocation models to design support mechanisms for renewable energy systems. However,

Dai et al. (2014) propose proportional resource allocation models to address how tradable emission permits can be allocated among a set of entities. Overall, resource allocation models provide the appropriate setting to aid decision makers in allocating scarce resources among self-interested parties. These models analyze the efficiency and fairness of different allocation schemes (Bertsimas et al. 2011, 2012), and this modeling framework has been used on a broad range of applications in operations management literature, such as healthcare management (McCoy and Lee 2014, Atasu et al. 2016), supply chain management (Cui et al. 2007, Wu and Niederhoff 2014), and recycling network design (Gui et al. 2015), among others. Using a resource allocation model to address profitability and fairness questions will provide new insights to determining the best ways to incentivize plants generating renewable energy.

3.3 Problem Description

Consider a supply chain consisting of biomass suppliers and coal-fired power plants. Plants face the issue of determining whether or not to cofire biomass, and if a plant decides to cofire, this plant must also decide how much biomass to use. Using coal to produce energy is cheaper than using biomass because the cost of collecting, transporting, and storing biomass is high, and biomass cofiring reduces plant efficiency. Consider that the supply chain is influenced by the policies established by a governmental entity, which faces a limited budget and the challenge of designing efficient and fair polices to encourage plants to generate renewable energy via biomass cofiring. The flexible approach proposed here presents policies that may (a) maximize system-wide profits, (b) ensure a fair distribution of budget to participating plants, or (c) maximize the kWh of renewable energy generated. The models developed here are used to evaluate the trade-offs that exist among a variety of policies.

These approaches are inspired by current U.S. and EU practices. For example, in the U.S., the PTC provides a flat tax credit per unit of renewable energy generated

to facilities that implement either full-scale biomass firing or closed-loop biomass cofiring. Full-scale biomass firing refers to using solely biomass in a power plant. Closed-loop biomass cofiring refers to the scenario when biomass is exclusively planted for the purpose of being used at power plant to produce electricity. However, plants that implement only partial cofiring are excluded and do not benefit from the PTC (Internal Revenue Code, §45). The EU uses FIT schemes to support biomass-related energy generation (Menanteau et al. 2003, Ragwitz et al. 2007, Fouquet and Johansson 2008). Finland has the largest number of biomass cofiring installations in the EU (78 biomass cofiring plants accroding to IEA Bioenrgy Task 32 database, 2017). Finland offers tax exemptions for the energy produced from biomass, provides investment subsidies for cofiring related projects, and offers an FIT of 133.5 €/MWh for combined heat and power (CHP) generation. A study by Ragwitz et al. (2007) evaluates the advantages of step-wise FIT schemes, in which plants are compensated based on plant characteristics, fuel types, and levels of renewable energy generation. For instance, in UK, coal-fired power stations that cofire more than 15% biomass, will receive twice as much support compared to lower levels of cofiring. In Germany, small bioenergy systems (<5MW) receive an FIT rate of \$0.1627/kWh and larger systems receive a rate of \$0.1087/kWh Croucher et al. (2010). The FIT programs are increasingly favored by EU countries to promote bioenergy and other renewables. This could be due to the fact that under FIT, the costs of support are directly passed on to end users of electricity (Dong 2012).

Based on these observations, our study extends these policies in the following directions: A ratio-based PTC which allows plants with the highest biomass-to-coal ratios to receive higher tax credits. A capacity-based PTC which provides a tax credit based on plant capacity, so smaller plants receive increased tax credit rates. These models capture two sides of this decision making process: First, the governmental entity decides the PTCs structure, if funds are allocated for cofiring. On the other side, power plants choose a cofiring strategy that maximizes profits because they depend on supply chain-related costs and revenues from the PTC.

The criteria that governments use to identify the best allocation of resources has been the subject of extensive studies in welfare economics (Mas-Colell et al. 1995, Young 1995, Sen and Foster 1997). The utilitarian approach refers to the common policy of a governmental entity identifying a distribution of resources that will maximize the sum of the utilities of all participants. Under the fairness principle, the governmental entity identifies a distribution of resources which optimizes some system fairness measure. Due to the subjective nature of fairness, no one principle is universally accepted as "the most fair." Thus, depending on the specific problem at hand and the fairness scheme definition applied, different fair solutions may apply. In light of those studies, here we investigate the distribution of renewable energy credits among the coal plants to help them obtain financial benefits from biomass cofiring. For instance, a solution to the max-min fairness scheme finds a distribution of resources that will maximize the minimum profit of all participating plants. Such a scheme results in the worst-case degradation of the max-profit objective (Bertsimas et al. 2012). In the context of this problem, a fair policy ensures a maximum number of small- and large-capacity power plants participate. Without fairness policies, only large-capacity plants may take advantage of tax incentives because large-capacity plants typically have large profit margins with the necessary cushion against uncertainties associated with investments in biomass cofiring. A fair policy also compensates based on the ratio of biomass-to-coal because the relationship between costs and the amount of biomass cofired is not linear.

Definitions: Let $\mathcal{C} = \{1, \ldots, C\}$ represent the set of plants in the supply chain. Let B_j represent the biomass cofiring strategy (the heat input ratio) adopted by plant j and the function $M_j^b(B_j)$ represent the amount of biomass required annually (in tons) to displace coal in plant j. Cofiring decisions at coal plants are impacted by biomass availability in the region, denoted by b. The set $\mathbf{B} := \{B_j | \sum_{j \in \mathcal{C}} M_j^b(B_j) \leq b\}$ represents all of the feasible cofiring strategies.

Let $\mathcal{T}$ represent the *resource set*, which is the set of all feasible allocations of PTC, i.e., each allocation that satisfies physical and monetary limitations that plants and the government face. Let $\mathbf{T} \in \mathcal{T}$ represent one of these PTC allocations where T_j is a tax

rate reduction in the form of $\$T_j$ per mega-watt hour (MWh) of electricity generated from biomass in plant j and $\mathbf{T} := \{T_j | \forall j \in \mathcal{C}\}$. The corresponding annual revenues from tax credits for each plant is a function $S_j^t(T_j, B_j)$ of the size of tax reduction and cofiring strategy. Let g represent the available annual assigned budget to support biomass cofiring through PTC, and let t^l, t^u represent a lower and an upper bound on the size of the tax rate. The resource set is defined as follows

$$\mathcal{T} := \{\mathbf{T} \in \mathbb{R}_+^n \mid \sum_{j \in \mathcal{C}} S_j^t(T_j, B_j) \leq g, B_j \in \mathbf{B}, t^l \leq T_j \leq t^u, \forall j \in \mathcal{C}\}.$$

For a given $\mathbf{T} \in \mathcal{T}$, assume that each coal plant can achieve a known profit level U_j via cofiring, and $\mathbf{U} := \{U_j | \forall j \in \mathcal{C}\}$. The amount of profit is a function of available PTC and cofiring strategy adopted by the plants ($U_j : (T_j, B_j) \rightarrow \mathbb{R}_+$). In Section 3.4.1, the details of deriving profit levels for plants are explained.

Profit maximization approach: Under this approach, the government selects a $\mathbf{T} \in \mathcal{T}$ to maximize the sum of profits of all participating plants:

$$U^* = \max_{\mathbf{T} \in \mathcal{T}} \quad \textstyle\sum_{j \in \mathcal{C}} U_j(T_j, B_j). \tag{3.1}$$

In practice, a profit maximization approach is not always favored since it may result in an unequal distribution of resources which may not be proportional to power plants efforts to generate renewable electricity. As a result, some of the plants may not receive a fair share of the available budget. Despite being likely impractical, this approach represents a fully efficient system and thus helps us to evaluate the other more practical approaches (capacity-based and ratio-based schemes).

Fairness approach: While identifying a fair distribution of resources among supply chain members is desired, no agreed-upon set of criteria define "fairness" in the literature. To quantify and compare the fairness of different allocation schemes, researchers use metrics such as the minimum system profit, the gap between minimum and maximum profit, and the Jain and Theil indices (Rawls 1971). The fairness metric used in this study is the

minimum guarantee of profit to all players and is obtained as follows

$$\overline{U} = \max_{\mathbf{T}\in\mathcal{T}} \min_{j\in\mathcal{C}} U_j(T_j, B_j). \tag{3.2}$$

As mentioned earlier the practical PTC schemes proposed and analyzed here are based on plant capacity and cofiring ratios. Let $\mathbb{S}$ represent the PTC scheme to be implemented by the government and $U_j^{\mathbb{S}}$ represent the optimal profit of plant j achieved under this scheme. Let $\underline{U}^{\mathbb{S}} = \min_{j\in\mathcal{C}} U_j^{\mathbb{S}}$ denote the minimum profit imposed by scheme $\mathbb{S}$. Bertsimas et al. (2012) define *fairness loss* of any scheme $\mathbb{S}$ as the difference between the fairness metric $\overline{U}$ and the resulted minimum profit $\underline{U}^{\mathbb{S}}$. Then, the relative loss in the minimum profit achieved under $\mathbb{S}$, as compared to the maximized minimum profit under max-min scheme, is the *price of efficiency* (PoE) and calculated as $PoE = \frac{\overline{U}-\underline{U}^{\mathbb{S}}}{\overline{U}}$. A fair allocation of resources leads to a loss of efficiency in the supply chain. The *price of fairness* (PoF) is a measure of efficiency loss due to implementing the fairness scheme, and is given by $PoF = \frac{U^*-\sum_{j\in\mathcal{C}} U_j^{\mathbb{S}}}{U^*}$. A PoF value equal to 0 indicates that both of the profit maximization and fair approaches have equal system efficiencies.

3.4 Developing the Optimization Models

3.4.1 Calculating a Plant's Profit

Revenues are obtained via savings from the PTC, plus savings due to displacing coal with biomass. Recall S_j^t, which represents revenues due to PTC. Let S_j^c represent the annual revenues due to displacing coal with biomass, and let M_j^c represent the amount of coal substituted by biomass at plant j. Both S_j^c and M_j^c are functions of cofiring ratio B_j. If p_j^c is the unit purchase cost of coal in plant j, then, the corresponding annual revenues (in \$) from coal displacement is equal to $S_j^c(B_j) = p_j^c M_j^c(B_j)$.

Costs of biomass cofiring include biomass delivery, ash disposal, coal plant retrofitting investments, and operations and maintenance (O&M) (IEA-ETSAP and IRENA 2013).

Biomass *delivery* cost accounts for the cost of purchasing and transportation. The unit delivery cost is denoted by c^d (in \$/ton). Ash generated from burning coal alone is a byproduct with a market value; however, ash generated from cofiring with biomass is not suitable and should be disposed at some cost (Tharakan et al. 2005). The unit ash disposal cost is denoted by c^a (in \$/ton). Let V_j denote the total annual costs due to biomass delivery and ash disposal: $V_j(B_j) = \left(c^b + c^a\right) M_j^b(B_j)$. The investment costs consist of the fixed annual operating O&M costs $\mathcal{F}_j$ (in \$ per MW) and the overnight capital costs I_j (in \$ per MW). Capital costs occur at the beginning of a cofiring project. Let c^f be the capital charge factor used to calculate the annual equivalent cost over the project's lifetime. Parameter N_j represents the plant's capacity in MW. Equation (3.3) presents the annual investment costs at plant j.

$$\mathcal{I}_j(B_j) = \Big(B_j \mathcal{F}_j + c^f I(B_j)\Big) N_j. \tag{3.3}$$

The profit achieved at plant j is calculated by subtracting total revenues from total costs as

$$U_j(T_j, B_j) = S_j^t(T_j, B_j) + S_j^c(B_j) - \mathcal{I}_j(B_j) - V_j(B_j). \tag{3.4}$$

3.4.2 Max-Profit Optimization Model

Following a profit maximization approach, the governmental entity uses model (3.1) to identify a credit allocation that will maximize the total profits of power plants. Let the ordered set $L := \left\{\beta_1, \beta_2, \ldots, \beta_{|L|}\right\}$ contain all the potential values for cofiring strategy B_j. This assumption is not restrictive, since, in real-world decision making about cofiring strategies, only certain cofiring strategies (e.g. 5%, 10%, or 20%) are implemented in a plant (see, for axample, DEBCO (2013)). Moreover, if needed, additional cofiring strategies can be evaluated by simply increasing the size of L. Accordingly, let the binary variable Y_{lj} $(\forall l \in L; j \in \mathcal{C})$ take the value 1 if $B_j = \beta_l$ and 0 otherwise. The binary variables Y_{lj} represents the cofiring strategy $\beta_l, l \in L$ adopted by plant j, therefore, $B_j = \sum_{l \in L} \beta_l Y_{lj}$,

where $\sum_{l \in L} Y_{lj} = 1$. Furthermore, in order to ease exposition we let $m_{lj} := M_j^b(B_j = \beta_l)$, $v_{lj} := V_j(B_j = \beta_l)$, $\mathcal{I}_{lj} := \mathcal{I}(B_j = \beta_l)$, and $s_{lj}^c := S_j^c(B_j = \beta_l)$. The optimization model for this approach can be formulated by the following mixed integer bilinear program (MIBP). We refer to this as model (MP).

$$\text{(MP)} \qquad \max : U(\mathbf{T}, \mathbf{Y}) = \sum_{l \in L} \sum_{j \in \mathcal{C}} m'_{lj} T_j Y_{lj} + \sum_{l \in L} \sum_{j \in \mathcal{C}} (s_{lj}^c - v_{lj} - \mathcal{I}_{lj}) Y_l j \quad (3.5a)$$

s.t.

$$\sum_{l \in L} Y_{lj} = 1, \ \ \forall j \in \mathcal{C}, \tag{3.5b}$$

$$\sum_{l \in L} \sum_{j \in \mathcal{C}} m_{lj} Y_{lj} \leq b, \tag{3.5c}$$

$$\sum_{l \in L} \sum_{j \in \mathcal{C}} m'_{lj} T_j Y_{lj} \leq g, \tag{3.5d}$$

$$T_j \in [t^{min}, t^{max}], \ \ \forall j \in \mathcal{C}, \tag{3.5e}$$

$$Y_{lj} \in \{0, 1\}, \ \ \forall l \in L, j \in \mathcal{C}, \tag{3.5f}$$

where m'_{lj} is the amount of renewable energy produced at plant j under strategy β_l and $m'_{lj} = H^b m_{lj}$ (H^b is the heating value of biomass feedstock). In this formulation, constraints (4.1) guarantee that each plant will select exactly one cofiring strategy, and constraint (4.2) sets an upper bound on the total amount of biomass available for cofiring. Constraint (4.3) limits the total revenues when tax revenues are less than or equal to the available budget, and constraints (4.5) set bounds for $\mathbf{T}$, while constraints (4.6) are the binary variables.

Model (MP) is non-convex due to the presence of mixed integer bilinear terms $T_j Y_{lj}$ in the objective function and constraints. Now, we provide a tight linear relaxation of the model using the McCormick relaxation technique (McCormick 1976). This relaxation converts model (MP) into a mixed integer linear program (MILP). Furthermore, since Y_{lj}'s are binary variables, this relaxation is tight (Adams and Sherali 1993). Based on this method, a convex relaxation of a non-convex functions is obtained using convex over-estimators and under-estimators of the function over its domain. Accordingly, the MILP formulation for

the max-profit model is represented as the model (LMP) below

$$\text{(LMP)} \quad \max : U(\mathbf{T}, \mathbf{Y}, \mathbf{W}) = \sum_{l \in L} \sum_{j \in \mathcal{C}} m'_{lj} W_{lj} + \sum_{l \in L} \sum_{j \in \mathcal{C}} (s^c_{lj} - v_{lj} - \mathcal{I}_{lj}) Y_l j \tag{3.6a}$$

s.t.

$(4.1), (4.2), (4.5), (4.6),$

$$\sum_{l \in L} \sum_{j \in \mathcal{C}} m'_{lj} W_{lj} \leq g, \tag{3.6b}$$

$$W_{lj} \geq t^{min} Y_{lj}, \ \ \forall l \in L, j \in \mathcal{C}, \tag{3.6c}$$

$$W_{lj} \geq t^{max} Y_{lj} + T_j - t^{max}, \ \ \forall l \in L, j \in \mathcal{C}, \tag{3.6d}$$

$$W_{lj} \leq t^{max} Y_{lj}, \ \ \forall l \in L, j \in \mathcal{C}, \tag{3.6e}$$

$$W_{lj} \leq t^{min} Y_{lj} + T_j - t^{min}, \ \ \forall l \in L, j \in \mathcal{C}, \tag{3.6f}$$

$$W_{lj} \in \mathbb{R}^n_+, \ \ \forall l \in L, j \in \mathcal{C}, \tag{3.6g}$$

where the optimal solution of the model (LMP) provides an optimal solution to the model (MP).

3.4.3 Max-Min Optimization Model

In this section we propose an optimization model for the max-min fairness scheme, which identifies a tax incentive to maximize the minimum profit of participating plants. That is,

$$\max \min_{j \in \mathcal{C}} \sum_{l \in L} m'_{lj} W_{lj} + \sum_{l \in L} (s^c_{lj} - v_{lj} - \mathcal{I}_{lj}) Y_l j, \tag{3.7}$$

s.t.

$(4.1), (4.2), (4.5), (4.6), (3.6b) - (3.6g).$

We can transform this model into an MILP model as follows:

$$\text{(MM)} \quad \max Z, \tag{3.8a}$$

s.t.

$$Z \leq \sum_{l \in L} m'_{lj} W_{lj} + \sum_{l \in L} (s^c_{lj} - v_{lj} - \mathcal{I}_{lj}) Y_l j, \;\; j \in \mathcal{C}, \tag{3.8b}$$

$$(4.1), (4.2), (4.5), (4.6), (3.6b) - (3.6g).$$

The optimal solution of the model (MM) will provide the necessary information to evaluate the relative fairness loss for the proposed PTC schemes.

3.5 Designing Flexible PTC Schemes

This section proposes flexible tax incentive schemes with respective optimization models. These flexible incentives are step-wise schemes that are functions of plant capacity and the cofiring ratio. The capacity-based scheme for compensation could provide more support for small-capacity plants to help manage uncertainties associated with adopting new technologies. The ratio-based scheme compensates plants based on the ratio of biomass-to-coal used. Since high-ratio cofiring is known to be more expensive than small-ratio cofiring and plants often need to undergo some infrastructural changes for high ratio cofiring, the ratio-based scheme provides greater support for such decisions (see an example in Table 3.1).

Table 3.1: Example of flexible incentive schemes to support biomass cofiring

Capacity-based scheme		Ratio-based scheme	
Plant capacity	Credit	Biomas to coal ratio	Credit
Less than 100 MW	\$0.020/kWh	*Less than 5%*	\$0.010/kWh
		Between 5-25%	\$0.015/kWh
More than 100 MW	\$0.015/kWh	*More than 25%*	\$0.025/kWh

3.5.1 Ratio-Based Schemes

This scheme rewards plants based on the cofiring strategy selected. Under such a scheme, the tax credit received by plant j, T_j, is proportional to the cofiring strategy adopted, B_j. We start with partitioning the set of cofiring strategies L into K subsets, such that $L_k = \{l \in L | \delta_{k-1} \leq \beta_l < \delta_k\}$ for $k = 1, \ldots, K$ and $0 = \delta_0 < \delta_1 < \ldots < \delta_K$. This scheme could provide larger incentives to plants that adopt higher cofiring ratios (see Figure 3.1).

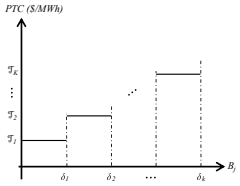

Figure 3.1: PTC versus cofiring ratio in the ratio-based scheme

In order to capture the structure of PTC under the ratio-based scheme, we introduce variables $\mathcal{T}_k, k = 1, \ldots, K$ as follows

$$T_j = \begin{cases} \mathcal{T}_1 & 0 \leq B_j < \delta_1 \\ \vdots & \\ \mathcal{T}_K & \delta_{K-1} \leq B_j < \delta_K \end{cases} \qquad \forall j \in \mathcal{C}$$

where $t_k^{min} \leq \mathcal{T}_k \leq t_k^{max}$ for $k = 1, \ldots, K$, and $t_{k-1}^{max} \leq t_k^{min}$ for $k = 2, \ldots, K$. Also note that $t_1^{min} = t^{min}$ and $t_K^{max} = t^{max}$ to keep the values for PTCs within the limits defined by resource set T. The optimization model for the ratio-based PTC scheme is

$$\text{(RS)} \quad \max: U^{\mathbb{S}}(\mathfrak{T}, \mathbf{Y}, \mathbf{W}) = \sum_{l\in L}\sum_{j\in\mathcal{C}} m'_{lj} W_{lj} + \sum_{l\in L}\sum_{j\in\mathcal{C}} (s^c_{lj} - v_{lj} - \mathcal{I}_{lj}) Y_l j \quad (3.9a)$$

s.t.

$(4.1), (4.2), (4.6), (3.6g)$,

$$W_{lj} \geq t_k^{min} Y_{lj}, \ \ \forall l \in L_k, k = 1, \ldots, K, \forall j \in \mathcal{C}, \quad (3.9b)$$

$$W_{lj} \geq t_k^{max} Y_{lj} + \mathfrak{T}_k - t_k^{max}, \ \ \forall l \in L_k, k = 1, \ldots, K, \forall j \in \mathcal{C}, \quad (3.9c)$$

$$W_{lj} \leq t_k^{max} Y_{lj}, \ \ \forall l \in L_k, k = 1, \ldots, K, \forall j \in \mathcal{C}, \quad (3.9d)$$

$$W_{lj} \leq t_k^{min} Y_{lj} + \mathfrak{T}_k - t_k^{min}, \ \ \forall l \in L_k, k = 1, \ldots, K, \forall j \in \mathcal{C}, \quad (3.9e)$$

$$\mathfrak{T}_k \in [t_k^{min}, t_k^{max}], \ \ k = 1, \ldots, K. \quad (3.9f)$$

Note that this scheme is simpler to implement compared to the profit maximization approach since, instead of deciding a separate PTC for each plant, each plant will have K options (i.e. $K = 2, 3, \ldots$) for PTC, depending on the levels of renewable energy generated.

Proposition 1. The optimal objective function value of (RS) is a lower bound to the optimal objective function value of the max-profit model (LMP).

Proof: See the Appendix B.

3.5.2 Capacity-Based Schemes

This scheme rewards plants based on their capacity, i.e. small-sized plants receive a higher PTC than large-sized plants, so smaller-capacity plants have an incentive to participate in cofiring. It is often observed that smaller plants can hardly overcome the burdens of implementing cofiring technology. It is shown that using flat rate PTC, larger plants with greater investments tend to have better opportunities to reap the benefits of PTC (Toke 2005). The reason behind this is the fact that PTC can only be used against passive income and those with already higher incomes are the ones that can utilize the full benefits of PTC. Considering the significant number of small and average coal plants in the U.S. (48% of coal plants in the country have less than 250 MW capacity) encouraging these plants to utilize biomass resources would help with nationwide demands to increase renewable energy

production. Similar capacity-based incentives are in place in some European countries. For instance, in Ireland, small biomass CHP plants receive about 16% higher FITs compared to larger facilities (Boekhoudt and Behrendt 2015).

Following an approach similar to the ratio-based schemes discussed above, coal plants are classified by partitioning the set C into K subsets $C_k = \{j \in \mathcal{C} | \nu_{k-1} \leq N_j < \nu_k\}$ for $k = 1, \ldots, K$ and $0 = \nu_0 < \nu_1 < \ldots < \nu_K$. As depicted in Figure 3.2, the biggest PTCs are provided in descending order, with the smallest power plants receiving the largest credits and the largest accepting the smallest.

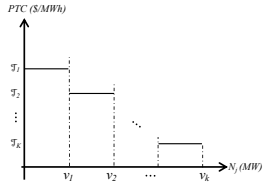

Figure 3.2: PTC versus plants' capacity in the capacity-based scheme

The variables $\mathcal{T}_k, k = 1, \ldots, K$ are defined to capture the proposed scheme in the optimization model:

$$T_j = \begin{cases} \mathcal{T}_1 & 0 \leq N_j < \nu_1 \\ \vdots & \\ \mathcal{T}_K & \nu_{K-1} \leq N_j < \nu_K \end{cases} \qquad \forall j \in \mathcal{C}$$

where $t_k^{min} \leq \mathcal{T}_k \leq t_k^{max}$ for $k = 1, \ldots, K$, and $t_{k-1}^{max} \geq t_k^{min}$ for $k = 2, \ldots, K$. Also, $t_K^{min} = t^{min}$ and $t_1^{max} = t^{max}$. The optimization model for the capacity-based PTC scheme

can be represented as

$$\text{(CS)} \quad \max: U^{\mathbb{S}}(\mathfrak{T}, \mathbf{Y}, \mathbf{W}) = \sum_{l \in L} \sum_{j \in \mathcal{C}} m'_{lj} W_{lj} + \sum_{l \in L} \sum_{j \in \mathcal{C}} (s^c_{lj} - v_{lj} - \mathcal{I}_{lj}) Y_l j \tag{3.10a}$$

s.t.

$(4.1), (4.2), (4.6), (3.6g)$,

$$W_{lj} \geq t_k^{min} Y_{lj}, \ \ \forall l \in L_k, k = 1, \ldots, K, \forall j \in \mathcal{C}, \tag{3.10b}$$

$$W_{lj} \geq t_k^{max} Y_{lj} + \mathfrak{T}_k - t_k^{max}, \ \ \forall l \in L_k, k = 1, \ldots, K, \forall j \in \mathcal{C}, \tag{3.10c}$$

$$W_{lj} \leq t_k^{max} Y_{lj}, \ \ \forall l \in L_k, k = 1, \ldots, K, \forall j \in \mathcal{C}, \tag{3.10d}$$

$$W_{lj} \leq t_k^{min} Y_{lj} + \mathfrak{T}_k - t_k^{min}, \ \ \forall l \in L_k, k = 1, \ldots, K, \forall j \in \mathcal{C}, \tag{3.10e}$$

$$\mathfrak{T}_k \in [t_k^{min}, t_k^{max}], \ \ k = 1, \ldots, K. \tag{3.10f}$$

Proposition 2. The optimal objective function value of (CS) is a lower bound to the optimal objective function value of the max-profit model (LMP).

Proof: See Proposition 1 proof.

3.6 Numerical Results

In this section we design a case study and provide managerial insights into tax incentives for biomass cofiring. First, we present the case study which is developed using data from nine southeastern U.S. states because the region is rich in biomass. Next, the results of sensitivity analysis on the PTC schemes are summarized, and managerial insights are provided. Information about the platform and computational performance of the optimization solvers are presented in Appendix B.

3.6.1 Case Study Development

This case study focuses on the following nine states located in the southeast U.S.: Alabama, Arkansas, Florida, Georgia, Louisiana, Mississippi, North Carolina, South Carolina, and Tennessee. The data about biomass availability comes from the Knowledge Discovery Framework (KDF) database provided by the Oak Ridge National Laboratory (KDF

Accessed 12.10.2013). The database provides detailed, county-level information about the availability of different types of biomass feedstock, such as forest products and residues, as well as agricultural products and residues. This study only focuses on woody biomass since it is shown to be the biomass of choice for cofiring projects (Fernando 2005). The data about the characteristics of existing coal-fired power plants, such as nameplate capacity, capacity factor, and operational hours, is provided by the U.S. Energy Information Administration (EIA, 2010).

The data about capital and O&M costs are collected from related articles in the literature. Different references in the literature estimate capital costs for biomass power that range between $50 and $400 per kW of installed capacity. The main reason for this variability in cost estimation is the difference among the quality of energy fuels analyzed and the status of the existing infrastructures at respective power plants (IEA-ETSAP and IRENA 2013). These costs do not seem to be significant when cofiring ratio is 5% -10% because the existing infrastructure of the coal plants can efficiently be utilized without additional investments. According to Sondreal et al. (2001), the expected capital cost is usually close to $50 per kW of installed capacity when cofiring ratio is less than 5%. These costs are typically between $150 and $300 per kW of installed capacity when cofiring ratio is 10-20% (Zhang et al. 2009).

Studies show that in most of the existing cofiring projects, displacing upto 50% of coal with biomass is technically achievable (IEA-ETSAP and IRENA 2013). However, cofiring at a ratio higher than 20% would increase the risk of fouling and slagging in the boilers leading to a significant drop in boiler efficiency. Pulverized coal (PC), fluidized bed (FB), and stoker boilers are the three most common types of combustion boilers in existing coal plants. It is known that FB and stoker boilers are better fits for cofiring higher percentages of biomass (Fernando 2012). In case that either of those type of boilers are already in use at a coal plant, the retrofit costs for cofiring will not be significantly higher compared to lower ratio cofiring. High ratio cofiring in PC boilers often involves with higher risks of slagging and corrosion and plant owners should invest in different type

of boilers for combustion (Basua et al. 2011). We assume an average capital cost of $400 per kW of installed capacity when cofiring is at a ratio between 25% and 50%. Equation (3.11) presents capital costs as a function of cofiring ratio. The O&M costs are estimated to be 2.5-3.5% of the overall capital costs.

$$\mathcal{C}(B_j) = \begin{cases} \$50/\text{kW} & 0.00 < B_j \leq 0.05 \\ \$150/\text{kW} & 0.05 < B_j \leq 0.15 \\ \$300/\text{kW} & 0.15 < B_j \leq 0.25 \\ \$400/\text{kW} & 0.25 < B_j \leq 0.50 \end{cases} \qquad \forall j \in \mathcal{C}. \tag{3.11}$$

Using biomass results in an efficiency loss and reduces the plants' nameplate capacity. The plants' nameplate capacity is used to calculate the investment costs since the retrofit costs are calculated based on nameplate capacity (Cuellar 2012).

We set $t^{min} = \$0/\text{MWh}$ and $t^{max} = \$20/\text{MWh}$. We use the same bounds for all schemes. In order to keep the proposed fair schemes simple, the following setups are considered. For the step-wise schemes proposed, we only consider $K = 2$ and $K = 3$. This approach is inspired by common practices in step-wise FIT schemes (see, for example, Germany's FIT policies in Couture et al. (2010)). The corresponding (RS) models developed are referred to as the *2-level* and *3-level* ratio-based schemes. The selected ranges for 2-level ratio-based schemes are

$$T_j = \begin{cases} \mathcal{T}_1 & 0 \leq B_j < 0.05, \\ \mathcal{T}_2 & 0.05 \leq B_j < 0.5, \end{cases} \qquad \forall j \in \mathcal{C},$$

where $\$0 \leq \mathcal{T}_1 \leq \$10$, and $\$10.01 \leq \mathcal{T}_2 \leq \$20$. And for the 3-level ratio-based schemes,

$$T_j = \begin{cases} \mathcal{T}_1 & 0 \leq B_j < 0.05 \\ \mathcal{T}_2 & 0.05 \leq B_j < 0.25 \\ \mathcal{T}_3 & 0.25 \leq B_j < 0.5 \end{cases} \qquad \forall j \in \mathcal{C},$$

where $\$0 \leq \mathcal{T}_1 \leq \$10$, $\$10.01 \leq \mathcal{T}_2 \leq \$15$, and $\$15.1 \leq \mathcal{T}_3 \leq \$20$.

Similarly, for the *capacity-based schemes*, we partition the set of coal plants $\mathcal{C}$ into two and three subsets based on capacity by setting $K = 2$ and $K = 3$. The corresponding (CS) models developed are referred to as the *2-level* and *3-level* capacity-based schemes. The corresponding ranges for 2-level and 3-level capacity-based schemes are, respectively,

$$T_j = \begin{cases} \mathcal{T}_1 & 0 \leq N_j < 500 \\ \mathcal{T}_2 & 500 \leq N_j \end{cases} \qquad \forall j \in \mathcal{C},$$

where $\$10.01 \leq \mathcal{T}_1 \leq \$20$, and $\$0 \leq \mathcal{T}_2 \leq \$10$,

$$T_j = \begin{cases} \mathcal{T}_1 & 0 \leq N_j < 500 \\ \mathcal{T}_2 & 500 \leq N_j < 2000 \\ \mathcal{T}_3 & 2000 \leq N_j \end{cases} \qquad \forall j \in \mathcal{C},$$

where $\$15.1 \leq \mathcal{T}_1 \leq \$20$, $\$10.01 \leq \mathcal{T}_2 \leq \$15$, and $\$0 \leq \mathcal{T}_3 \leq \$10$.

The total number of potential cofiring strategies in all cases is set to $|L| = 201$, thus, each plant can potentially cofire at ratios of $B_j \in L = \{0, 0.0025, 0.005, \ldots, 0.5\}$.

3.6.2 Comparing the PTC Schemes

This section uses numerical analyses to evaluate the impacts that the max-profit, max-min and other PTC schemes have on profitability and renewable energy production. Table 3.2 summarizes the total profits, and Table 3.3 summarizes the total biomass utilized when solving the models proposed (maximum values are in bold). For these instances the available budget of individual states is set to $\$300M$. For the SE problem set, the budget is set at $\$3,000M$. Since these numbers may not reflect the budgets actually available, sensitivity analyses are also conducted based on a broad range of available budgets (Figures 3.3 and 3.4).

Results show that, similar to max-profit model, the flat rate model maximizes the

total profits in the supply chain. The profits from the capacity-based models are typically lower, with very few exceptions, than the profits from the ratio-based models. Therefore, the relative loss in profits, as indicated by the PoF, is greatest for the capacity-based model: The average PoF is 18%, and the maximum PoF is 70%, compared to the PoF for ratio-based models of only 3.3%. For a few problems, the ratio-based model gives the same results as the max-profit model. The average PoF for flat rate models is 0%. Table 3.3 presents

Table 3.2: Total profits under the profit maximization approach and other schemes ($\$10^6$)

Problem	(LMP)	(MM)	(CS)		(RS)		Flat rate
			2-level	3-level	2-level	3-level	
AL	**268.53**	173.43	240.01	251.36	265.03	256.33	**268.53**
AR	**163.53**	141.33	48.43	118.31	**163.53**	144.56	**163.53**
FL	**273.69**	106.42	234.84	260.38	269.85	255.32	**273.69**
GA	**271.40**	145.83	247.02	258.12	268.62	260.85	**271.40**
LA	**176.07**	146.08	64.98	134.90	175.24	157.82	**176.07**
MS	**227.96**	**227.96**	176.45	184.26	**227.96**	218.71	**227.96**
NC	**275.80**	16.52	256.60	265.11	272.33	265.13	**275.80**
SC	**270.68**	16.60	251.10	263.05	269.53	259.27	**270.68**
TN	**268.57**	25.16	186.46	232.63	268.15	253.36	**268.57**
SE	**2,675.18**	1,235.45	2,347.55	2,490.96	2,666.20	2,551.38	**2,675.18**

the optimal solution of the problems in terms of the percentage of the biomass available and how much is being used. The maximum values for each problem appear in bold. As expected, the profit maximization approach does not guarantee to maximize the amount of biomass used at a plant or, consequently, the amount of renewable electricity generated. Indeed, the profit maximization approach, compared to the other schemes, leads to utilize less amounts of biomass. Likewise, the flat rate approach does not maximize the amount of biomass nor renewable energy. On the other hand, the capacity-based models use the maximum amount of biomass. Two problem instances in the 3-level capacity-based model, AR and SC, use 100% of the biomass available in the region. The average biomass usage for 2-level capacity-based models is about 80% of the total amount available. On average, biomass usage for the 2-level and 3-level ratio-based models is 56% and 67%, respectively, of the total amount available. These results indicate that the flat rate model, while easy to implement, is not as effective as the capacity-based or ratio-based models in encouraging power plants to generate renewable energy. The ratio-based schemes are sensitive to the

Table 3.3: Optimal biomass usage under profit maximization approach and other schemes (in %)

Problem	(LMP)	(MM)	(CS)		(RS)		Flat rate
			2-level	3-level	2-level	3-level	
AL	48.68	**94.73**	79.45	65.08	48.73	62.67	48.68
AR	54.05	56.72	**90.09**	66.67	54.05	54.05	54.05
FL	84.62	98.19	**100.00**	**100.00**	84.62	99.99	84.62
GA	48.29	71.77	**79.34**	62.19	48.38	62.74	48.29
LA	35.34	35.37	**50.56**	44.18	35.32	39.70	35.34
MS	41.91	41.91	**62.86**	55.21	41.91	43.17	41.91
NC	42.32	**99.87**	65.50	54.23	42.32	54.94	42.32
SC	66.43	**98.85**	89.29	78.02	66.61	83.59	66.43
TN	84.78	81.36	**100.00**	**100.00**	84.80	98.66	84.78
SE	57.46	**90.78**	85.09	74.73	57.49	69.56	57.46
Average	56.39	76.96	**80.22**	70.03	56.42	66.91	56.39

value of cofiring ratio B_j, which is directly related to the decision variable Y_{lj} (recall that $Y_{lj} = 1$ if $B_j = \beta_l$). This decision variable appears in the profit maximizing objective function along with the constraints (4.1)-(4.3), and when higher incentives T_j are provided for bigger cofiring ratios, profits are maximized rather than enforcing more participation or renewable energy generation (the term $T_j Y_{lj}$ positively impacts the objective function). Note that, B_j is not a direct measure of plant characteristics, i.e. two plants with equal cofiring strategies may have different sizes, capacity factors, etc. On the other hand, the capacity-based schemes are directly related to the plants installed capacity N_j, a parameter that only appears in the objective function and biomass limit constraint (4.2) (recall that the biomass amount m_{lj} is a function of N_j, F_j, and O_j - Chapter 2. and Appendix B.). Fixing the incentive value for different ranges of N_j does not help improve the objective function, unlike the case for the ratio-based approach. However, providing higher incentives for plants with smaller capacities better increases the utilization of the biomass limit constraint, which leads to increased renewable energy production. The capacity-based approach more accurately represents power plant characteristics, and effective capacity-based schemes may encourage more plants to participate and produce more renewable energy.(See Appendix B. for a simple numerical example).

Furthermore, in Table 3.4, we summarize the quantity of biomass used for cofiring per each dollar of incentive provided under profit maximization and other schemes. Consis-

tent with results of the Table 3.3, capacity-based schemes lead to higher biomass usage per dollar of credit provided. It is interesting to observe that this quantity is not significantly different between ratio-based schemes and the profit maximization and flat rate schemes.

Table 3.4: The amount of biomass used (kg) per dollar of provided subsidy under different schemes

Problem	(LMP)	(MM)	(CS)		(RS)		Flat rate
			2-level	3-level	2-level	3-level	
AL	8.12	15.80	13.25	10.86	8.13	8.13	8.12
AR	8.12	8.52	13.53	10.01	8.12	8.12	8.12
FL	8.12	9.42	9.59	9.60	8.12	8.12	8.12
LA	8.12	8.13	11.62	10.15	8.11	8.11	8.12
GA	8.12	12.07	13.34	10.46	8.13	8.13	8.12
MS	8.06	8.06	12.10	10.62	8.06	8.06	8.06
NC	8.12	19.16	12.57	10.40	8.12	8.12	8.12
SC	8.12	12.08	10.91	9.54	8.14	8.14	8.12
TN	8.12	7.79	9.58	9.58	8.12	8.12	8.12
SE	8.12	12.83	12.02	10.56	8.12	8.12	8.12
Average	8.11	11.39	11.85	10.18	8.12	8.12	8.11

Our analysis show that the total budget available to fund incentives such as the PTC can significantly impact renewable energy generation and plant profitability. In Figure 3.3(a) we plot profits versus budget limit, and in Figure 3.3(b) we plot the amount of biomass used versus budget limit. These plots correspond to the SE problem set, and for all the proposed schemes.

Based on these results, the flat rate and 2-level ratio-based schemes maximize profits. The 2-level capacity-based scheme results in largest biomass usage; and the max-profit, flat rate, and 2-level ratio-based schemes use the least amount of biomass. The results indicate that, the profits of the 2-level capacity-based model do not change for a budget greater than \$3,500M. This is mainly because the plants have used all the available biomass in the region. A similar observation is made for the max-profit, flat rate and 2-level ratio-based schemes. However, these schemes reach this point when the budget equals \$5,300M. That is, the same amount of renewable electricity is generated when implementing the 2-level ratio-based scheme -as compare to the max-profit, flat rate and 2-level ratio-based schemes- for about \$1,500M less.

The analysis presented here shows that the total budget available to fund incentives

like the PTC can significantly impact renewable energy generation and plant profitability. Figure 3.3(a) plots profits against budget limits, and Figure 3.3(b) shows the amount of biomass used versus budget limits. These plots correspond to the SE problem set and all the proposed schemes. Based on these results, flat rate and 2-level ratio-based schemes maximize profits. The 2-level capacity-based scheme results in the largest biomass usage, and max-profit, flat rate, and 2-level ratio-based schemes use the least amount of biomass. The results indicate that the profits of the 2-level capacity-based model do not change for a budget greater than \$3,500M because the plants will have used all the available biomass in the region. A similar observation is made for the max-profit, flat rate, and 2-level ratio-based schemes. However, these schemes reach this point when the budget equals \$5,300M. The same renewable amount of renewable electricity is generated when implementing the 2-level ratio-based scheme, as compared to the max-profit, flat rate, and 2-level ratio-based schemes, for about \$1,500M less. Figure 3.3(c) plots the PoF against budget availability. This graph shows that the values of PoF are sensitive to the available budget. When the budget is less than $\$800M$, the ratio-based schemes result in the highest PoF. When the budget is greater than $\$800M$, the capacity-based schemes result in the highest PoF. Recall that PoF measures the relative gap between the max-profit and fairness schemes, so as PoF increases, the relative gap between these two approaches increases as well. On the other hand, capacity-based schemes result in plants using the most biomass, as demonstrated above. These results could help policy makers design credit allocation policies that balance efficiency and fairness. Capacity-based schemes result in the most renewable energy generated, while ratio-based schemes balance profitability and biomass utilization. PoE values for the SE problem set were 100% because at least one plant decided not to cofire ($\underline{U}^{\mathbb{S}} = 0$) no matter what budget level was tested. However, not all of the individual states embraced such a policy (for instance, see Mississippi's results below).

We further analyze the fairness in distribution of subsidies among coal plants by calculating the Gini coefficients for each of the incentive schemes proposed. Figure 3.3(d) represents the Gini coefficient curves of different subsidy distribution schemes for coal plants

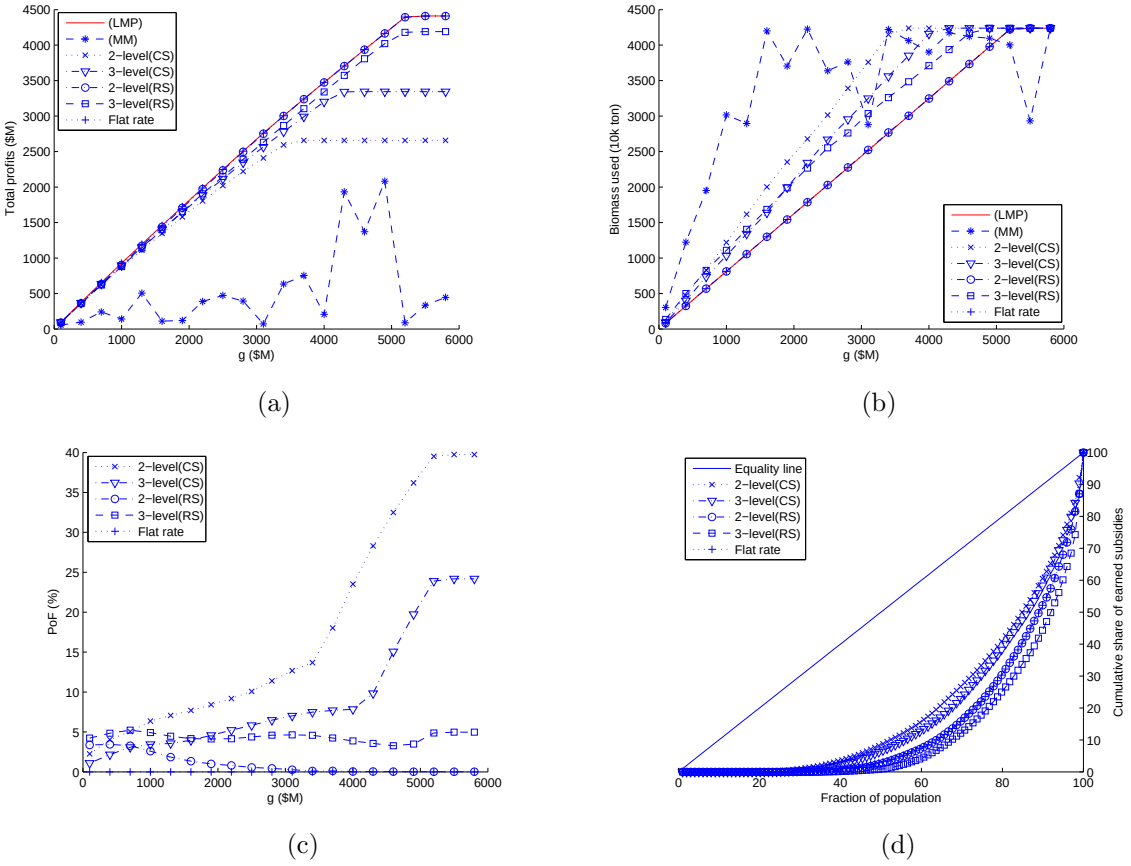

Figure 3.3: (a) Total profits, (b) biomass usage, (c) PoF (all versus the total budget), and (d) Gini coefficient curves for SE

in the southeast U.S. The calculated Gini coefficients are 0.59 and 0.62 for 2-level and 3-level capacity-based schemes, 0.69 and 0.74 for 2-level and 3-level ratio-based schemes, and 0.69 for flat rate scheme. These results are consistent with PoF measure of fairness as discussed above. The capacity-based schemes lead to smaller Gini coefficients compared to ratio-based and flat rate schemes suggesting that, in general, the distribution of incentives is fairer under capacity-based schemes. Using PoF and PoE metrics, the efficiency and fairness balance is measured by comparing the results with max-profit and max-min models deemed as the most efficient and most fair models, respectively. The capacity-based schemes result in higher PoF and lower PoE values compared to flat rate and ratio-based schemes, implying a fairer distribution of subsides which comes with the cost of larger loss of efficiency.

The PoF and PoE values for different levels of budget availability in Mississippi are depicted in Figure 3.4. Similar to the case of problem set SE, by increasing the available budget, the capacity-based schemes tend to result in a larger loss of profits (48% on average) than the flat rate (0%) and ratio-based schemes (2% on average). However, capacity-based schemes lead to smaller PoE than other schemes. For a budget level of $\$250M$, both the 2-level and 3-level capacity-based schemes result in zero PoE, while the ratio-based schemes both lead to highest relative PoE of 100%. Table 3.5 summarizes the optimal

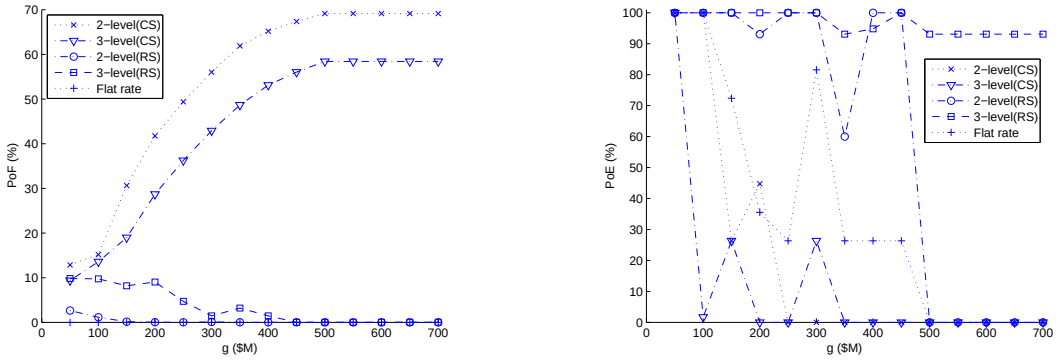

(a) (b)

Figure 3.4: (a) The PoF, and (b) PoE, versus the total budget for the state of Mississippi

values of T_j, biomass cofiring strategy B_j, and average CO_2 reductions for each of the plants in Mississippi. We estimate the amount of avoided emissions at coal plants using the default IPCC emission factors for stationary combustion in the energy industries: 340.6 $kgCO_2$/MWh for bituminous coal used for power generation and 363 $kgCO_2$/MWh for lignite coal (Intergovernmental Panel on Climate Change (IPCC) 2008). These results suggest: (i) All the plants participate in cofiring in the 3-level capacity-based model, but plant participation is lowest in this model, followed by the max-profit and flat rate models. (ii) High rate tax incentives do not guarantee that every plant participates in cofiring. The flat rate model provides the same incentive ($19.99 per MWh) to all plants; however, only a few plants participate since the revenues from such an incentive do not cover their expenses.

Plant 1, although of greater capacity than plant 3, participates only in the 3-level

Table 3.5: Optimal PTCs, cofiring strategies, and avoided emissions (in ton) for MS coal plants

Plant	Capacity (MW)	(CS) 2 level T^*	B^*	CO_2 avoided	(CS) 3 level T^*	B^*	CO_2 avoided	(RS) 2 level T^*	B^*	CO_2 avoided	(RS) 3 level T^*	B^*	CO_2 avoided	Flat rate T^*	B^*	CO_2 avoided
1	513	10	0.00	0	15	0.04	117999	0	0	0	0	0	0	19.99	0	0
2	59	20	0.03	1413	20	0.15	7064	0	0	0	0	0	0	19.99	0	0
3	400	20	0.50	1086198	20	0.50	1086198	20	0.15	325859	20	0.35	760339	19.99	0.15	325859
4	2229	10	0.14	1159352	10	0.04	331243	20	0.14	1159352	15	0.15	1242162	19.99	0.15	1242162
5	1215	10	0.04	128400	15	0.15	481501	20	0.06	192600	0	0	0	19.90	0.04	128400

capacity-based scheme because the plant currently uses lignite coal, and other plants use bituminous coal (see parameter values at the end of this chapter). Lignite coal has a smaller heating value and is cheaper than bituminous coal, so the revenues from displacing coal are not significant. Thus, this plant does not find biomass cofiring economically attractive.

Finally, the information about avoided emissions can help us to compare the schemes in terms of cofiring expenses per ton of CO_2 reduction. The unit costs per ton of CO_2 avoided are \$100.6 and \$99 for 2-level and 3-level capacity-based schemes, \$90.6 and \$90.7 for 2-level and 3-level ratio-based schemes, and \$89.6 for flat rate scheme. The capacity-based schemes turn out to be more expensive per each unit of avoided CO_2 when compared to ratio-based and flat rate schemes. This difference is mainly due to the fact that capacity-based schemes lead to higher amount of biomass usage and the coal plants need to invest more on their infrastructure in order to cofire higher percentages of biomass.

3.6.3 Managerial Insights

We now summarize some observations and insights produced by our case study. Provided that there is a limited budget to support biomass cofiring through PTC:

- *The flat rate model leads to the fewest kWh of renewable energy produced and favors large-sized plants.* The flat rate model behaves similar to the max-profit model. Such a model maximizes system's efficiency, that is, total profits. However, these profits are collected by the large-sized plants mainly.

- *Capacity-based models lead to the most renewable energy produced and increased number of participating plants in cofiring.* The 2-level and/or 3-level capacity-based models

result in plants utilizing the greatest amount of biomass in all the problems solved, which implies that plants will generate the most renewable energy if these incentive models are implemented. All the plants, smallest to largest, participate in the 3-level capacity-based model. While this scheme does not maximize a systems efficiency, it distributes the assigned budget more fairly to all the plants in the region.

- *Ratio-based models balance the PoF.* Under these models, smaller amounts of renewable energy are produced, but more profits are obtained than from the capacity-based models. These models generate more renewable energy than flat rate and max-profit models, but the proposed models also produce lower profits.

- *Capacity-based models lead to fairer incentive schemes. Regarding the fairness issue in distribution of subsidies among the coal plants, capacity-based schemes lead to fairer distributions compared to ratio-based and flat rate schemes as suggested by PoF/PoE metrics and Gini coefficients.*

- *The size of the budget influences biomass cofiring decisions both for power plants and governments.* Ratio- based models lead to plants using more biomass than capacity-based models when budgets are relatively small; capacity-based models lead to plants using more biomass when budgets are larger. This fact impacts governmental decisions about which allocation scheme to use and the size of tax rates. From the plants point of view, the selected scheme and the size of tax rates impact decisions about whether to participate in cofiring and, if so, how much biomass to cofire.

3.7 Conclusions

This chapter investigates the impacts of governmental incentives on renewable energy generation via biomass cofiring in coal-fired power plants. The literature indicates that biomass cofiring is readily available technology that is relatively easy to implement and will significantly reduce CO_2 emissions among existing coal-fired power plants.

We consider a resource allocation framework that allows the government to encourage power plants to cofire by providing credits in the form of the PTC to help plants absorb the additional costs incurred from biomass cofiring. We start with developing the max-profit and max-min models which guarantee to find an allocation scheme to maximize achievable total profits and highest minimum profit of participating plants, respectively. These approaches provide a basis for evaluating the proposed schemes in terms of relative loss in system's efficiency and fairness. Next, flexible PTC schemes are proposed, based both on plants capacity and the cofiring strategies used, to incorporate fairness in these allocation problems. The capacity-based and ratio-based schemes offer more financial support to smaller plants and those adopting higher cofiring ratios, respectively. The corresponding optimization models are non-convex, which are computationally difficult to solve. We reformulate the non-convex MIP as a linear MIP by using the McCormick relaxation of bilinear terms with binary variables.

Computational experiments are conducted using case studies based on information from nine southeastern U.S. states. We first compare the computational performance of solving linear MIPs by using Gurobi and non-convex MIPs by using BONMIN and COUENNE. Results show that the MIP solver outperforms the other two solvers in terms of CPU time and optimality gap for all of the instances. Then, we solve the case studies when ratio-based and capacity-based scheme are applied in profit optimization models.

The study in this chapter demonstrates the potential of different governmental incentives to promote renewable energy production via biomass cofiring. Our results indicate that the existing flat PTC could maximizes system's efficiency, but does not make the best use of the available biomass to generate renewable energy. One the other hand, capacity-based schemes result in highest levels of biomass utilization in most of the cases. Roughly speaking, it seems that ratio-based schemes provide a good balance between profitability and renewable energy production. However, the ratio-based schemes do not necessarily offer an economically attractive option for some plants (see the results from Mississippi). These observations provide insights to policy makers in state and federal levels to assist them in de-

signing better tax scheme frameworks, considering available budgets and emission reduction goals.

Parameters Values

Table 3.6: Values assigned for the main parameters used in this chapter (Wang (2008), IEA-ETSAP and IRENA (2013), US Energy Information Administration (2010), Cuellar (2012), US National Renewable Energy Laboratory (NREL) (2004))

Parameter	Unit	Value
FOM	($/$kWh$ yr)	12
TPC	($/$ton$)	50
c_f	(/yr)	0.15
c^{ash}	($/$ton$)	10
A	(%)	2
c^{coal} -Bituminous-	($/$ton$)	64.92
c^{coal} -Subbituminous-	($/$ton$)	14.28
c^{coal} -Lignite-	($/$ton$)	20.18
LHV^{bm}	(kWh/ton)	4926.8
LHV^{coal} -Bituminous-	(kWh/ton)	6582.5
LHV^{coal} -Subbituminous-	(kWh/ton)	6154.5
LHV^{coal} -Lignite-	(kWh/ton)	4396.1

Chapter 4

A Biobjective Optimization Model to Evaluate the Economic and Environmental Impacts of Biopower Supply Chain under Uncertainty

4.1 Introduction

Economic interests and environmental regulations are two main drivers to adopting GHG reduction technologies by coal-fired power plants. Many developed countries have designed and implemented policies which penalize GHG emissions or incentivise renewable electricity generation (Boekhoudt and Behrendt 2015). A recent meeting of the Intergovernmental Panel on Climate Change (IPCC) resulted in an agreement and commitment to control GHG emissions in order to keep the global average temperature well below 2°C (3.6°F) above pre-industrial levels (Paris Agreement, COP21 (2015)). The 5th Assessment

Report (AR5) of the IPCC proposes different scenarios that fossil-based energy systems can use to achieve large-scale, emission reductions during the upcoming decades. Power plants can adopt any single or combination of the following approaches to meet the IPCC environmental goals (Change 2014): invest in improving the efficiency of their system; invest in carbon dioxide (CO_2) capture and storage (CCS) technology; and substitute fossil fuels with fuels which have low carbon content (e.g. natural gas) or are carbon neutral (e.g. hydro, nuclear, biomass, etc) fuels.

Coal plants would typically start with efficiency improvement activities since they require little to no infrastructural changes. Other actions a plant take usually depend on the available capital and environmental performance of the plant. The implementation of CCS or natural gas technologies is a complex process which typically requires high investment costs. The co-combustion of biomass (typically woody biomass) with coal, known as *biomass cofiring*, is another appealing mid-term solution that can help coal plants to meet environmental goals and have a smoother transition to a full technology conversion in the long run if necessary. Biomss cofiring is a relatively inexpensive and efficient technology to mitigate GHG emissions in coal plants (Baxter 2005). It usually requires insignificant infrastructural change since solid biomass has similar physical characteristics to coal and can be burned in the same boilers designed for coal combustion.

It has been shown that increasing biomass content in cofiring by 1% (based on energy input ratio) would result in about 1.3% drop in global warming potential of the corresponding energy system (Mann and Spath 2001). Another pathway to utilize biomass feedstock is conversion to cellulosic ethanol to power internal combustion vehicles. A study by Campbell et al. (2009) suggests that using biomass to generate electricity (as in biomass cofiring) results in bigger emission offsets compared to ethanol. However, the extent of environmental impact of this technology will ultimately depend on the total life cycle emissions, including biomass supplier activities, feedstock transportation, and processes at power plants. It has also been shown that cofiring helps with reducing waste (e.g. wood waste, agricultural waste) and the environmental problems associated with it's disposal (Tillman

2000). According to Sebastián et al. (2011), if the biomass is not utilized for cofiring and remains in the environment, the CH_4 emissions related to its natural biodegradation would contribute to the life cycle GHG emissions.

Economic viability of biomass cofiring depends on the availability of resources and governmental support mechanisms. It is shown that biomass cofiring is economical when there are rich sources of biomass in close vicinity of plants, i.e. within 50-90 miles radius (Nicholls et al. 2006, Roni et al. 2014). Otherwise, government incentives are necessary to help plants to reach a break-even point (Ekşioğlu et al. 2016). Currently, the main financial incentive for biomass related electricity generation in the US is a production tax credit (PTC), a fixed rate credit ($¢/kWh$) which is provided for each unit of electricity generated from a renewable resource. As mentioned earlier, utilizing biomass leads to reduced emissions from coal plants. However, in order to investigate the feasibility of plants to comply with environmental regulations, it is important to investigate the GHG footprint of the corresponding supply chain. For example, a significant increase in GHG emissions due to feedstock transportation may offset emission reductions at the power plants. According to Khorshidi et al. (2014), the level of biomass cofiring (biomass to coal ratio) is another factor that directly impacts the GHG footprint of this technology. These observations motivated the development of a biobjective optimization model to analyze the influence of logistic and operational decisions on economic benefits and environmental impacts of biomass cofiring which is proposed in this paper. This type of industry-specific study of sustainability in biopower supply chains is rarely addressed in literature (**?**). In order to better capture the environmental impacts of cofiring, we integrate its life cycle assessment (LCA) into the proposed optimization framework. LCA is known to be a powerful tool to estimate the GHG emissions of biomass and biofuel supply chains (Muench and Guenther 2013).

This paper makes the following contributions to the literature. First, we develop a biobjective optimization model that captures the interactions between two (often) conflicting goals of energy systems, i.e. maximizing the profit-earning potential and minimizing

GHG emissions. The proposed model considers the biopower supply chain including biomass feedstock suppliers, transportation activities, and power plants. The proposed model captures the inherent uncertainties in the system. In order to capture the environmental impacts of the supply chain we incorporate the LCA impact results within the optimization framework. This type of modeling and analysis of biomass cofiring under uncertainty has not appeared in the literature before. Second, we develop a realistic example where a utility company which owns a number of coal-fired power plants decides to evaluate the feasibility of including biomass in their fuel portfolio. Third, we evaluate the performance of different approaches used to solve the biobjective optimization model under uncertainty. This analysis helps decision makers to understand the trade-offs that exist between solution accuracy and solution time of different approaches.

4.2 Literature Review

The literature related to biomass cofiring has grown significantly and across several disciplines in the last decade. In this section we mainly focus on studies related to biomass cofiring supply chains and studies which integrate life cycle assessment with optimization models.

4.2.1 Biomass cofiring supply chains

Most of the literature on supply chain management and design focus on the utilization of biomass for producing biofuels and biorefinery operations (Ekşioğlu et al. 2009, Sharma et al. 2013, Yue et al. 2014, De Meyer et al. 2014, Ba et al. 2016). There are fewer studies which focus on the utilization of solid biomass for cofiring supply chain, also known as biopower supply chain (Aguilar et al. 2012, Roni et al. 2014, Cinar et al. 2015, Ekşioğlu et al. 2016). In this study, we focus on models that integrate transportaiton and investment decisions with operational decisions to provide a clear picture of what happens in real-wold projects (Memişoğlu and Üster 2015, Ekşioğlu et al. 2016). In Memişoğlu and Üster (2015),

an integrated network planning model was developed that covers both strategic and tactical level decisions. The developed model is a large scale MIP and the authors propose an efficient solution algorithm based on Benders decomposition method. This model focuses on biomass-to-biofuel supply chains. Ekşioğlu et al. (2016) have introduced a model for integrating transportation and operational decisions for biomass cofiring in power plants. In addition to considering supply chain decisions, this model also considers the impacts of governmental incentives and efficiency losses due to cofiring at power plants. The developed model is an MINLP. The authors use Lagrangian relaxation to calculate lower bounds and propose an efficient linearization scheme to reformulate the model as an MIP. The work presented in thid study is an extension of the model by Ekşioğlu et al. (2016). This model extends the scope of the study by incorporating environmental impacts of the biopower supply chain via an additional objective function. The proposed model also captures the uncertainties associated with biomass quality. The models assumes centralized decision making where coal plants are managed by a single utility company.

Most of the optimization models that study biomass supply chains are deterministic, however, a few models consider the uncertain nature of of biomass supply and costs (Kim et al. 2011, Chen and Fan 2012, Gebreslassie et al. 2012, Marufuzzaman et al. 2014, Cinar et al. 2015). Kim et al. (2011), Chen and Fan (2012), Marufuzzaman et al. (2014) present the optimal design and operation of supply chain networks for biofuels under the supply, demand, and/or market price uncertainties. Gebreslassie et al. (2012) proposed a multiobjective stochastic optimization model for a hydrocarbon biorefinery supply chain. In order to capture the uncertainties, the authors modeled their problem as a two-stage stochastic program. The first objective function minimizes the supply chain costs. The second objective function minimizes the financial risk through conditional value-at-risk measure. This objective incorporates the government incentives that support biofules. A literature review carried out in Cinar et al. (2015) emphasized that there is a need to show the effect of uncertainties in cofiring supply chain network design and determination of optimal fuel combination. According to Mehmood et al. (2014), the specific chemical content and prop-

erties of biomass used in cofiring have a critical role in the efficiency of electricity generation process. In this study, we model the impact of uncertainty in quality of biomass feedstock used for cofiring via a probabilistic (chance) constraint.

4.2.2 Life cycle assessment and multiobjective optimization

Life cycle assessment is a tool which is most commonly used to estimate the GHG emissions of biomass and biofuel chains (Rabl et al. 2007, Muench and Guenther 2013). Mann and Spath (2001) is one of the earliest LCA studies on biomass cofiring. Their study shows a cofiring rates as small as 5% can result in a 5.4% reduction of GHG footprint of a coal plant. Similar studies were published by Heller et al. (2003), Cherubini et al. (2009), Sebastián et al. (2011); and Ruhul-Kabir and Kumar (2012) in later years. One of the shortcomings of conventional LCA is its inability to provide a systematic way to compare and analyze the impacts of different supply chain decisions to find the best viable approach. An approach to overcome this limitation is by integrating LCA into an optimization framework (Azapagic and Clift 1999). This is a fairly new approach in biomass and bioenergy context (You and Wang 2011, Čuček et al. 2011, You et al. 2012). Multiobjective optimization provides an appropriate framework when we want to analyze conflicting goals in the system such as minimizing the environmental impacts and maximizing the potential profits. Such approach to evaluate the environmental and economic performance in biomass supply chains have appeared in Santibanez-Aguilar et al. (2011), Čuček et al. (2012), Cambero et al. (2016), Dias et al. (2016). All of the mentioned studies focus on the design or planning of biomass-to-biofuel supply chains while in our study we investigate the biomass cofiring supply chain by means of LCA and economic evaluation under uncertainty.

Only a few studies in OR literature about biomass supply chains address the uncertainty in their problems (Gebreslassie et al. 2012, Cambero and Sowlati 2014). Gebreslassie et al. (2012) propose a biobjective optimization model which minimizes the cost and financial risk of a hydrocarbon biorefinery supply chain design. In this study, a number of problem parameters, such as market price, supply, and demand are assumed to be random

variables. To the best of our knowledge, this study is the first one to investigate the impacts of uncertain problem parameters within a multiobjective optimization framework for biomass cofiring.

There are a few studies in literature where the chance constraints (CCs) are used in the multiobjective models to analyze the perfomance of the supply chains (Bilsel and Ravindran 2011, Xu et al. 2011, Kalinina et al. 2013). In order to find the Pareto optimal solutions under uncertainty, Bilsel and Ravindran (2011) applied a goal programming approach and Xu et al. (2011) used fuzzy programming to reformulate their model. Kalinina et al. (2013) replaced the CC with its deterministic equivalent. We follow the approach in Kalinina et al. (2013) to find the Pareto optimal solutions in the proposed model. Furthermore, we apply the sample average approximation approach as explained in Kim and Ryu (2011) to evaluate its performance with respect to Pareto optimal solutions. For a review of different approaches used to solve stochastic multiobjective optimization models we refer the reader to Gutjahr and Pichler (2016).

4.3 Problem Description

In this study we investigate the economic and environmental impacts of cofiring in a setting where an electric utility company decides to introduce solid biomass as a renewable fuel to be cofired with coal in its existing coal-fired power plants. According to (IEA-ETSAP and IRENA 2013) most of the existing coal plants can potentially do up to 50% cofiring (biomass to coal heat ratio). Biomass cofiring can be a source of potential profits due to displacement of cheaper biomass with coal. Plants may also be eligible to receive financial incentives and credits from state and local governments due to biomass utilization. On the other hand, the extensive use of biomass may involve significant logistic costs and efficiency reductions at coal plants. A number of studeis show that biomass cofiring reduces emissions at the coal plant Mann and Spath (2001), Heller et al. (2003). However, the impact of cofiring on emissions is not well understood when emissions from biomass supply

chain are also taken into consideration. The biobjective optimization model we propose is expected to help utility companies to understand the trade-offs which exist between profits and emissions for different cofiring strategies (biomass to coal ratio).

The economic objective function maximizes the potential profits due to biomass cofiring. cofiring generates revenues from governmental incentives (credits) and from coal displacement. In the US, a main governmental incentive for electricity generation from biomass is production tax credit (PTC), a fixed rate credit which is provided per unit of electricity generated ($¢/kWh$). In our problem, we assume that all of the participating coal plants are eligible to receive this incentive. Furthermore, the objective function captures the retrofit costs due to adding cofiring capabilities, logistic and operational costs, as well as efficiency loss due to using biomass in the boilers. We follow the instructions proposed in Ekşioğlu et al. (2016) to derive the cost components and capture the efficiency reductions.

4.3.1 Estimating Environmental Impacts of Cofiring via LCA

In order to capture the environmental impacts of biomass cofiring and the underlying supply chain we employ the conventional life cycle assessment approach. LCA is commonly used to estimate GHG emissions of biomass and biofuel chains (Rabl et al. 2007). We consider a cradle-to-grave approach to estimate annual GHG emissions (CO_2-equivalent) during the life cycle of biomass used for cofiring.This LCA analysis follows the standards and principles proposed by the ISO 14044:2006 (ISO 2006). The four main steps of LCA as outlined in ISO 14044 for our study is described below.

Goal and scope definition: The goal of the LCA analysis is to determine the life cycle environmental impacts of biomass cofiring. This analysis is intended to provide useful information for electric utility companies that want to use biomass as a renewable fuel to be cofired with coal in their coal-fired power plants. In this analysis we are only looking at use phase emissions from the power plants. Utility companies may be required to report GHG emissions throughout the fuel supply chain to comply with regulations or to receive

renewable energy credits [1]. The functional unit considered for this analysis is the mass amount of biomass used at coal plants (Ton). The system boundary for LCA is depicted in Figure 4.1.

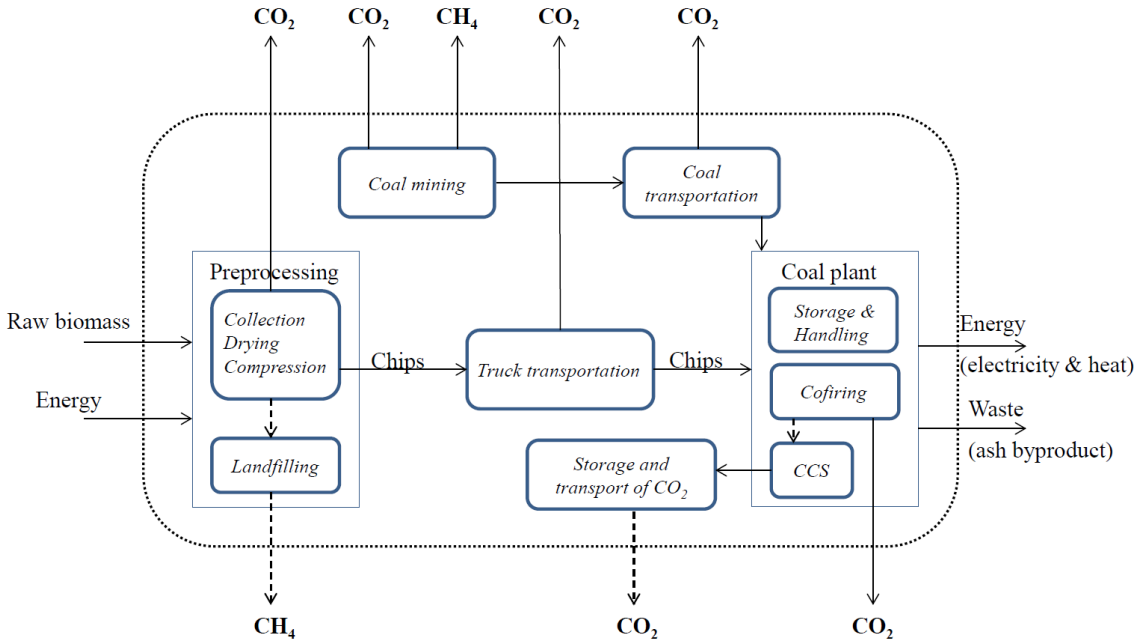

Figure 4.1: The system boundary to analyze the biomass cofiring life cycle

The life cycle boundary for our analysis include the following three main phases:

- Phase 1: *Raw material acquisition* includes the activities related to collection and processing of biomass, and coal extraction. It begins with acquiring solid biomass and coal mining, and ends with biomass and coal ready for transport.

- Phase 2: *Fuel transportation* includes transport of coal and biomass from the point of acquisition to the energy conversion facility.

[1]The Greenhouse Gas Protocol Initiative defines three scopes for emissions accounting and reporting (GHG Protocol 2011): (a) direct GHG emissions; (b) indirect GHG emissions associated with the generation of imported/purchased electricity; and (c) other indirect GHG emissions due to activities from sources owned or controlled by other companies (e.g. raw material acquisition or transportation of fuels)

- Phase 3: *Energy conversion facility* includes operation of the power plant and any modifications necessary to process and cofire biomass to generate electricity.

Inventory analysis: In this step, we analyze the input/output data associated with biomass cofiring supply chain and operations. The total life cycle emissions inventory accounts for raw material acquisition and preprocessing, coal and biomass transportation, and emissions at coal plants due to electricity generation and related operations. The total GHG emissions from each unit process is fed to the optimization model. The life cycle inventory entries, per functional unit of utilized biomass, is obtained from literature, several databases, and previous LCA analyses. We have used standard environmental databases that store emission data for similar processes, such as, EPA's Emissions & Generation Resource Integrated Database (eGRID) and the US Life Cycle Inventory Database (USLCI) by National Renewable Energy Laboratory (**?**). To conduct LCA, Argonne National Lab's GREET Life Cycle Analysis® tool (Wang 2008) is used. More details about the life cycle inventory entries and assumptions are provided in the Appendix.

Impact assessment and and integrating LCA in the biobjective optimization In third step, results of the life cycle inventory analysis are translated into potential environmental contributions. The main metric used for quantifying environmental concerns is global warming potential. In this work, emissions of two GHG gases CO_2 and CH_4 are grouped together in a single indicator in terms of carbon dioxide equivalent emissions (CO_2-equivalent/ton). The relative global warming potential of CH_4 to CO_2 is assumed to be $25:1$ based on a time horizon of 100 years suggested as part of Kyoto Protocol(IPCC, 2007).

The conventional LCA does not provide a systematic way to compare the environmental impacts of different supply chain decisions. An excellent approach to overcome this limitation is through integrating the outcomes of impact assessment into a multiobjective optimization framework. This allows decision makers to evaluate diverse supply chain design and operations alternatives that may be implemented to improve environmental performance while also assessing other aspects of the system such as economic and

social impacts. In order to integrate the LCA into the optimization model we follow the approaches proposed by Azapagic and Clift (1999) where the functional input is represented by decision variables, and relative impact of each activity is represented by objective function coefficients. This method is defined as the "problem oriented" approach to Impact Assessment (Heijungs et al. 1992).

Interpretation In last step of LCA analysis, results of the biobjective optimization model are analyzed and a set of practical strategies, which may help with the improvement of environmental and economic performance, are recommended. Solving the optimization model results in a set of optimal trade-off (Pareto optimal) solutions. These solutions represent a range of operational alternatives to utilize biomass in order to achieve best possible emission reductions and economic benefits. The proposed optimization approach provides additional insights into biomass cofiring. The Pareto optimal solutions help us to understand the inherent trade-offs that exist between economic and environmental objectives.

4.3.2 Mathematical formulation

In this section we present a chance constrained, biobjective, mixed integer programming (BCCMIP) model to analyze the economic and environmental impacts of biopower supply chain. We consider a set of coal plants have decided to cofire. These plants decide about biomass utilization and supply chain design and operations. The first objective function maximizes the average annual system-wide profits. The second objective minimizes net annual GHG emissions of biomass supply chain. These emissions are presented in terms of total CO_2-equivalent emissions.

The list of notations used in the BCCMIP model is presented below:

Sets

S	set of biomass suppliers ($i \in S$)
C	set of coal plants ($j \in C$)
C_i	set of coal plants that can receive biomass shipment from supplier i ($C_i \subset C$, $i \in S$)
K	set of price levels for biomass feedstock ($k \in K$)
L	set of potential cofiring strategies, i.e. $L := \{0, 0.01, 0.02, \ldots, 0.5\}$ ($l \in L$)

Decision variables

X_{ijk} continuous variable representing the amount of biomass of price $k \in K$ transported annually from supplier $i \in S$ to plant $j \in C$ (Ton)

Y_{lj} binary variable that takes the value 1 if plant $j \in C$ decides to use the cofiring strategy $l \in L$ and takes the value 0 otherwise

Parameters

σ^t_{lj} amount of savings at plant j via tax incentives (PTC) when cofiring at level l (\$)

σ^p_{lj} amount of saving at plant j from displacing coal with biomass by cofiring at level l (\$)

$\mathcal{I}_{lj}$ annualized investment costs due to cofiring at plant j when cofiring at level l (\$)

c_{ijk} unit purchase cost of biomass from supplier i delivered to plant j at price level k (\$/Ton)

v_{ijk} unit variable cost due to O&M, storage, and handling of biomass at plant j (\$/Ton)

$\overline{\mathrm{e}}^a_{lj}$ average GHG emissions impact due to the extraction and mining of coal to be burned in plant j at cofiring level l ($kgCO_2 - eq/Ton$)

$\overline{\mathrm{e}}^t_{lj}$ average GHG emissions impact of coal transportation to be burned in plant j at cofiring level l ($kgCO_2 - eq/Ton$)

e^p_{lj} GHG emissions impact due to biomass and coal co-combustion on plant j at cofiring level l ($kgCO_2 - eq/Ton$)

m_{lj} amount of required annual biomass feedstock if plant j decides to cofire at level l (Ton)

e^s_i GHG emissions impact due to the activities (skidding, debarking, chipping) at biomass supplier facility i ($kgCO_2 - eq/Ton$)

e^{avoid}_i impact of GHG emissions avoided from natural biodegradation of biomass as CH_4 ($kgCO_2 - eq/Ton$)

d_{ij} geographical distance from supplier i to plant j for biomass transportation using great-circle method ($mile$)

e^t GHG emissions impact of transporting biomass feedstock via trucks ($kgCO_2 - eq/Ton - mile$)

e^p_j GHG emissions impact due to handling, drying, and storage of biomass feedstock at plant j ($kgCO_2 - eq/Ton$)

s_{ik} maximum amount of available biomass at supplier i at price level k (Ton)

g limit on the financial incentives obtainable from government due to biomass utilization (\$)

h_i random variable representing the level of energy content in biomass provided by supplier i ($MMBtu/Ton$)

$\mathcal{E}_{lj}$ total required energy from burning biomass to meet the baseload requirement of plant j when cofiring at level l ($MMBtu$)

The proposed optimization model, BCCMIP, is presented as follows.

$$max \quad Z^1(Y,X) := \sum_{l\in L}\sum_{j\in C}\left(\sigma^t_{lj} + \sigma^p_{lj} - \mathcal{I}_{lj}\right) Y_{lj} - \sum_{i\in S}\sum_{j\in C_i}\sum_{k\in K}\left(c_{ijk} + v_{ijk}\right) X_{ijk}$$

$$min \quad Z^2(Y,X) := \sum_{l\in L}\sum_{j\in C}\left(\overline{\mathrm{e}}^a_{lj} + \overline{\mathrm{e}}^t_{lj} + \mathrm{e}^p_{lj}\right) m_{lj} Y_{lj} + \sum_{i\in S}\sum_{j\in C}\sum_{k\in K}\left(e^s_i - e^{avoid}_i + d_{ij}e^t + e^p_j\right) X_{ijk}$$

s.t.

$$\sum_{l \in L} Y_{lj} = 1, \qquad \forall j \in C, \tag{4.1}$$

$$\sum_{j \in C_i} \sum_{k \in K} X_{ijk} \leq s_{ik}, \qquad \forall i \in S, k \in K, \tag{4.2}$$

$$\sum_{l \in L} \sum_{j \in C} \sigma_{lj}^{t} Y_{lj} \leq g, \qquad \forall l \in L, j \in C, \tag{4.3}$$

$$Pr(\sum_{i \in S} \sum_{k \in K} h_i X_{ijk} \geq \sum_{l \in L} \mathcal{E}_{lj} Y_{lj}) \geq 1 - \gamma, \qquad \forall j \in C, \tag{4.4}$$

$$X_{ijk} \in \mathbb{R}_{+} \qquad \forall i \in S, j \in C_i, k \in K \tag{4.5}$$

$$Y_{lj} \in \{0, 1\} \qquad \forall l \in L, j \in C, \tag{4.6}$$

Constraints (4.1) guarantee that each power plant will adopt exactly one cofiring strategy (including 0% cofiring). Constraints (4.2) limit the amount of biomass delivered to be less than or equal the available feedstock at each supplier facility. Constraint (4.3) puts a limit on the amount of credit obtained by utility company. Constraint 4.4 represent the CCs at a reliability level of γ. These constraints impose, for at lease $(1 - \gamma)100\%$ of times, total energy value of delivered biomass is greater or equal to the energy requirements of each plant. Constraints (4.5)-(4.6) represent non-negative and binary decision variables.

4.4 Methodology

In this section we introduce the methodological approaches used to capture the uncertainties in the model and find the Pareto optimal solutions. The model BCCMIP proposed in previous section contains parameter randomness, conflicting objective functions, as well as mixed integer decision variables and which make solving the problem quite challenging. First we address the approach used to find the Pareto optimal solutions.

Since the developed optimization model is a multiple criteria decision making prob-

lem, there is no unique optimal solution to minimize/maximize both of the objective functions simulataneously, rather we find the Pareto optimal (Pareto efficient) solutions. Readers are referred to Ehrgott (2013) for a comprehensive review of the theory and applications of multicriteria optimization.

In order to simplify the exposition, we represent the introduced model in previous section as the simplified model (Q) below

$$\begin{aligned} (Q) \qquad & min\ \mathbf{f}(x) := (f_1(x), f_2(x)) \\ & P\left(\mathtt{E}(x,h) \leq 0\right) \geq 1-\gamma, \\ & x \in \mathcal{X}, \end{aligned}$$

where $f_1, f_2 : \mathbb{R}^{n_1} \times \mathbb{Z}^{n_2} \to \mathbb{R}$, $x := (x^1, x^2) \in \mathbb{R}^{n_1} \times \mathbb{Z}^{n_2}$. $\mathtt{E}(x,h) = -hx^1 + b_1x^2$ is the energy function determining the total energy content of the used feedstcok, $\mathcal{X} = \{(x^1, x^2) \in \mathbb{R}^{n_1} \times \mathbb{Z}^{n_2} \mid A_1x^1 + A_2x^2 \leq b_2\}$, is the discrete feasibility set defined by problem conditions, and $\gamma \in (0, 1]$ is the reliability level priory fixed by the Decision Maker. Heating values for provided biomass fuels $h_i, i = 1, \ldots, n_1$ are defined on the probability space (Ω, Σ, P). Note that the economic maximization objective function can turn to a minimization with a simple multiplication by (-1).

Definition 1. A feasible solution x' to (Q) is called *weakly efficient solution*, if there is no other feasible x such that $f_k(x) < f_k(x')$ for $k = 1, 2$. If x' is weakly efficient, then $\mathbf{f}(x')$ is called a *weakly efficient objective function value*. The set of all weakly efficient objective function values is referred to as *weakly efficient frontier*

Definition 2. A feasible solution x^* to (Q) is called *efficient* or *Pareto optimal*, if there is no other feasible x such that $f_k(x) \leq f_k(x*)$ for $k = 1, 2$ and $\mathbf{f}(x) \neq \mathbf{f}(x^*)$. If x^* is efficient, then $\mathbf{f}(x^*)$ is called a *Pareto optimal objective function value*. The set of all efficient solutions $x' \in \mathcal{X}$ is denoted by $\mathcal{X}_E$. The set of all Pareto optimal objective function values is referred to as *Pareto frontier* or *efficient frontier*. In Figure 4.2 the geometric representation

of the efficient and weakly efficient frontiers for the model BCCMIP is shown.

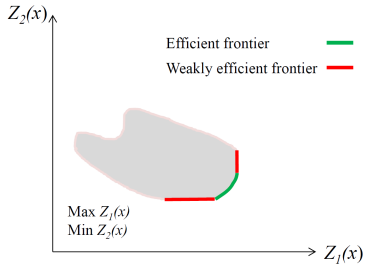

Figure 4.2: Efficient and weakly efficient frontiers for BCCMIP

4.4.1 Capturing the Uncertainties

One of the major uncertainties in this problem that may impact decision making is the energy content (measured as the lower heating value, h_i) of the biomass feedstock imported to the coal plant. Coal plants generally require that total energy potential of the replaced biomass be as good as the replaced coal to satisfy the baseload electricity output of the plant. However, this is not a rigid requirement that must be satisfied all the times. In case that the energy content of the initially decided biomass ratio is not enough, coal plants may decide to reduce the amount of utilized biomass or accept a negligible reduction in plant output if the provided incentives or resulted emission reductions are appealing.

The chance constraint programming is an appropriate approach to deal with this type of uncertainty in our model. Constraints 4.4 introduced in previous section indicate that for at least $(1-\gamma)100\%$ of the times (γ values are typically small, e.g., 1%, 5%, etc.) the total energy potential of the imported biomass feedstock is greater or equal to the energy content of the displaced coal. We assume the vector of heating values, $h : \Omega \rightarrow \mathbb{R}^{n_1}$, follows a multivariate normal distribution. We explain two different approaches we applied to model CC's. In the computational analysis we implement both approaches and compare the advantage and disadvantages of each. For a review of different approaches to model and solve the CCs in the context of stochastic multiobjective optimization refer to (Abdelaziz

2012).

4.4.1.1 True efficient frontier

Lemma 1.1. (Kataoka 1963) Suppose $h = (h_1, \ldots, h_n)$ has a multivariate normal distribution with mean $\mathbb{E}(h) = (\mathbb{E}(h_i), \ldots, \mathbb{E}(h_n))$, and let $cov(h_i, h_j)$ be the covariance of h_i and h_j. Then, for any $x \in \mathbb{R}^n$, the inner product $hx = h_1x_1 + \ldots + h_nx_n$ is normally distributed with mean

$$\mathbb{E}(hx) = \mathbb{E}(h_1)x_1 + \ldots + \mathbb{E}(h_n)x_n$$

and variance

$$Var(hx) = x'Var(h)x = \sum_{i=1}^{n}\sum_{j=1}^{n} x_i cov(h_i, h_j)x_j.$$

Proposition 1.1.(γ-satisfying efficient solution) Suppose for any $i = 1, \ldots, n_1$, the random variables h_i are normally distributed and independent. Then a point $x^* \in \mathbb{R}^{n_1} \times \mathbb{Z}^{n_2}$ is a γ-satisfying efficient solution for problem (Q) if and only if x^* is Pareto optimal for the deterministic problem (Q') below:

$$\begin{aligned}(Q') \qquad & min(f_1(x), f_2(x)) \\ & b_1x^2 - \sum_{i=1}^{n_1}\mathbb{E}(h_i)x_i^1 + \Phi^{-1}(1-\gamma)\sqrt{x^{1\prime}Var(h)x^1} \leq 0, \\ & x \in \mathcal{X},\end{aligned}$$

where $\Phi(x) = \frac{1}{\sqrt{2\pi}}\int_{-\infty}^{x} e^{\frac{-y^2}{2}}\mathrm{d}y$.

Proof. Assume that x^* is a γ-satisfying efficient solution of problem (Q). We show that the first constraint of problem (Q) is the exact equivalent to

$$b_1x^2 - \mathbb{E}(hx^1) - \Phi^{-1}(1-\gamma)\sqrt{x^{1\prime}Var(h)x^1} \leq 0.$$

Based on the definition $\mathtt{E}(x,h) = -hx^1 + b_1x^2$. By Lemma 1.1., $\mathtt{E}(x,h)$ is normally distributed with the expected value $\mathbb{E}(\mathtt{E}(x,h)) = -\sum_{i=1}^{n_1}\mathbb{E}(h_i)x_i^1 + b_1x^2$ and variance

$Var\left(\mathtt{E}(x,h)\right) = x^{1\prime}Var(h)x^1$. The CC in problem (Q), $P(\mathtt{E}(x,h) \leq 0) \geq 1-\gamma$, can be expressed as

$$P\left(\frac{\mathtt{E}(x,h) - \mathbb{E}(\mathtt{E}(x,h))}{\sqrt{Var\left(\mathtt{E}(x,h)\right)}} \leq \frac{-\mathbb{E}(\mathtt{E}(x,h))}{\sqrt{Var\left(\mathtt{E}(x,h)\right)}}\right) \geq 1-\gamma.$$

Note that $P(\mathtt{E}(x,h) \leq 0) = \Phi\left(\frac{-\mathbb{E}(\mathtt{E}(x,h))}{\sqrt{Var(\mathtt{E}(x,h))}}\right)$. Therefore the CC is equivalent to

$$\Phi\left(\frac{-\mathbb{E}(\mathtt{E}(x,h))}{\sqrt{Var\left(\mathtt{E}(x,h)\right)}}\right) \geq 1-\gamma,$$

that is

$$\frac{-\mathbb{E}(\mathtt{E}(x,h))}{\sqrt{Var\left(\mathtt{E}(x,h)\right)}} \geq \Phi^{-1}(1-\gamma),$$

which leads to $\mathbb{E}(\mathtt{E}(x,h)) + \Phi^{-1}(1-\gamma)\sqrt{Var\left(\mathtt{E}(x,h)\right)} \leq 0$.

By replacing $\mathbb{E}(\mathtt{E}(x,h))$ and $Var\left(\mathtt{E}(x,h)\right)$ with their equivalents based on Lemma 1.1. we would get the deterministic equivalent of the CC as:

$$b_1 x^2 - \sum_{i=1}^{n_1} \mathbb{E}(h_i)x_i^1 + \Phi^{-1}(1-\gamma)\sqrt{x^{1\prime}Var(h)x^1} \leq 0. \tag{4.7}$$

■

The set of Pareto optimal objective function values resulted from γ-satisfying efficient solutions is referred to as *True efficient frontier*. Note that the new constraints (4.7) are in the form of second order cone constraints (SOCCs). Modern optimization solvers can effectively solve problems with these types of constraints. However, it is known that solving the multiobjective optimization models with SOCCs is generally more expensive than the case where all constraints are linear. To avoid such difficulties researchers may develop linear or convex approximations of the nonlinear constraints (Ağpak and Gökçen 2007, Bilsel and Ravindran 2011) or find average approximations of the CCs through scenario generation (Luedtke and Ahmed 2008, Pagnoncelli et al. 2009).

4.4.1.2 Approximate efficient frontier

The other well-known approach to treat the CC is through a sampling procedure. In this approach, a set of realizations for the random parameter is generated prior to solving the problem. Using the generated scenarios, the CC is replaced with a set of new constraints (linear) that reflect the approximate behavior of the CC. This method is known as the sample average approximation (SAA) introduced initially by Charnes and Cooper (1959).

Given that the random parameter follows a known probability distribution, we use a simulation approach (e.g. Monte Carlo) to generate a set of realizations for random variable h, as h^s, $s = 1, \ldots, N$. The sample average approximation of CC is obtained by replacing the original probability distribution P by the empirical measure P_N. Let $\mathbb{1}_{(0,\infty)} : \mathbb{R} \to \{0, 1\}$ be the indicator function of (0,∞), i.e.

$$\mathbb{1}_{(0,\infty)}(t) := \begin{cases} 1 & \text{if} \quad t > 0, \\ 0 & \text{if} \quad t \leq 0. \end{cases}$$

Note that $P\left(\mathtt{E}(x, h)) \leq 0\right) \geq 1 - \gamma$ is equivalent to $P\left(\mathtt{E}(x, h)) > 0\right) \leq \gamma$. Using this indicator function the CC can be formulated as $\mathbb{E}_P\left[\mathbb{1}_{(0,\infty)}(\mathtt{E}(x, h))\right] \leq \gamma$. Then, the CC can be approximated by

$$\mathbb{E}_{P_N}\left[\mathbb{1}_{(0,\infty)}(\mathtt{E}(x, h))\right] = \frac{1}{N}\sum_{s=1}^{N} \mathbb{1}_{(0,\infty)}(\mathtt{E}(x, h^s)) \leq \gamma. \tag{4.8}$$

By introducing a binary variable V^s we can reformulate the SAA constraint (4.8) as the following

$$\begin{aligned} &\mathtt{E}(x, h^s) \leq mV^s,\ s = 1, \ldots, N, \\ &\sum_{s=1}^{N} V^s \leq N\gamma, \\ &V^s \in \{0, 1\},\ s = 1, \ldots, N, \end{aligned}$$

where m is a large constant to make the firs constraint redundant in case $V^s := 1$.

The set of Pareto optimal objective function values resulted from solving problem (Q) using the SAA constraints above is called SAA_N *efficient frontier*. In Appendix C., we show that under mild assumptions, the sequence of SAA_N efficient frontiers converge to the True efficient frontier as $N \to \infty$ with probability **1**.

4.4.2 Finding the Efficient Frontiers

We implement the **ϵ-constraint** method (Changkong and Haimes 1983) to generate a set of Pareto optimal solutions for the multiobjective model BCCMIP. In this method, the biobjective model is turned into a single objective model by keeping one of the objective functions and converting the other objective function into a bounded constraint. To generate the set of Pareto optimal solutions we start by solving each of the single objective optimization models while systematically changing the values of the constrained objective. Especially, for our BCCMIP model we solve the following two single objective models

$$\max \quad f_1(x) \tag{4.9}$$

$$x \in \mathcal{X}, \tag{4.10}$$

$$f_2(x) \leq \epsilon_2, \tag{4.11}$$

where the economic objective is maximized and the environmental objective is constrained with an upper bound limit, and

$$\min \quad Z_2(x) \tag{4.12}$$

$$x \in \mathcal{X}, \tag{4.13}$$

$$Z_1(x) \geq \epsilon_1, \tag{4.14}$$

where the environmental objective is minimized and the economic objective is constrained with a lower bound limit. $\mathcal{X}$ is the feasible region resulted from intersection of set $\mathcal{X}$ introduced in previous section and the CC $P\left(\mathtt{E}(x,h) \leq 0\right) \geq 1-\gamma$. Depending on how we model the CC, either by the deterministic equivalent or SAA approach, we will get either of True efficient frontier or SAA_N efficient frontier respectively.

To find the Pareto optimal solutions, we start by finding the range of parameters ϵ_1 and ϵ_2 in the set of Pareto optimal solutions. We first construct the payoff table (as shown in Table 4.2), by solving problems (4.9-4.10) and (4.12-4.13).

Table 4.2: The payoff table

	Problem Solved	
	$\max_{x\in\mathcal{X}} f_1(x)$	$\min_{x\in\mathcal{X}} f_2(x)$
z_1 (\$M)	ϵ_1^{max}	ϵ_2^{max}
z_2 (\$M)	ϵ_1^{min}	ϵ_2^{min}

The payoff table indicates the greatest value and smallest value that parameters ϵ_1 and ϵ_2 can take respectively. The ϵ-constraint method follows the Algorithm 1 explained below to find a set of Pareto optimal solutions.

4.5 Computational Results

4.5.1 Data Description

For our computational analyses we develop a case study using data from coal-fired power plants owned by Duke Energy Carolinas LLC. This electric power holding company supplies electricity for customers in the states of North and South Carolina. We consider 7 main coal plants with over 50MW capacity spread across the two states to meet the baseload electricity requirements of the company (Figure 14). All the plants are equipped with pulverized coal boilers which is shown to be compatible for biomass cofiring (Tillman et al. 2010). Information about plants characteristics are collected from energy.gov and Duke Energy website. For details about the economics of biomass cofiring and relevant supply chain costs, we refer the reader to Ekşioğlu et al. (2016) and Karimi et al. (2017).

Algorithm 1 The ϵ-constraint algorithm

procedure PARETOFRONT($\mathbf{Z}$)
  input Pareto optimal set $\mathbb{L}$, number of intervals k
  Build the payoff table and calculate the range of the parameters ϵ_1 and ϵ_2
  Calculate the step size $\Delta\epsilon_1 = \frac{\epsilon_1^{max} - \epsilon_1^{min}}{k}$, $\Delta\epsilon_2 = \frac{\epsilon_2^{max} - \epsilon_2^{min}}{k}$.
  for $i = 0$ to k **do**
    $\epsilon_1 = \epsilon_1^{min} + i\Delta\epsilon_1$
    Solve (4.9-4.11)
    if (4.9-4.11) feasible **then**
      Add solution to $\mathbb{L}$
    end if
  end for
  for $i = 0$ to k **do**
    $\epsilon_2 = \epsilon_2^{max} - i\Delta\epsilon_2$
    Solve (4.12-4.14)
    if (4.12-4.14) feasible **then**
      Add solution to $\mathbb{L}$
    end if
  end for
  return $\mathbb{L}$
end procedure

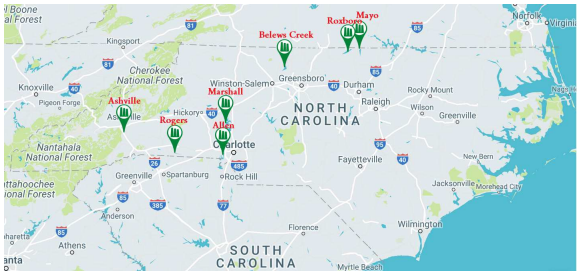

Figure 4.3: Coal-fired power plants owned by Duke Energy Carolinas LLC

Biomass availability data by state and county is extracted from the Knowledge Discovery Framework (KDF) database, an outcome of the US Billion Ton Study led by the Oak Ridge National Laboratory (KDF Accessed 12.10.2013). This database provides the amount of biomass available at the county level in the form of forest products, agricultural products, agricultural residues, etc. The database provides the amount of biomass available at different market prices, which vary from \$20 to \$200 per ton of biomass feedstock. We consider

a total of 90 suppliers of woody biomass in South and North Carolina. These suppliers are located within 80 mile radius of plants (Figure 4.4). We only focus on the wood processing residues and forest management residues resources for biomass cofiring. These resources have little to no impact on land use change and are not significantly useful otherwise.

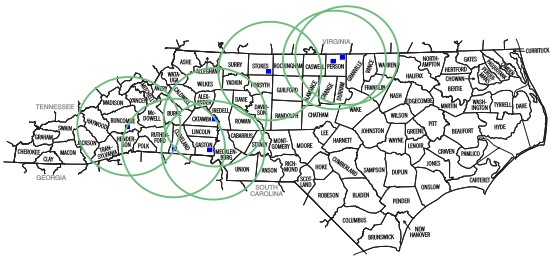

Figure 4.4: Biomass suppliers counties within 80-mile radius of coal plants

The data extracted from eGRID and USLCI databases is logged into Argonne Lab's GREET Life Cycle Analysis® tool for life cycle assessments (more details about LCA in the Appendix A).

Finally, the solution algorithms are implemented using Julia language and optimization models are build using Julia for Mathematical Programming (JuMP, **?**). Computational analyses to compare the true and approximate frontiers are run on a personal laptop with Intel(R) Core(TM) i5-4300U CPU with 1.90GHz, 2.50GHz, and 8.00GB of RAM. The solutions to the case study problems, which are summarized in Table 4.3, are found by running the algorithm on Clemson University's high performance computing nodes (Palmetto Cluster). MIP and MISOCP models are solved using Gurobi 7.0.1 solver.

4.5.2 True vs. Approximate Efficient Frontiers

In our analysis, we are interested in comparing the performance of the two approaches introduced in Section 4.4 to capture the uncertainties. As explained, the true frontier model is a biobjective MIQCP and the SAA frontier model is a biobjective MIP. Typically MIQCPs are harder to solve compared to MIP due to the presence of quadratic

constraints. In Figure 4.5 the true efficient frontiers and a group of SAA frontiers for different scenario sizes (N) with a 95% reliability level is depicted. It is shown that the SAA frontiers provide lower bounds for the environmental objective function and upper bounds for the economic objective function. By increasing the scenario size the SAA frontiers get closer to the true frontier. This is a promising indicator that by increasing the parameter N we can have a good approximation of the true frontier and avoid the difficulties of solving the biobjective MIQCP model. But how difficult is it to find the true frontier?

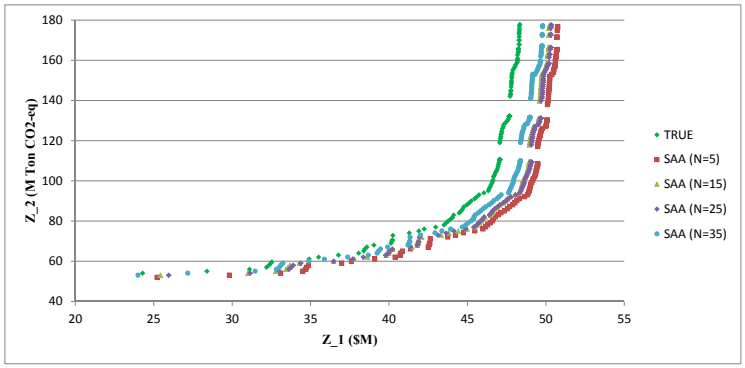

Figure 4.5: True efficient frontier and SAA frontiers with different sample sizes ($\gamma = 0.05$)

In Figure 4.6 the computational times for finding the true and SAA frontiers are presented (both models are solved using the ϵ-constraint method). The average CPU seconds for finding the true frontier is around 1600 seconds. On the other hand, the computational time for SAA frontier has an exponential growth as we increase the scenario size. The reason is by increasing N the number of constraints (**??**)-(**??**) increases and it contributes to the exponential growth of the MIP model. Despite the presence of quadratic constraints in MIQCP, the problem size remains fixed and we are able to find the true frontier with less difficulty compared to SAA frontiers when $N > 35$. For the rest of the results presented in this section we only report on the true frontiers.

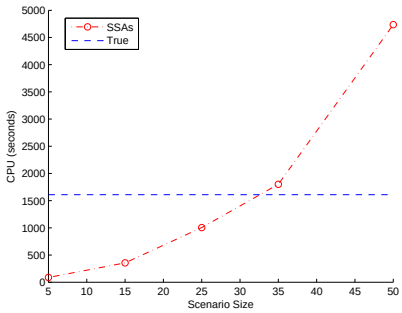

Figure 4.6: Average computaion times to calaculate the efficient frontiers (solver times)

4.5.3 Evaluating the Impacts of Cofiring

Figure 4.7 represents the efficient frontiers for different ranges of cofiring.The x-axis represents the total annual profits from biomass cofiring in all the seven plants. A negative value in the x-axis means the total costs associated with adopting cofiring is more than the savings and this leads to economic loss for the utility company. The y-axis represents the total annual emissions across all coal plants. These estimates capture emissions due to burning of coal, and emissions due to biomass transportation and suppliers activities. The total annual emissions without cofiring are estimated to be 64.34M Ton CO_2-eq. The graph represents the total emissions for the following scenarios: coal plants are required to displace 0-15% of coal with biomass; displace 0-25% of coal with biomass; displace 5-25% of coal with biomass; displace 5-50% of coal with biomass; and displace 0-50% of coal with biomass. As mentioned in the problem definition, we assume centralized decision making, thus, cofiring decisions are made by the utility company in collaboration with coal plants with the goal of optimizing system's performance. Figure 4.7 shows that giving each plant more flexibility in decision making, would result in greater profits and emission reductions. For example, when plants are to do cofiring between 5 and 25%, higher profits are achieved (compared to 0-25% scenario) since all plants do cofiring and utilize biomass. However, total emissions still remain high due to more biomass transportation and suppliers activities. Allowing plants to do cofiring between 0 and 50% results in better quality solutions. Such solutions allow plants that are located close to suppliers to cofire more than other plants, thus, leading

to higher profits while achieving higher emission reductions.

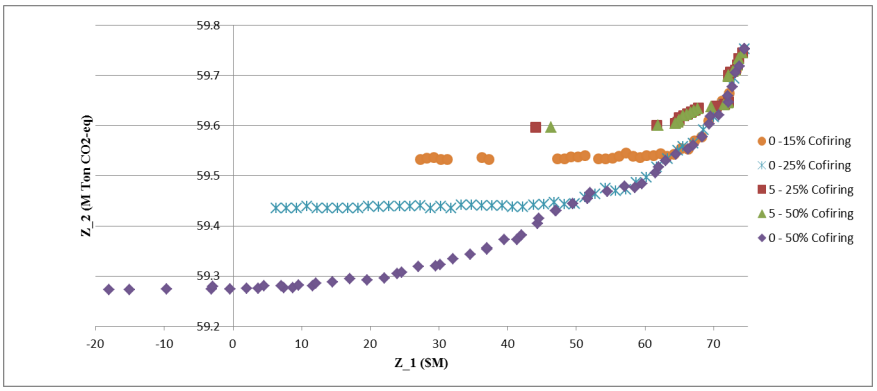

Figure 4.7: Efficient frontiers for different ranges of cofiring ratio

Table 4.3 summarizes the efficient frontiers for cofiring scenarios presented in Figure 4.7. First row represents the base case which assumes no cofiring. For the cofiring scenarios, range, standard deviation, and mean of Pareto optimal objective values are reported. These results imply some interesting observations. Total emission reductions for all scenarios is around 7% in average. There is no significant difference in reductions when high-ratio cofiring (e.g. 25-50%) is imposed. This is due to the fact that by increasing biomass usage, despite greater reduction in coal consumption, emissions due to transportation and suppliers activities compromise the emission reductions at coal plants. Table 4.3 results show that there are more deviations in profit making potentials for similar levels of emissions reduction. For the scenario when plants are allowed to do cofiring from 0 to 50%, total profits can be as much as \$74M and as low as -\$22M. Respectively, emissions reduction ranges from 6.4% to 8%. Every Pareto optimal solution represents an alternative cofiring and logistic plan for coal plants. The cofiring and supply chain decisions have crucial roles in economic attractiveness of biopower.

Next, we illustrate how these Pareto optimal solutions can lead to operational decisions regarding cofiring at individual plants. It is up to the decision makers to choose a strategy based on the environmental regulations and company interests. In Figure 4.8, three

Table 4.3: Emission reductions and profits for different ranges of cofiring

Cofiring range	Emissions (MTon CO_2-eq)				Biopower profits ($M)				Emissions reduction	
	min	max	std	mean	min	max	std	mean	min (%)	max (%)
0%	-	-	-	64.34	-	-	-	0	-	-
0-15%	59.53	59.74	0.05	59.56	27.28	74.25	14.15	50.72	7.1%	7.5%
0-25%	59.43	59.75	0.07	59.48	6.27	74.54	20.41	40.65	7.1%	7.8%
5-25%	59.60	59.74	0.04	59.66	44.08	74.24	5.34	70.07	7.1%	7.4%
5-50%	59.60	59.74	0.04	59.66	46.31	74.24	5.02	70.16	7.1%	7.4%
0-50%	59.27	59.75	0.17	59.44	-22.24	74.54	30.84	37.02	6.3%	8%

Pareto optimal solutions are selected to represent three types of possible decision making for biomass cofiring. Figures 4.9 a-c show the cofiring strategy, profits, and life cycle emissions for each plant that are informed by these representative Pareto solutions.

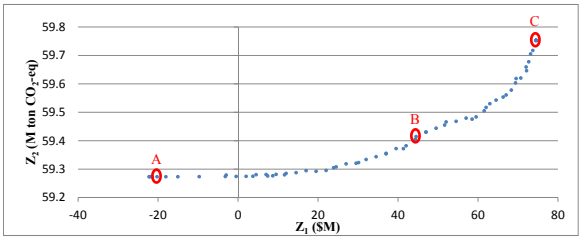

Figure 4.8: Three representative Pareto optimal solutions based on the true efficient frontier for 0-50% cofiring

Point A in Figure 4.8 corresponds to a Pareto optimal point that we would like to call an environmentally friendly solution. This solution leads to the greatest reduction on life cycle emissions due to biomass cofiring. Chart (a) in Figure 4.9 represents the resulted cofiring strategies, emissions and the amount of profits attainable for each plant. The chart shows that under this solution some of the smaller coal plants will undergo economic loss while the bigger plants will gain negligible profits. The point B corresponds to a more moderate Pereto optimal solution where none of the plants undergo economic loss, but the total emission reduction is not as big as the previous solution (Chart (b), Figure 4.9). Finally the point C at top of the efficient frontier represents a conservative solution where all of the plants gain profits, however, the emission reductions is at the lowest attainable

levels.

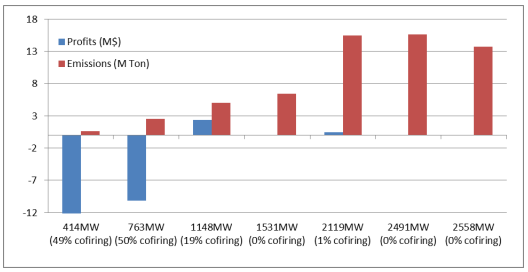

(a) Pareto optimal solution A

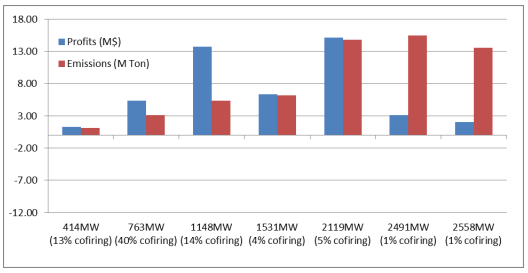

(b) Pareto optimal solution B

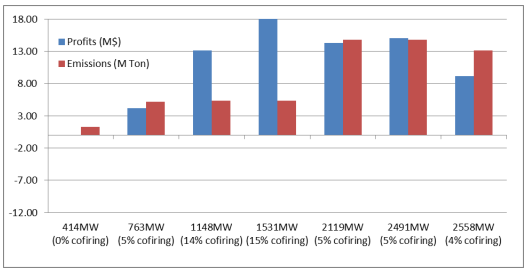

(c) Pareto optimal solution C

Figure 4.9: Cofiring strategies, profits, and emissions for three Pareto optimal solutions in Figure 4.8

Comparing the cofiring strategies of big and small plants at points A and C would help with understanding the different outcomes for emissions. At point A the two smallest plants cofire at rates of 49% and 50% (maximum possible), with total biomass use of 1.66M ton, while the two largest plants choose not to use biomass. At point C the two smallest plants cofire at rates of 0% and 5%, and the two largest plants cofire at rates 5% and 4%. The total biomass usage for these plants at point C is 0.87M ton. Biomass utilization at point A is almost twice as much for point C and this leads to higher emission reductions

at point A. An important note should be taken into account for the case when large plants decide to do cofiring. It is known that under current flat rate PTC, larger plants with greater investments tend to have better opportunities to reap the financial benefits (Toke 2005, Karimi et al. 2017). For this case study, we have assumed a total limit of \$150M for the savings obtainable from PTC (constraint 4.3). When large coal plants do cofiring the limit on PTC savings is reached and further biomass usage is not economically feasible. That is why for point C the total profits are higher but biomass usage and emissions reductions are lower. Whereas point A represents a solution for which smaller plants do maximum possible cofiring without reaching the limit on PTC savings and that leads to higher biomass usage and emission reductions.

Finally, we explain an example of how this model can aid the decision making in presence of some environmental regulations. Currently, there is no nation-wide carbon tax or carbon cap policies in place. Some of the states (e.g. California) have started imposing such policies and it is likely that other states will start to implement such policies in near future. By assuming a limit imposed by government on the total emissions allowable for a company (i.e. a Carbon cap policy), our model can be helpful on deciding the best operational and logistic plan to comply with such policy yet gain the most benefits from available incentives (Figure 4.10). In Figure 4.10 we assume a limit on the total annual GHG emissions allowed for a company. All the Pareto optimal solutions below the limit line are associated with operational and logistic plans that would satisfy this requirement. A viable solution which is to the right-most end of the Pareto curve may lead to the highest profits. In Figure 4.11, the best viable logistic and cofiring plans associated with the red-circled point in Figure 4.10 is illustrated. This solution can potentially lead to a $\$44.3M$ profit for Duke Energy.

This company may not need to consider extra reductions in GHG emissions as long

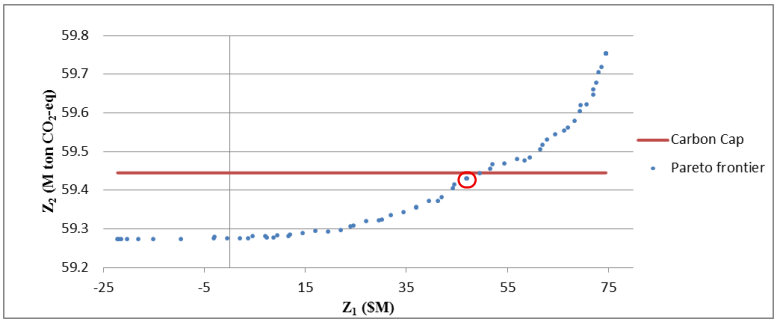

Figure 4.10: A carbon cap limit and viable Pareto optimal solutions to comply with

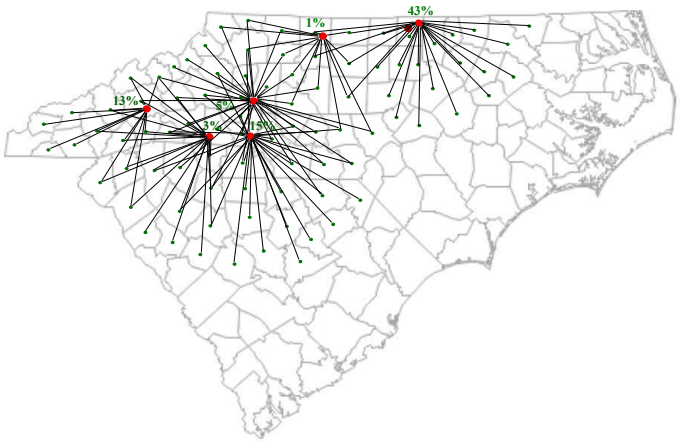

Figure 4.11: Logistic and cofiring decisions associated with the best viable Pareto solution (red circle in Figure 4.10)

as the representative solution is under the limit line. If, for example, the logistic and operational decisions associated with the point A in Figure 4.8 had chosen to follow, even though this solution meets the emission limit, it would result in an economic loss of $\$15M$.

4.6 Conclusions

In this paper, we develop an optimization model to evaluate the economic and environmental impacts of utilizing solid biomass for cofiring in a set of coal-fired power plants owned by a central utility company. We aim at facilitating the decision making regarding the operational and logistic plans to cofire by assessing the potential economic benefits and GHG emissions throughout the supply chain of biomass. The economic benefits

are mainly due to the financial incentives provided by the governments while considering the costs associated with procurement of biomass and capital investments. To estimate the GHG impacts, we utilize the well known LCA methodology and integrate its outcomes in our optimization framework. Furthermore, because of the importance of feedstock quality in the efficiency of electricity generation process, we take into account the uncertainty in energy content (heating value) of the utilized biomass in the model via chance constraints. The proposed model developed is called BCCMIP.

In our computational experiments, we start by implementing two distinct approaches to model the uncertainties implied by CCs and find the Pareto frontiers. First, by deriving the deterministic equivalent of the CCs we reformulate the model as a biobjective MIQCP. This model would result in the true efficient frontier and is typically harder to solve compared to MIPs. Second, we apply a sampling procedure known as SAA to reformulate the model as biobjective MIP and find the approximate Pareto frontiers. We use the ϵ-constraint algorithm to find the Pareto frontiers in both models. The computational results show that by increasing the size of sample scenarios in SAA the approximate frontier get closer to the true frontier; however, the average computation time increases exponentially. For scenario sizes where $N > 35$ the true frontier was faster to calculate than the SAA frontiers.

In our case study, we work on the problem of biomass cofiring for a utility company with coal plants in the states of North and South Carolina. Our numerical analysis show that by taking into account the footprint of the supply chain, including the suppliers activity, fuel transportation, and coal plants emissions, the total GHG emission reductions is in the range of 6 to 8% annually. Results show that there is not significant variation in emissions reduction for difference ranges of cofiring ratios. Especially, we observed that, higher biomass utilization rate (high ratio cofiring) does not guarantee a better environmental performance. This might be due to the fact that using more biomass is associated with higher transportation emissions and this counterbalances the reductions at coal plants. Regarding profitability, there were more variations for similar levels of GHG reductions which implies

a significant sensitivity on operational and logistic decisions. We showcased an example on how this model can be helpful to find the best strategies in response to Carbon cap and similar policies. By considering the goal of complying to a Carbon limit policy, we presented a set of Pareto optimal logistic and operational decisions that potentially lead to economic profits and another set of Pareto optimal solutions that lead to economic loss due to poorer logistic and operational decisions.

This research can be extended in several directions. One important subject of interest is analyzing the impacts of cofiring in conjunction with CCS technology (bio-CCS). Some preliminary studies show that bio-CCS may lead to negative emissions, but a comprehensive study of life cycle impacts throughout the supply chain, similar to what we did here, is necessary. Another extension of current research may involve the inclusion of an expanded and more complicated supply chain structure for biomass. Biomass feedstock may be imported from farther resources using different transportation modes, such as train, barge, or intermodal transportation. Our problem can also be modified to take into account more uncertainty elements such as random market prices, biomass availability or seasonality, and electricity demand.

Appendices

Appendix A Boundary Implications of Nonlinear Models in Chapter 2

Theorem 1: *I*n an optimal solution $X^* = \{X_1^*, X_2^*, \ldots, X_l^*\}$ to the single plant problem, at most one of the suppliers' is used partially. That means, $X_i^* = s_i$, $\forall i \in S^*/k$; $X_k^* = \gamma$; and $X_i^* = 0$ for $i \notin S^*$. Where, S^* is the set of suppliers selected in the optimal solution.

Proof:

Let's assume that the suppliers within set S are sorted in an increasing order of the size of variable unit costs $(c_i + c_i^{bm})$. Thus, $(c_1 + c_1^{bm}) \leq \ldots \leq (c_i + c_i^{bm}) \leq \ldots \leq (c_l + c_l^{bm})$, where, $l = |S|$. Let the unit profit be $\overline{c}_i = \left(\sigma^p + \sigma^t - c_i - c_i^{bm}\right)$. Thus, the unit profits are decreasing, and $\overline{c}_1 \geq \overline{c}_2, \ldots, \geq \overline{c}_l$.

Let's divide the interval $[0, 0.5]$ into k smaller subintervals as follows $[0, B_1], [B_1, B_2], ...[B_{k-1}, 0.5]$. The breakpoint B_1 represents what percentage of coal that could be displaced if all the biomass available at supplier 1 is being used by the plant. Next, B_2 represents the percentage of coal that can be displaced if biomass supply available at suppliers 1 and 2 was used; and so on. Without loss of generality, we assume that $l \geq k$.

Increasing the value of B impacts the amount of biomass used at the plant, thus, the right hand-side values of constraints (4.3) increase with B. Let $M_1, M_2, \ldots, M_k$ represents the amount of biomass required at $B_1, B_2, \ldots, B_k$. Indeed, $M_1 = s_1$ since we assumed that supplier 1 is being used to meet the demand for biomass as B increases from 0 to B_1; $M_2 = s_1 + s_2$; and so on.

For fixed values of B, we can also calculate corresponding investment costs using equations (4) and (5). Let $I_1, I_2, ...I_k$ be the investment costs at the corresponding breakpoints $B_1, B_2, \ldots, B_k$.

Let $\mathcal{Z}_1, \mathcal{Z}_2, \ldots, \mathcal{Z}_k$ denote the total cost for $B \in \{B_1, B_2, \ldots, B_k\}$. Therefore, $\mathcal{Z}_l = \sum_{i=1}^{l} \overline{c}_i X_i - I_l$ for $l = 1, \ldots, k$.

Theorem 1 implies that in an optimal solution the total amount of biomass used is

equal to: $M^* = \sum_{i=1}^{j} X_i^* = \sum_{i=1}^{j-1} s_i + \gamma$, and $\gamma \leq s_j, j \leq k$. We prove this by contradiction. Let's assume that $X^* = \{X_1^*, X_2^*, \ldots, X_f^*\}$ is an optimal solution to the single plant problem. This solution is such that more than one of the suppliers is used partially. That means: $X_1^* < s_1, X_2^* < s_2, \ldots, X_f^* < s_f$, and $\sum_{i=1}^{f} X_i^* = M^*$. Let I^* denote the corresponding investment costs. Since X^* is the optimal solution to this problem, then $\mathcal{Z}(X^*) \geq \mathcal{Z}(X)$ for any feasible X. Let $X = \{X_1, X_2, \ldots, X_j\}$ be a feasible solution such that: $X_1 = s_1, X_2 = s_2, \ldots, X_{j-1} = s_{j-1}, X_j = \gamma$; and $\sum_{i=1}^{j} X_i = M^*$. Since the total amount of biomass used in both solutions is the same, M^*, the corresponding investment costs are the same. In solution X all the suppliers are completely used, thus, $j < f$.

$$\mathcal{Z}(X^*) - \mathcal{Z}(X) = \left(\sum_{i=1}^{f} \overline{c}_i X_i^* - I^*\right) - \left(\sum_{i=1}^{j} \overline{c}_i X_i - I^*\right) = \sum_{i=1}^{f} \overline{c}_i X_i^* - \sum_{i=1}^{j-1} \overline{c}_i s_i - \overline{c}_j \gamma =$$

$$= \sum_{i=1}^{f} \overline{c}_i X_i^* - \sum_{i=1}^{j-1} \overline{c}_i X_i^* - \sum_{i=1}^{j-1} \overline{c}_i (s_i - X_i^*) - \overline{c}_j \gamma$$

$$= \sum_{i=j}^{f} \overline{c}_i X_i^* - \sum_{i=1}^{j-1} \overline{c}_i (s_i - X_i^*) - \overline{c}_j \gamma.$$

Since $\sum_{i=1}^{f} X_i^* = \sum_{i=1}^{j} X_i$, this is true: $\sum_{i=j}^{f} X_i^* = \sum_{i=1}^{j-1} (s_i - X_i^*) + \gamma$. Since $\overline{c}_1 \geq \overline{c}_2, \ldots \geq \overline{c}_j \ldots \geq \overline{c}_f$, the following holds true:

$$\mathcal{Z}(X^*) - \mathcal{Z}(X) = \sum_{i=j}^{f} \overline{c}_i X_i^* - \sum_{i=1}^{j-1} \overline{c}_i (s_i - X_i^*) - \overline{c}_j \gamma \leq \overline{c}_j \sum_{i=j}^{f} X_i^* - \overline{c}_j \sum_{i=1}^{j-1} (s_i - X_i^*) - \overline{c}_j \gamma = 0.$$

Therefore, $\mathcal{Z}(X^*) \leq \mathcal{Z}(X)$. This contradicts the assumption that $\mathcal{Z}(X^*)$ is an optimal solution for the single plant problem. Therefore, in an optimal solution at most one of the suppliers is used partially. ■

Theorem 2. *T*he special case of problem (**P**) -when there is a single plant in the supply chain- can be solved to optimality via an $O(|S|log(|S|))$ algorithm.

Proof:

Let's assume that the suppliers within set S are sorted in an increasing order of the size of variable unit costs $(c_i + c_i^{bm})$. Let's divide the interval $[0, 0.5]$ into k smaller subintervals $[0, B_1], [B_1, B_2], ...[B_{k-1}, 0.5]$ in a similar way as explained in Theorem 1. Without loss of generality, we assume that $\overline{c}_i > 0$ for $i = 1, \ldots, k$. We analyze the characteristics of the solution to (**P**) for $B \in [0, 0.04]$, $B \in [0.04, 0.221)$, and $B \in (0.221, 0.5]$.

Case 1: $B^* \in [0, 0.04]$.

Let (X^*, B^*, Y^*) denote a solution to the single plant case of problem (**P**). Since $B^* \leq 0.04$, then $Y^* = 1$. Let's assume that suppliers $1, \ldots, i$ were selected in the optimal solution. Thus, $B^* \in [B_{i-1}, B_i]$. Based on Theorem 1, and since constraints (22) are binding (Proposition **9**), the optimal objective function value is

$$\mathcal{Z}(B^*) = \sum_{j=1}^{i-1} \overline{c}_j s_j + \overline{c}_i \left(\frac{M^{coal} \rho^b B^*}{(1 - \alpha B^*)(\rho^b - 0.0044(B^*)^2 - 0.0055)} - \sum_{j=1}^{i-1} s_j \right) - I^{cap} \left(\frac{B^*}{1 - B^*} \right).$$

Let function

$$f_i^1(B) = \frac{\left(\overline{c}_i M^{coal} \rho^b\right) B}{(1 - \alpha B)(\rho^b - 0.0044 B^2 - 0.0055)}$$

and

$$f_i^2(B) = I^{cap} \left(\frac{B}{1 - B} \right).$$

Thus,

$$\mathcal{Z}(B^*) = \sum_{j=1}^{i-1} \overline{c}_j s_j - \overline{c}_i \sum_{j=1}^{i-1} s_j + f_i^1(B^*) - f_i^2(B^*) = \sum_{j=1}^{i-1} (\overline{c}_j - \overline{c}_i) s_j + f_i^1(B^*) - f_i^2(B^*).$$

Functions $f_i^1(B)$ and $f_i^2(B)$ are continuous functions of B for $B \in [B_{i-1}, B_i]$. Thus, the objective function $\mathcal{Z}(B)$ is also continuous on B (Stromberg 2015). Since $\mathcal{Z}(B)$ is the difference of two convex functions, we cannot conclude that it is concave, or, that it is convex. Let $\delta_i^1(B)$ denote the slope of function $f_i^1(B)$; and $\delta_i^2(B)$ denote the slope of

function $f_i^2(B)$. Since both functions are increasing, $\delta_i^1(B) > 0$ and $\delta_i^2(B) > 0$. The following cases could be encounter for $B \in [B_{i-1}, B_i]$.

(a) $\delta_i^1(B) > \delta_i^2(B)$: since the slope of $\mathcal{Z}(B) > 0$, $\mathcal{Z}(B)$ is increasing, thus, $B^* = B_i$.

(b) $\delta_i^1(B) < \delta_i^2(B)$: since the slope of $\mathcal{Z}(B) < 0$, $\mathcal{Z}(B)$ is decreasing, thus, $B^* = B_{i-1}$.

(c) $\delta_i^1(\overline{B}) = \delta_i^2(\overline{B})$ for some $\overline{B} \in [B_{i-1}, B_i]$: Since both $f_i^1(B)$ and $f_i^2(B)$ are strictly increasing in B, the slope of these lines could be equal in at most two points. Thus, $\mathcal{Z}(B)$ could be quasi-convex, or quasi-concave, or have one minimum and one maximum in $B \in [B_{i-1}, B_i]$. If $\mathcal{Z}(B)$ is quasi-convex, $B^* = \arg\max\{\mathcal{Z}(B_{i-1}), \mathcal{Z}(B_i)\}$. If $\mathcal{Z}(B)$ is quasi-concave, or have one minimum and one maximum, then, $B^* \in (B_{i-1}, B_i)$.

Case 2: $B^* \in [0.04, 0.221)$.

The optimal objective function value is

$$\mathcal{Z}_i(B^*) = \sum_{j=1}^{i-1} \overline{c}_j s_j + \overline{c}_i \left(\frac{M^{coal} \rho^b B^*}{(1-\alpha B^*)(\rho^b - 0.0044(B^*)^2 - 0.0055)} - \sum_{j=1}^{i-1} s_j \right)$$
$$- I^h \left(\frac{B^*}{1-B^*} \right)^{0.9554} - \left(I^s + I^{cd} \right) \left(\frac{B^*}{1-B^*} \right)^{0.5575}.$$

Let function

$$f_i^1(B) = \frac{\left(\overline{c}_i M^{coal} \rho^b\right) B}{(1-\alpha B)(\rho^b - 0.0044B^2 - 0.0055)} - \left(I^s + I^{cd} \right) \left(\frac{B}{1-B} \right)^{0.5575}$$

and

$$f_i^2(B) = I^h \left(\frac{B}{1-B} \right)^{0.9554}.$$

Thus,

$$\mathcal{Z}_i(B^*) = \sum_{j=1}^{i-1} (\overline{c}_j - \overline{c}_i) s_j + f_i^1(B^*) - f_i^2(B^*)$$

Functions $f_i^1(B)$ and $f_i^2(B)$ are continuous functions of B. Thus, the objective function $\mathcal{Z}(B)$ is also continuous on B (Stromberg 2015). Function $f_i^1(B)$ is convex since it is the difference of a convex and a concave function. However, we cannot say the same for function $\mathcal{Z}(B)$ since it is the difference of two convex function. Let $\delta_i^1(B)$ denote the slope of function $f_i^1(B)$; and $\delta_i^2(B)$ denote the slope of function $f_i^2(B)$. Since both functions are increasing, $\delta_i^1(B) > 0$ and $\delta_i^2(B) > 0$. The following cases could be encounter for $B \in [B_{i-1}, B_i]$.

(a) $\delta_i^1(B) > \delta_i^2(B)$: since the slope of $\mathcal{Z}(B) > 0$, $\mathcal{Z}(B)$ is increasing, thus, $B^* = B_i$.

(b) $\delta_i^1(B) < \delta_i^2(B)$: since the slope of $\mathcal{Z}(B) < 0$, $\mathcal{Z}(B)$ is decreasing, thus, $B^* = B_{i-1}$.

(c) $\delta_i^1(\overline{B}) = \delta_i^2(\overline{B})$ for some $\overline{B} \in [B_{i-1}, B_i]$: If $\mathcal{Z}(B)$ is quasi-convex, $B^* = \arg\max\{\mathcal{Z}(B_{i-1}), \mathcal{Z}(B_i)\}$. If $\mathcal{Z}(B)$ is quasi-concave, or have one minimum and one maximum, then, $B^* \in (B_{i-1}, B_i)$.

Case 3: $B \in (0.221, 0.5]$.

The optimal objective function value is

$$\mathcal{Z}_i(B^*) = \sum_{j=1}^{i-1} \overline{c}_j s_j + \overline{c}_i \left(\frac{M^{coal} \rho^b B^*}{(1 - \alpha B^*)(\rho^b - 0.0044(B^*)^2 - 0.0055)} - \sum_{j=1}^{i-1} s_j \right)$$

$$- I^h \left(\frac{B^*}{1 - B^*} \right)^{0.9554} - \left(I^s + I^{cd} \right) \left(\frac{B^*}{1 - B^*} \right)^{0.5575}.$$

Let function

$$f_i^1(B) = \frac{\left(\overline{c}_i M^{coal} \rho^b \right) B}{(1 - \alpha B)(\rho^b - 0.0044 B^2 - 0.0055)}$$

and

$$f_i^2(B) = I^h \left(\frac{B}{1 - B} \right)^{0.9554} + \left(I^s + I^{cd} \right) \left(\frac{B}{1 - B} \right)^{0.5575}.$$

Thus,

$$\mathcal{Z}_i(B^*) = \sum_{j=1}^{i-1}(\overline{c}_j - \overline{c}_i)s_j + f_i^1(B^*) - f_i^2(B^*)$$

Functions $f_i^1(B)$ and $f_i^2(B)$ are continuous functions of B. Thus, the objective function $\mathcal{Z}(B)$ is also continuous on B (Stromberg 2015). Function $f_i^2(B)$ is convex since it is the sum of two convex functions. We cannot conclude whether function $\mathcal{Z}(B)$ is concave or convex since it is the difference of two convex functions. Let $\delta_i^1(B)$ denote the slope of function $f_i^1(B)$; and $\delta_i^2(B)$ denote the slope of function $f_i^2(B)$. Since both functions are increasing, $\delta_i^1(B) > 0$ and $\delta_i^2(B) > 0$. The following cases could be encounter while solving $\mathcal{Z}_i(B)$.

(a) $\delta_i^1(B) > \delta_i^2(B)$: since the slope of $\mathcal{Z}(B) > 0$, $\mathcal{Z}(B)$ is increasing, thus, $B^* = B_i$.

(b) $\delta_i^1(B) < \delta_i^2(B)$: since the slope of $\mathcal{Z}(B) < 0$, $\mathcal{Z}(B)$ is decreasing, thus, $B^* = B_{i-1}$.

(c) $\delta_i^1(\overline{B}) = \delta_i^2(\overline{B})$ for some $\overline{B} \in [B_{i-1}, B_i]$: If $\mathcal{Z}(B)$ is quasi-convex, $B^* = \arg\max\{\mathcal{Z}(B_{i-1}), \mathcal{Z}(B_i)\}$. If $\mathcal{Z}(B)$ is quasi-concave, or have one minimum and one maximum, then, $B^* \in (B_{i-1}, B_i)$.

Implications of the results from Cases 1-3.

Based on Theorem 1, at most one supplier will be used partially in an optimal solution. Additionally, we did sort the suppliers in a decreasing order of their unit profit $\overline{c}$. That means, if suppliers $1, \ldots, j$ are selected in an optimal solution, supplier j (the last supplier selected) is the only one that could have been used partially. To find an optimal solution to the problem we need to compare the objective function values for each $B \in \{B_1, \ldots, B_l\}$.

■

Proposition 1: *A feasible solution to problem (***Q***) is feasible to the non-linear problem (***P***); and the objective function value of (***Q***) is a lower bound for problem (***P***).*

Proof: This is true due to the way we constructed model (**Q**). We built model (**Q**) by discretizing the continuous variable B_j. L is the set of the co-firing strategies that are

Table 4: A polynomial time algorithm for the single plant problem.

Step 1: Initialize: $S^* = \emptyset$; $B^* = 0$; $M_i = B_i = I_i = 0$ for $i = 1, \ldots, k$, $k \leq |S|$. $l = 1$

Step 2: Let $B^1 = 0.04, B^2 = 0.221, B^3 = 0.5$.

Step 3: **Sort** $s_i \in S$ in an ascending order of unit profit $\overline{c}_i$.

Step 4: **For** $i = 1, \ldots, k$:

Let $M_i = M_{i-1} + s_i$

Calculate B_i using equation (2)

Calculate $\mathcal{Z}(B_i)$

End For i

Step 5: **For** $p = 1, \ldots 3$:

For $i = l, \ldots k$:

If $\mathcal{Z}(B_i) > 0$

If $\mathcal{Z}(B_i) > \mathcal{Z}(B_{i-1})$ and $B_i \leq B^p$ then

$S^* = S^* \bigcup i$

$\phi = i$

Else

Find $B^{p*} \in [B_{i-1}, B_i]$ using Golden Search Algorithm

If $B^{p*} > B_{i-1}$, then $S^* = S^* \bigcup i$, $\phi = i$

End If

End If

End For i

$l = \phi$

End For p

$B^* = \arg\max\{\mathcal{Z}(B^{1*}), \mathcal{Z}(B^{2*}), \mathcal{Z}(B^{3*})\}$

Step 6: Report the optimal solution:

B^*

For $i = 1, \ldots, |S^*| - 1$, let $X_i^* = s_i$.

Let $j = |S^*|$. Calculate X_j^*.

If $B^* \leq 0.04$ then $Y^* = 1$, **Else**, $Y^* = 0$.

investigated, thus, it includes some, but clearly not all the potential values that B_j could take.

Let $\Xi(\mathbf{Q})$ be the set of solutions to problem $(\mathbf{Q})$, and $\Xi(\mathbf{P})$ be the set of solutions to problem $(\mathbf{P})$. Let $(X_{ij}^Q, Y_{lj}^Q) \in \Xi(Q)$ be a feasible solution to problem $(\mathbf{Q})$. We can use

this solution to derive a feasible solution for problem (**P**) in the following way.

$$X_{ij}^{P} = X_{ij}^{Q} \text{ for } i \in I, j \in C \tag{15}$$

$$B_{j}^{P} = \sum_{l \in L} L_l * Y_{lj}^{Q} for j \in C \tag{16}$$

$$Y_{j}^{P} = \begin{cases} 1 & \text{if } \sum_{l \in L} L_l * Y_{lj}^{Q} \leq 0.04 \\ 0 & \text{otherwise.} \end{cases} \tag{17}$$

Since (X_{ij}^{Q}, Y_{lj}^{Q}), a feasible solution to (**Q**), can be used to derive a feasible solution for (**P**); it can easily be verified that the corresponding objective function value of (**Q**) is a lower bound for (**P**). ■

Theorem 3: *As* $|L|$ approaches infinity, an optimal solution to (**Q**) is optimal to (**P**) with probability 1.

Proof: An optimal solution to problem (**Q**) could be transformed to a feasible solution for (**P**) using equations (15) to (17). Let, $\mathcal{Z}^{Q*}$ be the corresponding objective function value of (**Q**), and $\mathcal{Z}^{P}$ be the corresponding objective function value of (**P**). By construction, these two objective function values are equal. Next, we show that, under certain conditions, an optimal solution to (**P**) can be transformed to a feasible solution to (**Q**). Let $(X_{ij}^{P*}, B_{j}^{P*}, Y_{j}^{P*})$ be the optimal solution to problem (**P**).

CASE 1: $|L|$ is finite.

If $B_{j}^{P*} \in L$, then, we can derive a feasible solution for (**Q**) using the following equations.

$$X_{ij}^{Q} = X_{ij}^{P*} \text{ for } i \in I, j \in C \tag{18}$$

$$Y_{lj}^{Q} = \begin{cases} 1 & \text{if } B_{j}^{P*} = L_l \\ 0 & \text{otherwise} \end{cases} \quad \text{for } j \in C. \tag{19}$$

However, given that B_{j}^{P*} is a continuous variable, and L is a finite set, the probability that B_{j}^{P*} is represented in L is equal to zero.

If $B_j^{P*} \notin L$, then, we cannot derive an solution to model (**Q**) using a solution to (**P**).

CASE 2: $|L|$ is infinite.

In this case, $\lim_{|L|\to\inf} P(B_j^{P*} \in L) = 1$. This implies that, given an optimal solution to (**P**) we can derive a feasible solution to (**Q**) using equations (18) and (19). Let, $\mathcal{Z}^{P*}$ be the corresponding objective function value of (**P**), and $\mathcal{Z}^{Q}$ be the corresponding objective function value of (**Q**). These two objective function values are equal. By Proposition **1** and optimality theory, we have: $\mathcal{Z}^{P} \leq \mathcal{Z}^{P*} = \mathcal{Z}^{Q} \leq \mathcal{Z}^{Q*}$ and $\mathcal{Z}^{P*} \geq \mathcal{Z}^{Q}$. This implies that $\mathcal{Z}^{P*} = \mathcal{Z}^{Q*}$.

To summarize, as $|L| \to$ inf the optimal solutions to models (**Q**) and (**P**) are equal with probability 1. ■

Proposition 2:

$$B_j \leq \frac{1}{M_j^{coal}} \sum_{i \in S} X_{ij} \leq f_j \leq (B_j + \overline{a}_j) \qquad \forall j \in C.$$

Where, $\overline{a}_j = \frac{0.5\left(\rho_j^b - (1-0.5\alpha_j)(\rho_j^b - 0.0066)\right)}{(1-0.5\alpha_j)(\rho_j^b - 0.0066)}$.

Proof: Function f_j has the following properties: $f_j = 0$ if $B_j = 0$ and $f_j > B_j$ for $B_j > 0$. This is due to the way we construct f_j. If B_j represents the percentage of coal being substituted in plant j (by mass), then, f_j transforms this percentage into an equivalent percentage of biomass needed to enable this substitution. Thus, the linear function $\overline{f}_j = B_j$ is an inner approximation of f_j. Indeed, $\overline{f}_j$ underestimates f_j for $B_j \in (0, 0.5]$.

Function f_j is an increasing function of B_j. Thus the difference $f_j - B_j$ reaches its maximum when $B_j = 0.5$. This maximum difference is $\overline{a}_j$. To summarize,

$$f_j = 0 \quad \text{if} \quad B_j = 0$$

$$f_j = B_j + \overline{\alpha}_j \quad \text{if} \quad B_j = 0.5$$

$$B_j < f_j < B_j + \overline{\alpha}_j \quad \text{if} \quad 0 < B_j < 0.5.$$

■

Proposition 4: Function $f(B_j) = \frac{B_j}{(1-B_j)}$ is increasing in B_j, for $0 \leq B_j \leq 1$.

Proof: To proof this we show that for any $\epsilon > 0$, such that, $B_j + \epsilon < 1$, the following holds true $f(B_j + \epsilon) - f(B_j) \geq 0$.

Therefore,

$$f(B_j + \epsilon) - f(B_j) = \frac{B_j + \epsilon}{(1 - (B_j + \epsilon))} - \frac{B_j}{(1 - B_j)} = \frac{(B_j + \epsilon)(1 - B_j) - B_j(1 - (B_j + \epsilon))}{(1 - (B_j + \epsilon))(1 - B_j)} =$$

$$= \frac{B_j - B_j^2 + \epsilon - \epsilon B_j - B_j + B_j^2 + \epsilon B_j}{(1 - (B_j + \epsilon))(1 - B_j)} = \frac{\epsilon}{(1 - (B_j + \epsilon))(1 - B_j)} > 0.$$

■

Proposition 5: Functions $f(B_j) = \left(\frac{B_j}{1-B_j)}\right)^{0.5575}$ and $f(B_j) = \left(\frac{B_j}{1-B_j}\right)^{0.9554}$ are increasing in B_j, for $0 \leq B_j \leq 1$.

Proof: Via proposition **4** we show that $\frac{B_j}{1-B_j}$ is increasing in B_j. For $B_j \in [0, 0.5]$, $\frac{B_j}{1-B_j}$ takes values in $[0, 1]$. Therefore, $\frac{B_j}{1-B_j}$ in some power l $(0 < l < 1)$ is also an increasing function of B_j. ■

Proposition 6: Functions $f(B_j) = \left(\frac{B_j}{1-B_j)}\right)$ is strongly convex for $0 \leq B \leq 0.5$.

Proof: We prove this by investigating the second derivative of this function with respect to B_j.

$$\frac{df(B_j)}{dB_j} = \frac{1}{(1 - B_j)^2},$$

and

$$\frac{d^2 f(B_j)}{dB_j^2} = \frac{2}{(1 - B_j)^3}.$$

Clearly, $\frac{d^2 f(B_j)}{dB_j^2} \geq 2$ for $0 \leq B \leq 0.5$. Therefore, functions $f(B_j) = \left(\frac{B_j}{1-B_j)}\right)$ is strongly convex. ■

Proposition 7: Functions $f(B_j) = \left(\frac{B_j}{1-B_j)}\right)^{0.9554}$ is strictly convex for $0.04 \leq B \leq 0.5$.

Proof: We prove this by showing that the second derivative of this function with respect

to B_j is greater than zero for $0.04 \leq B \leq 0.5$.

$$\frac{df(B_j)}{dB_j} = \frac{0.9554}{(1-B_j)^2(\frac{B_j}{1-B_j})^{0.0446}},$$

and

$$\frac{d^2f(B_j)}{dB_j^2} = \frac{\frac{1.9108(1-B_j)}{\left(\frac{B_j}{1-B_j}\right)^{0.0446}} - \frac{0.0426108}{\left(\frac{B_j}{1-B_j}\right)^{1.0446}}}{(1-B_j)^4}.$$

For $0.04 \leq B \leq 0.5$, function $(1-B_j)^4 \geq 0$. Additionally, for $0.04 \leq B \leq 0.5$, the difference

$$\frac{1.9108(1-B_j)}{\left(\frac{B_j}{1-B_j}\right)^{0.0446}} - \frac{0.0426108}{\left(\frac{B_j}{1-B_j}\right)^{1.0446}} > 0.$$

Therefore, functions $f(B_j) = \left(\frac{B_j}{1-B_j)}\right)^{0.9554}$ is strictly convex for $0.04 \leq B \leq 0.5$. ■

Proposition 8: Functions $f(B_j) = \left(\frac{B_j}{1-B_j)}\right)^{0.5575}$ is strictly concave for $0.04 \leq B < 0.221$ and strictly convex for $0.221 < B \leq 0.5$.

Proof: We prove this by showing that the second derivative of this function with respect to B_j is less than zero for for $0.04 \leq B < 0.221$; and greater than zero for $0.221 < B \leq 0.5$.

$$\frac{d^2f(B_j)}{dB_j^2} = \frac{0.5575\left(\frac{2}{(1-B_j)^2} + \frac{2B_j}{(1-B_j)^3}\right)}{\left(\frac{B_j}{1-B_j}\right)^{0.4425}} - \frac{0.246694\left(\frac{1}{1-B_j} + \frac{B_j}{(1-B_j)^2}\right)^2}{\left(\frac{B_j}{1-B_j}\right)^{1.4425}}$$

The second derivative takes negative values for $0.04 < B_j < 0.221$ and takes positive values for $0.221 < B_j \leq 0.5$.

Therefore, functions $f(B_j) = \left(\frac{B_j}{1-B_j)}\right)^{0.5575}$ is strictly concave for $0.04 \leq B \leq 0.221$ and is strictly convex for $0.221 < B \leq 0.5$. ■

Proposition 9: In an optimal solution to model (**P**), constraints (4.3) are binding.

Proof: We prove this by contradiction.

Let (X^*, Y^*, B^*) be an optimal solution of (**P**). Let I^* denote the corresponding investment costs, and let S^* denote the set of suppliers selected. The optimal objective function value is $\mathcal{Z}^P(X^*, Y^*, B^*) = \sum_{i \in S^*} \overline{c}_i X_i^* - I^*$.

Let's assume that constraints (4.3) are not binding at (X^*, Y^*, B^*). Therefore,

$$\sum_{i \in S^*} X_i^* < \frac{(M^{coal} * \rho^b)}{(1/B^* - \alpha)(\rho^b - 0.0044(B^*)^2 - 0.0055)}.$$

Let (X, Y, B) be a feasible solution of (**P**). We create this solution by starting at (X^*, Y^*, B^*) and decreasing the value of B^* by $\epsilon > 0$ so that constraints (4.3) become binding.

Let's now calculate:

$$\mathcal{Z}^P(X^*, Y^*, B^*) - \mathcal{Z}^P(X, Y, B) = \left(\sum_{i \in S^*} \overline{c}_i X_i^* - I^* \right) - \left(\sum_{i \in S^*} \overline{c}_i X_i^* - I \right) = I - I^* \leq 0.$$

As shown in Propositions **4** and **5**, the investment cost functions do increase with B. Since $B < B^*$, then, $I < I^*$. Therefore,

$$\mathcal{Z}^P(X^*, Y^*, B^*) < \mathcal{Z}^P(X, Y, B).$$

This contradicts the initial assumption that (X^*, Y^*, B^*) be an optimal solution of (**P**). Therefore, at an optimal solution constraints (4.3) are binding.

■

Proposition 10: Function $f(B_j) = \frac{\rho_j^b B_j}{(1-\alpha_j B_j)(\rho_j^b - 0.0044 B_j^2 - 0.0055)}$ is strongly convex for $0 \leq B_j \leq 0.5$, $0 \leq \alpha_j \leq 1$, and $\rho_j^b > 0.0066$.

Proof: We prove this by showing that the second derivative of this function with respect to B_j is greater than zero for $0 \leq B_j \leq 0.5$, $0 \leq \alpha_j \leq 1$, and $\rho_j^b > 0$. The second derivative is:

$$\frac{d^2 f(B_j)}{dB_j^2} = \frac{0.00015488\rho_j^b B_j^3}{(1-\alpha_j B_j)(-0.0055+\rho_j^b-0.0044B_j^2)^3} + \frac{0.0088\rho_j^b B_j}{(1-\alpha_j B_j)(-0.0055+\rho_j^b-0.0044B_j^2)^2} =$$

$$= \frac{0.0088\rho_j^b B_j}{(1-\alpha_j B_j)(-0.0055+\rho_j^b-0.0044B_j^2)^2}\left(1+\frac{0.0176B_j^2}{(-0.0055+\rho_j^b-0.0044B_j^2)}\right)$$

For $0 \leq \alpha_j \leq 1$ and $\rho_j^b > 0$, the following holds true: $\left(\frac{0.0088\rho_j^b B_j}{(1-\alpha_j B_j)(-0.0055+\rho_j^b-0.0044B_j^2)^2}\right) > 0$.

Expression $\left(1+\frac{0.0176B_j^2}{(-0.0055+\rho_j^b-0.0044B_j^2)}\right) > 0$ if $(-0.0055+\rho_j^b-0.0044B_j^2) > 0$.

The minimum value that expression $(-0.0055+\rho_j^b-0.0044B_j^2)$ can take is when $\rho_j^b = 0$ and $B_j = 0.5$. In this case, the value of this expression is -0.0066. If $\rho_j^b > 0.0066$, then, $\frac{d^2 f(B_j)}{dB_j^2} > 0$ and function $f(B_j) = \frac{\rho_j^b B_j}{(1-\alpha_j B_j)(\rho_j^b-0.0044B_j^2-0.0055)}$ is strictly convex. ■

Step 1: Initialize λ, UB, n, u, ξ, ϵ, N

Step 2: Let $LB = \mathcal{Z}^Q(X, Y)$

Step 3: Solve subproblems $(\text{SP})_j$ for $j \in C$

Step 4: Compute the upper bound:

$$UB^n = \sum_{j \in J} \mathcal{Z}_j^{SP}(X, Y, B) + \sum_{i \in S} s_i \lambda_i$$

If $UB^n > UB$, then

$UB = UB^n$

$\epsilon = \frac{UB^n - LB}{LB}$

End If

Let $n = n + 1$

Step 5: **If** $\epsilon \leq 0.01$**, then STOP**

ELSE

Let $u^n = \frac{\xi^n (UB - LB)}{\sum_{i \in S} (s_i - \sum_j X_{ij}^n)^2}$

Let $\lambda_i^n = \lambda_i^{n-1} + u^n (s_i - \sum_j X_{ij})$

Step 6: **If** $n > N$, then, **STOP**

ELSE go to **Step 3**

Figure 12: Lagrangean relaxation algorithm

Appendix B Computational Performance and Problem Structure of Models in Chapter 3

B.1 Computational Performance

We model the MIBP problem (MP) in GAMS 23.7 and solve the problem using BONMIN and COUENNE solver packages. We model the corresponding MIP reformulation, model (LMP), in AMPL 20141128 and solve it using GUROBI 6.5.0. The computations are done in a Dell personal computer with Intel(R) Core(TM) $i5-4300U$ CPU 2.50 GHz processor, and with 8.00 GB of RAM.

The performance measures used for models (MP) and (LMP) are presented in Table 5. This table summarizes the size of the problems solved, the running time in CPU seconds, and the optimality gap reported by each solver. Each problem corresponds to one of the states in the southeastern U.S. The last problem set (SE), corresponds to the whole Southeast. Two stopping criteria apply: (i) CPU running time of no more than 4,000 seconds, and (ii) relative optimality gap of no more than e^{-06}. The results from Table 5 indicate

Table 5: The performance of the solution approaches proposed

		Model (MP)						Model (LMP)			
	Nr. of	Number of		BONMIN		COUENNE		Number of		Gurobi	
Problem	Plants	Variables	Constraints	CPU	Gap	CPU	Gap	Variables	Constraints	CPU	Gap
AL	11	4,000	2,211	13	$4.06e^{-01}$	124	e^{-06}	4,411	8,813	0.4	e^{-06}
AR	4	352	804	6	$1.00e^{-06}$	40	e^{-06}	1,604	3,206	0.2	e^{-06}
FL	15	4,000	3,015	17	$3.76e^{-01}$	309	e^{-06}	6,015	12,017	0.9	e^{-06}
GA	12	2,965	2,814	16	$1.00e^{-06}$	253	e^{-06}	5,614	11,216	0.3	e^{-06}
LA	4	4,000	804	6	$8.19e^{-01}$	29	e^{-06}	1,604	3,206	0.8	e^{-06}
MS	5	4,000	1,005	7	$4.66e^{-01}$	51	e^{-06}	2,005	4,007	0.3	e^{-06}
NC	23	1,531	5,025	27	$5.00e^{-06}$	157	e^{-06}	10,025	20,027	0.4	e^{-06}
SC	16	4,000	3,216	18	$8.79e^{-01}$	925	e^{-06}	6,416	12,818	0.4	e^{-06}
TN	9	4,000	2,010	12	$4.92e^{-01}$	138	e^{-06}	4,010	8,012	0.3	e^{-06}
SE	99	4,000	20,904	106	$5.00e^{-03}$	4,000	$8e^{-03}$	41,704	83,306	2.5	e^{-06}

that using McCormick relaxation leads to finding the optimal solution for all problems in less than 3 CPU seconds, an approach which is much more efficient than using off-the-shelf nonlinear solvers. Additionally, for the majority of the problems solved, BONMIN stopped because it reached the maximum running time without providing the optimal solution.

B.2 Note on Capacity-based Schemes

Note on the increased biomass utilization under capacity-based schemes. The results of Tables 2. and 3. indicate that capacity-based schemes lead to higher levels of biomass utilization than with the ratio-based schemes, in most cases. This increased use of biomass seems counterintuitive since, under the ratio-based schemes, plants that adopt higher cofiring ratios have the opportunity to receive higher incentives and may, we hypothesize, use more biomass overall because of the optimization models structure. This phenomenon can be illustrated with an example of a single power plant model. Model (UB) for a single plant can be represented as follows:

$$\max : \alpha^1 TB - \alpha^2 B \tag{20a}$$

s.t.

$$\sum_{j \in \mathcal{C}} \alpha^3 B \leq b, \tag{20b}$$

$$\alpha^1 TB \leq g, \tag{20c}$$

$$T \in [t^{min}, t^{max}], \tag{20d}$$

$$B \in [0, 0.5]. \tag{20e}$$

Using the 2-level capacity-based and ratio-based schemes explained in Section 6.1., also assume two plants, with capacities 400MW and 2229MW, respectively, falling under the first and second levels of capacity ranges in the 2-level capacity-based scheme. Figure (13) illustrates the feasible region of the model (20) under these schemes and for the two plants. The marked point on each graph represents the optimal solution for the corresponding model. For the smaller plant, T is allowed to chose amounts greater than \$10.01 (Section 6.1.) under the capacity-based scheme, which allows the optimal points for both schemes to be the same values. However, for larger-sized plant, under the capacity-based scheme, T is only allowed to chose amounts less than \$10 and this provides a larger feasibility range for B. Consequently, the optimal point under the ratio-based model results in a smaller

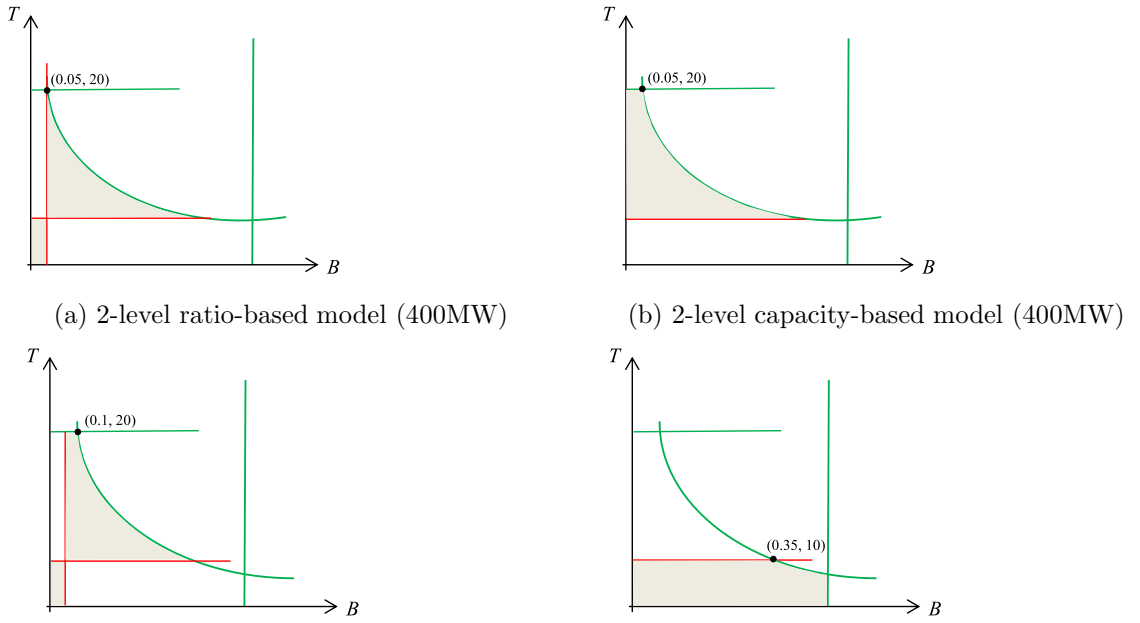

(a) 2-level ratio-based model (400MW)

(b) 2-level capacity-based model (400MW)

(c) 2-level ratio-based model (2229MW)

(d) 2-level capacity-based model (2229MW)

Figure 13: Feasible regions and optimal points for two plants under PTC scheme models

value for cofiring ratio. Therefore, a capacity-based model leads to greater B^* than the ratio-based model, despite the fact that ratio-based model provides greater incentive for high-ratio biomass cofiring.

B.3 Saving Functions

Proposition 1. Proof: The utilitarian approach identifies a PTC rate for each plant that maximizes system-wide profits, accounting for the existing limitations on budget (g) and the biomass supply in the region (b). Note that, for each plant j, T_j can take values within $[t^{min}, t^{max}]$. The proposed ratio-based scheme adds additional constraints to the model. These constraints limit PTC to taking values within smaller subintervals which are all contained within $[t^{min}, t^{max}]$. These additional limitations reduce the size of the feasible region for model (RS). Thus, its objective function value is a lower bound for model (UL). ■

Tax saving function. Each plant $j \in \mathcal{C}$ is characterized by its installed capacity N_j, the plant's capacity factor F_j, and the annual operating hours O_j. These characteristics define the amount of energy (in MWh) generated annually at a plant. The amount of energy, denoted with E_j, is function of N_j, F_j, O_j. Given these plants characteristics the amount of energy generated at a plant is equal to $E_j = N_j * F_j * O_j$. Then, if plant j is to cofire at a ratio of B_j, the amount of renewable energy generated would equal to $E_j * B_j$. Note that, the lower heating values for coal and biomass are not the same. If H^b represents the lower heating value of biomass (in kWh per ton), then the amount of biomass required annually (in tons) to displace coal equals

$$M_j^b(B_j) = \frac{B_j * E_j}{10^{-3} * H^b}. \tag{21}$$

Finally, if T_j represent the amount of PTC received by coal-fired power plant j, the annual saving due to PTC equals

$$S_j^t(T_j, B_j) = T_j * H^b * M_j(B_j).$$

Appendix C A Convergence Analysis of Biobjective Chance Constrained Programs

Let's assume the multiobjective model BCCMIP introduced in Chapter 4 can be relaxed as the simplified model below

$$\begin{aligned} (Q) \qquad & min\ (f_1(x), f_2(x)) \\ & P\left(\mathtt{E}(x,h) \leq 0\right) \geq 1-\gamma, \\ & x \in \mathcal{X}, \end{aligned}$$

where $f_1, f_2 : \mathbb{R}^n \to \mathbb{R}$ are continuous real-valued functions, the energy function $\mathtt{E}(x,h)$ consists of the continuous variable $x \in \mathbb{R}^n$, and random variable h defined on the probability space (Ω, Σ, P). $\mathcal{X}$ is a compact feasibility set defined by problem conditions, and $\gamma \in (0,1]$ is the reliability level priory fixed by the Decision Maker. In what follows we present a proof of the conjecture that *the sequence of SAA_N efficient frontiers converge to the True efficient frontier as $N \to \infty$ with probability **1**.*

We provide the proof based on constrained-objective scalarization of (Q). The ϵ-constraint problems $L_i(\epsilon)$, $i = 1, 2$ for the original problem (Q) are defined as

$$\begin{aligned} L_i(\epsilon) \qquad & min f_i(x) \\ & p(x) \leq \gamma, \\ & f_j(x) \leq \epsilon_j, \qquad\qquad j = 1,2, j \neq i \\ & x \in \mathcal{X}, \end{aligned}$$

where $p(x) = P\left(\mathtt{E}(x,h) \leq 0\right)$ and ϵ_1, ϵ_2 are upper bounds on the values of the objective functions $f_1(x)$ and $f_2(x)$.

We can apply the SAA approach to define approximate ϵ-constraint problems $\widehat{L}_{iN}(\epsilon)$,

$i = 1, 2$ as

$$\begin{aligned} \widehat{L}_{iN}(\epsilon) \qquad & min f_i(x) \\ & \hat{p}_N(x) \leq \gamma, \\ & f_j(x) \leq \epsilon_j, \qquad\qquad\qquad j = 1, 2, j \neq i \\ & x \in \mathcal{X}, \end{aligned}$$

where $\hat{p}_N(x) = \frac{1}{N} \sum_{s=1}^{N} \mathbb{1}_{(0,\infty)}(\mathtt{E}(x, h^s))$.

Definition 1. A sequence of extended real valued functions $f_k(x)$ is said to epi-converge to a function $f(x)$, written as $f_k \xrightarrow{e} f$, if for any x the following conditions hold:

(i) for any sequence x_k converging to x,

$$\liminf_{k\to\infty} f_k(x_k) \geq f(x)$$

(ii) there exists a sequence x_k converging to x such that

$$\limsup_{k\to\infty} f_k(x_k) \leq f(x)$$

Note that epi-convergence can be interpreted as a one-sided version of uniform convergence.

Definition 2. A function $f : X \to \mathbb{R}$ is lower semicontinuous if for every $\alpha \in \mathbb{R}$ the set $\{x \in X : f(x) > \alpha\}$ is an open set. If f is lower semicontinuous at x_0 we have that $\liminf_{x\to x_0} f(x) \geq f(x_0)$.

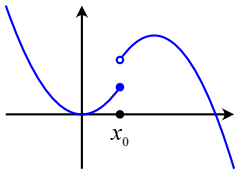

Figure 14: A lower semicontinuous function

Proposition 1.1 Pagnoncelli et al. (2009) If $\mathtt{E}(x, h)$ is a Carathéodory function

(i.e. h is measurable and x continuous), then $p(x)$ and $\hat{p}_N(x)$ are lower semicontinuous and $\hat{p}_N \xrightarrow{e} p$. **Proof.** Refer to Pagnoncelli et al. (2009).

Assumption 1.1 The problem $L_1(\epsilon)$ has an optimal solution x^* such that for any $\delta > 0$, there is $x \in \mathcal{X}$ with $\|x - x^*\| \leq \delta$, $p(x) \leq \gamma$, and $f_2(x) \leq \epsilon_2$.

In the other words, we assume the existence of a sequence $\{x_k\}$ of feasible points for problem $L_1(\epsilon)$ that converge to the an optimal solution x^*.

Proposition 1.2. Suppose $\mathtt{E}(x, h)$ is a Carathéodory function and $f_1(x)$ is a continuous function. Let Z^* and $\hat{Z}_N^*$ be the optimal objective function values for $L_1(\epsilon)$ and $\widehat{L_{1N}}(\epsilon)$ respectively. Then $\hat{Z}_N^* \to Z^*$ with probability 1 as $N \to \infty$.

Proof. From proposition 1.1. $\hat{p}_N(x)$ epi-converges to $p(x)$ $w.p.1$. Based on Assumption 1.1. problem $L_1(\epsilon)$ has optimal solution and there is $x \in \mathcal{X}$ such that $p(x) \leq \gamma$ and $f_2(x) \leq \epsilon_2$. Therefore $\hat{p}_N(x) \leq \gamma$ and problem $\widehat{L_{iN}}(\epsilon)$ has feasible solution $w.p.1$ for N large enough. By compactness of $\mathcal{X}$, bounded constraint $f_2(x) \leq \epsilon_2$, and lower semicontinuity of $\hat{p}_N(x)$, the feasible region of $\widehat{L_{1N}}(\epsilon)$ is compact; thus, $\widehat{L_{1N}}(\epsilon)$ has optimal solution $w.p.1$ for N large enough.

Now let us choose a feasible solution x for $\widehat{L_{1N}}(\epsilon)$ which is arbitrary close to x^*. Obviously $f_1(x) \geq \hat{Z}_N^*$. From Assumption 1.1. for any $\delta \geq 0$ we have $\|x - x^*\| \leq \delta$ and since $f_1(x)$ is continuous:

$$\limsup_{N \to \infty} \hat{Z}_N^* \leq f_1(x^*) = Z^* \qquad w.p.1 \tag{22}$$

Let $\hat{x}_N^*$ be the optimal solution to $\widehat{L_{1N}}(\epsilon)$, i.e. $\hat{x}_N^* \in \mathcal{X}$, $\hat{p}_N(\hat{x}_N^*) \leq \gamma$, $f_2(\hat{x}_N^*) \leq \epsilon_2$, and $\hat{Z}_N^* = f_1(\hat{x}_N^*)$. Both x^* and $\hat{x}_N^*$ belong to compact $\mathcal{X}$ so it is safe to assume $\hat{x}_N^*$ converges to x^* $w.p.1$, and since $\hat{p}_N \xrightarrow{e} p$ for any $x \in \mathcal{X}$ then

$$\liminf_{N \to \infty} \hat{p}_N(\hat{x}_N^*) \geq p(x^*) \qquad w.p.1 \tag{23}$$

Note that x^* is a feasible solution of $L_1(\epsilon)$, thus $p(x^*) \leq \gamma$, $f_2(x^*) \leq \epsilon_2$, and $f_1(x^*) \geq Z^*$.

It follows from (23) that

$$\liminf_{N\to\infty} f_1(\hat{x}_N^*) \geq Z^* \qquad w.p.1 \tag{24}$$

Finally, from (22) and (24) we conclude that $\hat{Z}_N^* \to Z^*$ and the proof is complete. ■

In above proposition we show the convergence of optimal objective function value of ϵ-constraint problem $\widehat{L_{1N}}(\epsilon)$ to that of problem $L_1(\epsilon)$. Similarly, same result can be shown for the optimal objective function values of the problems $L_2(\epsilon)$ and $\widehat{L_{2N}}(\epsilon)$ as $N \to \infty$. Next, we show how it is possible to find Pareto optimal solutions to problem (Q) via ϵ-constraint problems.

Definition 3. For a given point x^*, we use the symbols $L_i(\epsilon^*)$ and $\widehat{L}_{iN}(\epsilon^*)$, $i = 1, 2$, to represent the problems $L_i(\epsilon)$ and $\widehat{L}_{iN}(\epsilon)$, $i = 1, 2$, respectively, such that $\epsilon_j = \epsilon_j^* = f_j(x^*)$ for $j = 1, 2$ and $j \neq i$.

Theorem 1.1. Assume $x^* \in \mathbb{R}^n$ is a feasible solution to the biobjective problem (Q). As $N \to \infty$ the approximate problems $\widehat{L}_{iN}(\epsilon)$, $i = 1, 2$, will result in a true Pareto optimal solution x^* $w.p.1$, if and only if x^* is an optimal solution to $\widehat{L}_{iN}(\epsilon^*)$, $i = 1, 2$.

Proof. In Proposition 2.2. we showed that, as $N \to \infty$, the optimal objective function value of every problem $\widehat{L}_{iN}(\epsilon)$, $i = 1, 2$, converges to the optimal objective function value of corresponding problem $L_i(\epsilon)$, $i = 1, 2$, $w.p.1$. Consequently, for any optimizer x^* of $L_i(\epsilon)$, $i = 1$ or 2, there exists a sequence of optimizers $\{\hat{x}_N^*\}$ for $\widehat{L}_{iN}(\epsilon)$, $i = 1$ or 2 that converge x^* $w.p.1$. Now we outline the necessary and sufficient conditions for x^* to be a Pareto optimal solution to (Q), i.e. a true Pareto optimal solution.

Necessity: Let x^* be a Pareto optimal solution to problem (Q), then it is an optimizer to problems $\widehat{L}_{iN}(\epsilon^*)$, $i = 1, 2$. Let us assume that x^* does not solve at least one of the problems $\widehat{L}_{iN}(\epsilon^*)$, $i = 1$ or 2, optimally. Say $\widehat{L_{1N}}(\epsilon^*)$. Then there exists a feasible solution x such that $f_1(x) < f_1(x^*)$ and $f_2(x) \leq f_2(x^*)$ (constraint of $\widehat{L_{1N}}(\epsilon^*)$ based on Definition 3). This contradicts the Pareto optimality of x^* for (Q). In other words, x^* has to optimally solve any problem $\widehat{L}_{iN}(\epsilon^*)$, $i = 1, 2$.

Sufficiency: If x^* is an optimizer for problems $\widehat{L}_{iN}(\epsilon^*)$, $i = 1, 2$, then it is a Pareto

optimal solution for (Q). x^* is a feasible solution for (Q) by assumption. Since x^* is also an optimal solution to problems $\widehat{L}_{iN}(\epsilon^*)$, $i = 1, 2$, there is no other feasible solution x such that $f_1(x) < f_1(x^*)$ (for $\widehat{L_{1N}}(\epsilon^*)$) and $f_2(x) < f_2(x^*)$ (for $\widehat{L_{2N}}(\epsilon^*)$). This is the definition of Pareto optimality for x^*. ■

Based on the necessary and sufficient conditions outlined above, it is possible to find every true Pareto optimal solution to the problem (Q) via $\widehat{L}_{iN}(\epsilon^*)$, $i = 1, 2$ for N large enough. Therefore the proposed conjecture is true under mild assumptions. The experimental results reported on Chapter 4. support the conjecture as well (see Figure 15 below). Intuitively, since $\hat{p}_N \xrightarrow{e} p$ (convergence from below), seems that the resulted approximate frontiers also have a convergence from below towards the True frontier.

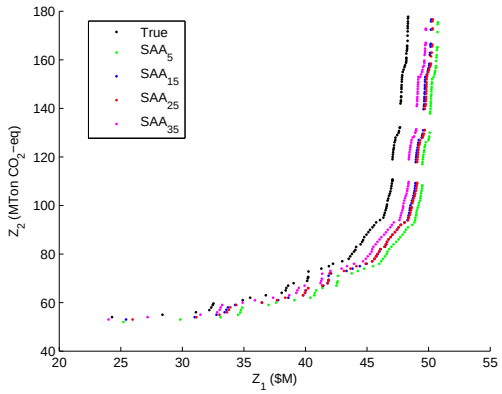

Figure 15: The convergence of SAA frontiers to True frontier in `BCCMIP`

Appendix D Life Cycle Assessment for the Environmental Objective Function

Basic assumptions

- Two categories of sustainable biomass considered for the study: forest management residues and wood processing residues.
- We do not take into account the environmental impacts due to direct and indirect land use change (forest residues and urban wood waste have marginal land use change impacts).
- We assume that the CO_2 uptake during the biomass growth is equal to the amount that is emitted during the combustion at the power plant (biogenic carbon is not tracked in the analysis).
- GHG emissions due to transmission of power from plants to final users were not included in the analysis.
- We assume if the biomass is not utilized for cofiring and remains in the environment, the CH_4 emissions related to natural biodegradation would contribute to the life cycle GHG emissions.

Raw materials acquisition

Extracting coal from the ground is the first phase of the fossil fuel life cycle. Mining and cleaning are the main processes to prepare coal to be transported to power plants. The emissions at this stage are mainly due to diesel emissions from mining and preparation equipment and methane (CH_4) emissions from the mine. The GHG estimations for coal mining are mainly adopted from Spath et al. (1999) and the Argonne National Laboratory's GREET (Greenhouse gases, Regulated Emissions, and Energy use in Transportation) model. We consider the two main types of coal, bituminous and subbituminous, as each of

the coal plants under the study uses either of the these types as their primary fuel. The subbituminous coal is relatively pure and can be prepared for transportation by removing large impurities and crushing it into smaller size pieces. The bituminous coal generally requires a jig washing process to separate heavier impurities Spath et al. (1999). The preparation of urban wood waste for cofiring is initially involved with the collection of waste, transferring to a depot, and crushing the matter into small pieces (wood chips). After transporting the wood chips to power plants, extra processes may be applied to make biomass a compatible fuel for combustion in PC boilers (e.g. drying or compression). We will consider the impact of these processes in the third phase. The collection of forest residues mainly done by skidders which gather the residues and pile them in a landing site. The average energy use for the collection of forest residues using medium sized grapple skidders is reported as 83.8 MBtu/dry Ton in Boardman et al. (2014). In the landing depot, branches and barks are removed from trees using a stroke-boom delimber or iron gate for larger trees. The delimbed trees are then loaded into a chipper. The energy use for debarking/delimbing and chipping using conventional methods are assumed to be 116.4 MBtu/dry Ton and 105.8 MBtu/dry Ton respectively (based on the report in Boardman et al. (2014)). The primary GHG impact of preprocessing phase arise from the use of diesel equipment and trucks. The carbon intensity of diesel fuel is assumed to be 95 kg CO_2-eq/MMBtu (Skone and Gerdes 2008).

Fuel transportation

We use the information provided in Boardman et al. (2014) to take into account the emissions due to coal transportation. In this model, it is assumed that 10% of coal is transported on a barge over 330 miles and the other 90% of coal is transported by train over 440 miles (Wang 2008). The amount of required coal for a year depends on the heating value of coal, plant characteristics, and cofiring strategy. It is assumed that biomass feedstock (in form of wood chips) is transported by diesel trucks from supplier facilities to coal plants. Based on the GHG conversion factors provided by UK's Department for Environment, Food

& Rural Affairs (DEFRA), the average emission rate of transporting wood is 0.275 kg CO_2-eq/Ton-mile (DEFRA 2016). Work by Bauer et al. (2010) evaluates the relationships that exist among vehicle fuel consumption, CO_2 emissions, and vehicle load for transporting different biomass feedstock. The specific parameter values for biomass transportation were obtained and validated using Argonne Greet Model (Wang 2008) and the U.S. Life Cycle Inventory Database. The geographical distance from suppliers to plants are calculated based on the great-circle distance method.

Electricity generation

In this phase of the life cycle we consider all of the processes typically carried out at a coal-fired power plant including those related to biomass fuel preparation and handling. The coal plants of interest use the pulverized coal (PC) boilers for fuel combustion. The majority of existing US coal plants use PC boilers, and this type of boiler can handle higher ratios of biomass cofiring (Tillman et al. 2010). The US Environmental Protection Agency (EPA) provides the environmental characteristics of current electricity generation utilities in the Emission & Generation Resource Integrated Database (eGRID). We use eGRID to find the annual GHG emission rates of the coal plants under study. eGrid provides the data for annual CO_2 equivalent output emission rates (kg CO_2-eq/MWh) for existing power plants in US. Using the efficiency factor and heat input of the primary fuel used at each plant we can estimate the output emission per ton of coal used $M_{coal} = \frac{1MWh}{\eta_0 LHV_{coal}}$. Regarding the avoided emissions, according to Mann and Spath (2001) The total CO_2 and methane avoided per ton of biomass are 1.117 ton 0.065 ton respectively (using global warming potential of greenhouse gases relative to CO_2 it adds up to $1.117 + 25 * 0.065 = 2.742$ ton CO_2-eq per ton of biomass avoided. However, in determining the net greenhouse gas emission balance for this system, it is important to recognize that not all of the emissions and avoided emissions will occur at the same time. While CO_2 will be emitted at the power plant as soon as biomass is fired, the release of CO_2 and methane from mulch, and particularly from landfills, will be delayed. Because it is exposed to the elements, the time

frame for complete decomposition of mulch would likely be on the order of just few years, and is reported to occur at a rate of 10% per year (Harmon et al. (1996)).

GREET® life cycle analysis tool (2015) is the main tool we used for LCA. A sample output for one of the plants with 763MW capacity which uses pulverized coal boilers and bituminous coal as the primary fuel is presented in Table 6.

Table 6: A sample GREET® LCA impact results

Activity	Description	GHG impact factor
Raw material acquisition		
Bituminous coal	Mining - cleaning	59.9 kg CO_2-eq/Ton
Forest residues	Collection (skidding) - debarking - chipping	29.1 kg CO_2-eq/Ton
Urban wood waste	Collection - chipping	18.4 kg CO_2-eq/Ton
Transportation		
Biomass	Truck (100%), depending on supplier location	0.27 kg CO_2-eq/Ton-mile
Coal	Barge (10%, 330 miles), rail (90%, 440 miles)	18.27 kg CO_2-eq/Ton
Energy conversion facility		
Handling	Unloading, dust collection, and cleaning	4.00 kg CO_2-eq/Ton
Drying	Using natural gas (0.07kgCO_2/MJ intensity)	65.95 kg CO_2-eq/Ton
Storage	Loading-unloading equipment	0.85 kg CO_2-eq/Ton
Co-combustion	Assuming the carbon neutrality of biomass	3041.6 kg CO_2-eq/Ton

Bibliography

Abdelaziz, Fouad Ben. 2012. Solution approaches for the multiobjective stochastic programming. *European Journal of Operational Research* **216**(1) 1–16.

Adams, W. P., H. D. Sherali. 1993. Mixed-integer bilinear programming problems. *Mathematical Programming* **59**(1-3) 279–305.

Aden, A., M. Ruth, K. Ibsen, J. Jechura, K. Neeves, J. Sheehan, B. Wallace, L. Montague, A. Slayton, J. Lukas. 2002. Lignocellulosic biomass to ethanol process design and economics utilizing co-current dilute acid prehydrolysis and enzymatic hydrolysis for corn stover. NREL/TP-510-32438, Golden Co: National Renewable Energy Laboratory.

Ağpak, Kürşad, Hadi Gökçen. 2007. A chance-constrained approach to stochastic line balancing problem. *European Journal of Operational Research* **180**(3) 1098–1115.

Aguilar, F.X., M.E. Goerndt, N. Song, S. Shifley. 2012. Internal, external and location factors influencing cofiring of biomass with coal in the us northern region. *Energy Economics* **34**(6) 1790–1798.

Al-Mansour, Fouad, Jaroslaw Zuwala. 2010. An evaluation of biomass co-firing in europe. *Biomass & Bioenergy* **34**(5) 620–629.

Alizamir, S., F. de Véricourt, P. Sun. 2016. Efficient feed-in-tariff policies for renewable energy technologies. *Operations Research* **64**(1) 52–66.

An, H., W. E. Wilhelm, S. W. Searcy. 2011. A mathematical model to design a lignocellulosic biofuel supply chain system with a case study based on a region in central Texas. *Bioresource Technology* **102** 7860–7870.

Atasu, A., B. Toktay, W. M. Yeo, C. Zhang. 2016. Effective medical surplus recovery. *Production and Operations Management* doi:10.1111/poms.12641.

Azapagic, Adisa, R Clift. 1999. Life cycle assessment and multiobjective optimisation. *Journal of Cleaner Production* **7**(2) 135–143.

Ba, Birome Holo, Christian Prins, Caroline Prodhon. 2016. Models for optimization and performance evaluation of biomass supply chains: An operations research perspective. *Renewable Energy* **87** 977–989.

Basua, P., J. Butler, M.A. Leona. 2011. Biomass co-fring options on the emission reduction and electricity generation costs in coal-fired power plants. *Renewable Energy* **36**(1) 282–288.

Bauer, J., T. Bektas, T. G. Crainic. 2010. Minimizing greenhouse gas emissions in intermodal freight transport: an application to rail service design. *Journal of the Operational Research Society* **61**(3) 531–542.

Baxter, Larry. 2005. Biomass-coal co-combustion: opportunity for affordable renewable energy. *Fuel* **84**(10) 1295–1302.

Bertsimas, D., V. F. Farias, N. Trichakis. 2011. The price of fairness. *Operations Research* **59**(1) 17–31.

Bertsimas, D., V. F. Farias, N. Trichakis. 2012. On the efficiency-fairness trade-off. *Management Science* **58**(12) 2234–2250.

Bilsel, R Ufuk, A Ravindran. 2011. A multiobjective chance constrained programming model for supplier selection under uncertainty. *Transportation Research Part B: Methodological* **45**(8) 1284–1300.

Bloomberg New Energy Finance. 2015. New energy outlook 2015: long-term projections of the global energy sector. http://www.seia.org/sites/default/files/resources/BNEF-NEO2015_Executive-summary.pdf (accessed May 2015).

Boardman, Richard D, Kara G Cafferty, Corrie Nichol, Erin M Searcy, Tyler Westover, Richard Wood, Mark D Bearden, James E Cabe, Corinne Drennan, Susanne B Jones, et al. 2014. Logistics, costs, and ghg impacts of utility scale cofiring with 20% biomass. Tech. rep., Pacific Northwest National Laboratory (PNNL), Richland, WA (US).

Boekhoudt, Andre, Lars Behrendt. 2015. *Taxes and incentives for renewable energy*. International Cooperative KPMG.

Cambero, Claudia, Taraneh Sowlati. 2014. Assessment and optimization of forest biomass supply chains from economic, social and environmental perspectives–a review of literature. *Renewable and Sustainable Energy Reviews* **36** 62–73.

Cambero, Claudia, Taraneh Sowlati, Mihai Pavel. 2016. Economic and life cycle environmental optimization of forest-based biorefinery supply chains for bioenergy and biofuel production. *Chemical Engineering Research and Design* **107** 218–235.

Campbell, JE, DB Lobell, CB Field. 2009. Greater transportation energy and ghg offsets from bioelectricity than ethanol. *Science* **324**(5930) 1055–1057.

Caney, S. 2009. Justice and the distribution of greenhouse gas emissions. *Journal of Global Ethics* **5**(2) 125–146.

Caputo, A.C., M. Palumbo, P.M. Pelagagge, F. Scacchia. 2005. Economics of biomass energy utilization in combustion and gasification plants: effects of logistic variables. *Biomass and Bioenergy* **28** 35–51.

Change, IPCC Climate. 2014. Mitigation of climate change. contribution of working group iii to the fifth assessment report of the intergovernmental panel on climate change. *Cambridge University Press, Cambridge, UK and New York, NY* .

Changkong, Vira, Yacov Y Haimes. 1983. Multiobjective decision making: Theory and methodology. *North-Holland Series in System Science and Engineering*, vol. 8. Elsevier Science Publishing Co New York NY.

Charnes, Abraham, William W Cooper. 1959. Chance-constrained programming. *Management science* **6**(1) 73–79.

Chen, Chien-Wei, Yueyue Fan. 2012. Bioethanol supply chain system planning under supply and demand uncertainties. *Transportation Research Part E: Logistics and Transportation Review* **48**(1) 150–164.

Cherubini, Francesco, Neil D Bird, Annette Cowie, Gerfried Jungmeier, Bernhard Schlamadinger, Susanne Woess-Gallasch. 2009. Energy-and greenhouse gas-based lca of biofuel and bioenergy systems: Key issues, ranges and recommendations. *Resources, conservation and recycling* **53**(8) 434–447.

Cinar, Didem, Panos M Pardalos, Steffen Rebennack. 2015. Evaluating supply chain design models for the integration of biomass co-firing in existing coal plants under uncertainty. *Handbook of Bioenergy*. Springer, 191–217.

COP21. 2015. *United Nations Climate Change Conference*. Paris, France.

Couture, T. D., K. Cory, C. Kreycik, E. Williams. 2010. Policymaker's guide to feed-in tariff policy design. Tech. rep., National Renewable Energy Laboratory (NREL), Golden, CO.

Crawford, P. B. 1998. Analyzing fairness principles in tax policy: A pragmatic approach. *Denv. UL Rev.* **76** 155.

Croucher, Matt, Ant Evans, Tim James, Jessica Raasch. 2010. *Market-Based Incentives*. Seidman Research Institute. WP Carey School of Business.

Čuček, Lidija, Jiří Jaromír Klemeš, P Varbanov, Zdravko Kravanja. 2011. Life cycle assessment and multi-criteria optimization of regional biomass and bioenergy supply chains. *Chemical Engineering Transactions* **25** 575–580.

Čuček, Lidija, Petar Sabev Varbanov, Jiří Jaromír Klemeš, Zdravko Kravanja. 2012. Total footprints-based multi-criteria optimisation of regional biomass energy supply chains. *Energy* **44**(1) 135–145.

Cuellar, Amanda Dulcinea. 2012. Plant power: The cost of using biomass for power generation and potential for decreased greenhouse gas emissions. Ph.D. thesis, Massachusetts Institute of Technology.

Cui, T. H., J. S Raju, Z. J. Zhang. 2007. Fairness and channel coordination. *Management Science* **53**(8) 1303–1314.

Dai, Q., Y. Li, Q. Xie, L. Liang. 2014. Allocating tradable emissions permits based on the proportional allocation concept to achieve a low-carbon economy. *Mathematical Problems in Engineering* **2014**.

Dasappa, S, PJ Paul, HS Mukunda, NKS Rajan, G Sridhar, HV Sridhar. 2004. Biomass gasification technology-a route to meet energy needs. *Current Science* **87**(7) 908–916.

De, S., M. Assadi. 2009. Impact of cofiring biomass with coal in power plants: A techno-economic assessment. *Biomass and Bioenergy* **33** 283–293.

De Meyer, Annelies, Dirk Cattrysse, Jussi Rasinmäki, Jos Van Orshoven. 2014. Methods to optimise the design and management of biomass-for-bioenergy supply chains: A review. *Renewable and sustainable energy reviews* **31** 657–670.

DEBCO. 2013. Demonstration of large scale biomass co firing and supply chain integration. FP7 Project.

Dias, Luis C, Carolina Passeira, João Malça, Fausto Freire. 2016. Integrating life-cycle assessment and multi-criteria decision analysis to compare alternative biodiesel chains. *Annals of Operations Research* 1–16doi:10.1007/s10479-016-2329-7.

Dong, C., Y. Yang, R. Yang, J. Zhang. 2010. Numerical modeling of the gasification based biomass co-firing in a 600mw pulverized coal boiler. *Applied Energy* **87**(9) 2834–2838.

Dong, N. 2012. Support mechanisms for cofiring secondary fuels. *IEA Clean Coal Centre, London, UK* .

Drake, D. F., P. R. Kleindorfer, L. N. Van Wassenhove. 2016. Technology choice and capacity portfolios under emissions regulation. *Production and Operations Management* **25**(6) 1006–1025.

Ehrgott, Matthias. 2013. *Multicriteria optimization*, vol. 491. Springer Science & Business Media.

EIA. 2011. Form eia-860: Annual electric generator report.

EIA. 2013a. Annual energy outlook 2013 URL http://www.eia.gov/forecasts/aeo/MT-electric.cfm#solar-photo.

EIA. 2013b. Annual energy outlook: Energy markets summary. *http://www.eia.gov/forecasts/steo/tables/pdf/1tab.pdf, accessed 2.08.13* .

EIA. 2013c. Most states have renewable portfolio standards. *http://www.eia.gov/todayinenergy/detail.cfm?id= 4850, accessed 26.07.13* .

EIA. 2014. Annual energy outlook 2014. URL http://www.eia.gov/forecasts/aeo/MT_emissions.cfm.

Eksioglu, S. D., A. Acharya, L. E. Leightley, S. Arora. 2009. Analyzing the design and management of biomass-to-biorefinery supply chain. *Computers & Industrial Engineering* **57** 1342–1352.

Ekşioğlu, S. D., H. Karimi, B. Ekşioğlu. 2016. Optimization models to integrate production and transportation planning for biomass co-firing in coal-fired power plants. *IIE Transactions* **48**(10) 901–920.

Ekşioğlu, S. D., S. Rebennack, P. M. Pardalos, eds. 2015. *Handbook of Bioenergy: Bioenergy Supply Chain - Models and Applications*. Springer Publishers.

Ekşioğlu, Sandra D, Ambarish Acharya, Liam E Leightley, Sumesh Arora. 2009. Analyzing the design and management of biomass-to-biorefinery supply chain. *Computers & Industrial Engineering* **57**(4) 1342–1352.

EPA. 2009. Future climate change. URL http://www.epa.gov/climatechange/science/future.html.

EPA. 2013. Environmental protection agency proposes carbon pollution standards for new power plants / agency takes important step to reduce carbon pollution from power plants as part of president obama's climate action plan. *http://yosemite.epa.gov/opa/admpress.nsf/0/da9640577ceacd9f85257beb006cb2b6!OpenDocument* .

Fernando, R. 2005. *Fuels For Biomass Cofiring*. IEA Coal Research, Clean Coal Centre.

Fernando, R. 2012. Cofiring high ratios of biomass with coal. *IEA Clean Coal Centre* .

Fischer, Carolyn, Richard G Newell. 2008. Environmental and technology policies for climate mitigation. *Journal of environmental economics and management* **55**(2) 142–162.

Fouquet, D., T. B. Johansson. 2008. European renewable energy policy at crossroads -focus on electricity support mechanisms. *Energy Policy* **36**(11) 4079–4092.

Garcia, A., J. M. Alzate, J. Barrera. 2012. Regulatory design and incentives for renewable energy. *Journal of Regulatory Economics* **41**(3) 315–336.

Gebreslassie, Berhane H, Yuan Yao, Fengqi You. 2012. Multiobjective optimization of hydrocarbon biorefinery supply chain designs under uncertainty. *Decision and Control (CDC), 2012 IEEE 51st Annual Conference on*. IEEE, 5560–5565.

GHG Protocol. 2011. The Greenhouse Gas Protocol: A Corporate Accounting and Reporting Standard. Standard, World Business Council for Sustainable Development (WBCSD) and the World Resources Institute (WRI).

Goerndt, M.E., F.X. Aguilar, K. Skog. 2013a. Drivers of biomass co-firing in U.S. coal-fired power plants. *Biomass & Bioenergy* **58** 158–167.

Goerndt, M.E., F.X. Aguilar, K. Skog. 2013b. Resource potential for renewable energy generation from co-firing of woody biomass with coal in the northern U.S. *Biomass and Bioenergy* **59** 348–361.

Goulder, L. H., A. R. Schein. 2013. Carbon taxes versus cap and trade: a critical review. *Climate Change Economics* **4**(03) 1350010.

Gui, L., A. Atasu, Ö. Ergun, L. B. Toktay. 2015. Efficient implementation of collective extended producer responsibility legislation. *Management Science* **62**(4) 1098–1123.

Gutjahr, Walter J, Alois Pichler. 2016. Stochastic multi-objective optimization: a survey on non-scalarizing methods. *Annals of Operations Research* **236**(2) 475–499.

Hansson, Julia, Göran Berndes, Filip Johnsson, Jan Kjärstad. 2009. Co-firing biomass with coal for electricity generation?an assessment of the potential in eu27. *Energy Policy* **37**(4) 1444–1455.

Harmon, Mark E, Janice M Harmon, William K Ferrell, David Brooks. 1996. Modeling carbon stores in oregon and washington forest products: 1900–1992. *Climatic Change* **33**(4) 521–550.

Heijungs, Reinout, Jeroen B Guinée, Gjalt Huppes, Raymond M Lankreijer, Helias A Udo de Haes, Anneke Wegener Sleeswijk, AMM Ansems, PG Eggels, R van Duin, HP De Goede, et al. 1992. Environmental life cycle assessment of products: guide and backgrounds (part 1) .

Heller, Martin C, Gregory A Keoleian, Timothy A Volk. 2003. Life cycle assessment of a willow bioenergy cropping system. *Biomass and Bioenergy* **25**(2) 147–165.

Huang, Y., C. W. Chen, Y. Fan. 2010. Multistage optimization of the supply chains of biofuels. *Transportation Research Part E* **46**(6) 820–830.

IEA. 2012. Carbon-dioxide emissions from fuel combustion: highlights. http://www.iea.org/co2highlights/co2highlights.pdf.

IEA Bioenergy Task-32. 2017. Database of biomass cofiring initiatives. http://task32.ieabioenergy.com/database-biomass-cofiring-initiatives/ (accessed July 2017).

IEA-ETSAP and IRENA. 2013. Technology Brief E21: Biomass Cofiring. https://www.irena.org (accessed May 2015).

Intergovernmental Panel on Climate Change (IPCC). 2008. 2006 IPCC Guidelines for National Greenhouse Gas Inventories. B. Metz, O.R. Davidson, P.R. Bosch, R. Dave, L.A. Meyer, eds., *A primer, Prepared by the National Greenhouse Gas Inventories Programme*. IGES, Japan.

ISO, ISO14040. 2006. 14040: Environmental management–life cycle assessment–principles and framework. *London: British Standards Institution* .

Kalinina, Maria, Leif Olsson, Aron Larsson. 2013. A multi objective chance constrained programming model for intermodal logistics with uncertain time. *International Journal of Computer Science Issues* **10**(6) 35–44.

Kangas, Hanna-Liisa, Jussi Lintunen, Jussi Uusivuori. 2009. The cofiring problem of a power plant under policy regulations. *Energy policy* **37**(5) 1898–1904.

Karimi, H., S. D. Ekşioğlu, A. Khademi. 2017. Analyzing tax incentives for producing renewable energy by biomass cofiring. *IIE Transactions* .

Kataoka, Shinji. 1963. A stochastic programming model. *Econometrica: Journal of the Econometric Society* 181–196.

Katoh, N., A. Shioura, T. Ibaraki. 2013. Resource allocation problems. *Handbook of Combinatorial Optimization*. Springer, 2897–2988.

KDF. Accessed 12.10.2013. Knowledge discovery framework. us department of energy. *https://bioenergykdf.net* .

Kelly, F. P., A. K. Maulloo, D. KH. Tan. 1998. Rate control for communication networks: Shadow prices, proportional fairness and stability. *Journal of the Operational Research society* **49**(3) 237–252.

Khorshidi, Zakieh, Minh T Ho, Dianne E Wiley. 2014. The impact of biomass quality and quantity on the performance and economics of co-firing plants with and without co_2 capture. *International Journal of Greenhouse Gas Control* **21** 191–202.

Kim, Jinkyung, Matthew J Realff, Jay H Lee. 2011. Optimal design and global sensitivity analysis of biomass supply chain networks for biofuels under uncertainty. *Computers & Chemical Engineering* **35**(9) 1738–1751.

Kim, K-K., Chi-Guhn L. 2012. Evaluation and optimization of feed-in tariffs. *Energy policy* **49** 192–203.

Kim, Sujin, Jong-hyun Ryu. 2011. The sample average approximation method for multi-objective stochastic optimization. *Proceedings of the Winter Simulation Conference*. Winter Simulation Conference, 4026–4037.

Koppejan, J., S. Van Loo. 2012. *The handbook of biomass combustion and co-firing*. Routledge.

Krass, D., T. Nedorezov, A. Ovchinnikov. 2013. Environmental taxes and the choice of green technology. *Production and Operations Management* **22**(5) 1035–1055.

Kroes, J., R. Subramanian, R. Subramanyam. 2012. Operational compliance levers, environmental performance, and firm performance under cap and trade regulation. *Manufacturing & Service Operations Management* **14**(2) 186–201.

Kumar, A., J. B. Cameron, P. C. Flynn. 2005. Pipeline transport and simultaneously saccharification of corn stover. *Bioresource Technology* **96**(7) 819–829.

Kumar, A., J. Kleinberg. 2006. Fairness measures for resource allocation. *SIAM Journal on Computing* **36**(3) 657–680.

Li, J., A. Brzdekiewicz, W. Yang, W. Blasiak. 2012. Co-firing based on biomass torrefaction in a pulverized coal boiler with aim of 100 percent fuel switching. *Applied Energy* **99** 344–354.

Lintunen, Jussi, Hanna-Liisa Kangas. 2010. The case of co-firing: The market level effects of subsidizing biomass co-combustion. *Energy Economics* **32**(3) 694–701.

Luedtke, James, Shabbir Ahmed. 2008. A sample approximation approach for optimization with probabilistic constraints. *SIAM Journal on Optimization* **19**(2) 674–699.

Luenberger, David G, Yinyu Ye. 2008. Linear and nonlinear programming. international series in operations research & management science. *Springer, Berlin.* **10** 978–0.

Luo, Y., S. Miller. 2013. A game theory analysis of market incentives for US switchgrass ethanol. *Ecological Economics* **93** 42–56.

Luss, H. 1999. On equitable resource allocation problems: a lexicographic minimax approach. *Operations Research* **47**(3) 361–378.

Mahmudi, H., P. Flynn. 2006. Rail vs. truck transport of biomass. *Applied Biochemistry and Biotechnology* **129**(1) 88–103.

Mann, Maggie, P Spath. 2001. A life cycle assessment of biomass cofiring in a coal-fired power plant. *Clean Products and Processes* **3**(2) 81–91.

Marufuzzaman, M., S.D. Eksioglu, Y. Huang. 2014. Two-stage stochastic programming supply chain model for biodiesel production via wastewater treatment. *Computers & Operations Research* **49** 1–17.

Mas-Colell, A., M. D. Whinston, J. Green. 1995. *Microeconomic Theory*, vol. 1. Oxford University Press, New York.

McCormick, G. P. 1976. Computability of global solutions to factorable nonconvex programs: Part I: Convex underestimating problems. *Mathematical Programming* **10**(1) 147–175.

McCoy, J. H., H. L. Lee. 2014. Using fairness models to improve equity in health delivery fleet management. *Production and Operations Management* **23**(6) 965–977.

McIlveen-Wright, DR, Ye Huang, S Rezvani, Jayanta Deb Mondol, David Redpath, Mark Anderson, NJ Hewitt, BC Williams. 2011. A techno-economic assessment of the reduction of carbon dioxide emissions through the use of biomass co-combustion. *Fuel* **90**(1) 11–18.

Mehmood, S., B. Reddy, M.A. Rosen. 2014. Exergy analysis of a biomass co-firing based pulverized coal power generation system. *International Journal of Green Energy, Available on-line* .

Memişoğlu, Gökhan, Halit Üster. 2015. Integrated bioenergy supply chain network planning problem. *Transportation Science* **50**(1) 35–56.

Menanteau, P., D. Finon, M-L. Lamy. 2003. Prices versus quantities: choosing policies for promoting the development of renewable energy. *Energy Policy* **31**(8) 799–812.

Moiseyev, A., B. Solberg, A. M. I. Kallio. 2014. The impact of subsidies and Carbon pricing on the wood biomass use for energy in the EU. *Energy* **76** 161–167.

Montgomery, James. May 2015. Biomass in the us: Finding our carrot and stick. *http://www.renewableenergyworld.com/articles/2013/04/biomass-in-the-us-finding-our-carrot-and-stick.html* .

Muench, Stefan, Edeltraud Guenther. 2013. A systematic review of bioenergy life cycle assessments. *Applied Energy* **112** 257–273.

Nemhauser, G. L., L. A. Wolsey. 1988. *Integer and combinatorial optimization*. John Wiley & Sons, Inc.

Nicholls, David L, Stephen E Patterson, Erin Uloth. 2006. *Wood and coal cofiring in interior Alaska: Utilizing woody biomass from wildland defensible-space fire treatments and other sources*, vol. 551. US Department of Agriculture, Forest Service, Pacific Northwest Research Station.

O'Mahoney, Amy, Fiona Thorne, Eleanor Denny. 2013. A cost-benefit analysis of generating electricity from biomass. *Energy Policy* **57** 347–354.

Pagnoncelli, BK, Shabbir Ahmed, A Shapiro. 2009. Sample average approximation method for chance constrained programming: theory and applications. *Journal of optimization theory and applications* **142**(2) 399–416.

Paudel, B. 2013. Feasibility and co-benefits of biomass co-firing: Case in Utah. *Utah State University, Logan, Utah, M.Sc. Dissertation* .

Perlack, R. D., A. T. Turhollow. 2002. Assessment of options for the collection, handling and transportation of corn stover. Available from: http://www.ornl.gov/~webworks/cppr/y2001/rpt/113127.pdf.

Petrolia, D. R. 2008. The economics of harvesting and transporting corn stover for conversion to fuel ethanol: a case study for Minnesota. *Biomass and Bioenergy* **32**(7) 603–612.

Piriou, B, G Vaitilingom, B Veyssière, B Cuq, X Rouau. 2013. Potential direct use of solid biomass in internal combustion engines. *Progress in Energy and Combustion Science* **39**(1) 169–188.

Rabl, Ari, Anthony Benoist, Dominique Dron, Bruno Peuportier, Joseph V Spadaro, Assaad Zoughaib. 2007. How to account for CO_2 emissions from biomass in an LCA. *The International Journal of Life Cycle Assessment* **12**(5) 281–281.

Radunović, B., J-Y. le Boudec. 2007. A unified framework for max-min and min-max fairness with applications. *IEEE/ACM Transactions on Networking (TON)* **15**(5) 1073–1083.

Ragwitz, M., A. Held, G. Resch, T. Faber, R. Haas, C. Huber, R. Coenraads, M. Voogt, G. Reece, S. G. Jensen P. E. Morthorst, I. Konstantinaviciute, B. Heyder. 2007. Assessment and optimisation of renewable energy support schemes in the European electricity market. https://ec.europa.eu/energy/intelligent/projects/en/projects/optres (accessed May 2016).

Rawls, J. 1971. A theory of justice. *Harvard University Press* .

Roni, Md., S. Eksioglu, E. Searcy, K. Jha. 2014. A supply chain network design model for biomass co-firing in coal-fired power plants. *Transportation Research Part E: Logistics and Transportation Review* **61** 115–134.

Ruhul-Kabir, M., A. Kumar. 2012. Comparison of the energy and environmental performances of nine biomass/coal co-firing pathways. *Bioresource Technology* **124** 394–405.

Santibanez-Aguilar, Jose Ezequiel, J Betzabe González-Campos, José María Ponce-Ortega, Medardo Serna-González, Mahmoud M El-Halwagi. 2011. Optimal planning of a biomass conversion system considering economic and environmental aspects. *Industrial & Engineering Chemistry Research* **50**(14) 8558–8570.

Searcy, E., P. Flynn, E. Ghafoori, A. Kumar. 2007. The relative cost of biomass energy transport. *Applied Biochemistry and Biotechnology* **137** 639–652.

Sebastián, F, J Royo, M Gómez. 2011. Cofiring versus biomass-fired power plants: Ghg (greenhouse gases) emissions savings comparison by means of lca (life cycle assessment) methodology. *Energy* **36**(4) 2029–2037.

Sen, A. K., J. E. Foster. 1997. On Economic Inequality. *Oxford: Clarendon Press.(1979), The Welfare Basis of Real Income Comparisons: A Survey, Journal of Economic Literature* **17**(1) 1–45.

Shao, Yuanyuan, Jinsheng Wang, Fernando Preto, Jesse Zhu, Chunbao Charles Xu. 2012. Ash deposition in biomass combustion or co-firing for power/heat generation. *Energies* **5**(12) 5171–5189.

Sharma, B., R.G. Ingalls, C.L. Jones, A. Khanchi. 2013. Biomass supply chain design and analysis: Basis, overview, modeling, challenges, and future. *Renewable and Sustainable Energy Reviews* **24** 608–627.

Shrimali, G., E. Baker. 2012. Optimal feed-in tariff schedules. *IEEE Transactions on Engineering Management* **59**(2) 310–322.

Skone, Timothy J, Kristin Gerdes. 2008. Development of baseline data and analysis of life cycle greenhouse gas emissions of petroleum-based fuels. *National Energy Technology Laboratory* **310**.

Smith, Irene M, Katerina Rousaki. 2002. *Prospects for co-utilisation of coal with other fuels-GHG emissions reduction*. IEA Coal Research, Clean Coal Centre.

Solomon, S., D. Qin, M. Manning, Z. Chen, M. Marquis, K.B. Averyt, M. Tignor, H.L. Miller. 2007. *Climate Change 2007: The Physical Science Basis. Contribution of Working Group I to the Fourth Assessment Report of the Intergovernmental Panel on Climate Change*. Cambridge University Press, Cambridge, United Kingdom and New York, NY, USA.

Sondreal, E.A., S.A. Benson, J.P. Hurley, M.D. Mann, J.H. Pavlish, M.L. Swanson. 2001. Review of advances in combustion technology and biomass cofiring. *Fuel Process Technology* **71** 7–38.

Spath, PL, MK Mann, DR Kerr. 1999. Life cycle assessment of coal-fired power production. Tech. rep., National Renewable Energy Lab. (No. NREL/TP-570-25119), Golden, CO (US).

Steer, J., R. Marsh, A. Griffiths, A. Malmgren, G. Riley. 2013. Biomass co-firing trials on a down-fired utility boiler. *Energy Conversion and Management* **66** 285–294.

Stromberg, Karl R. 2015. *An introduction to classical real analysis*, vol. 376. American Mathematical Soc.

Tchapda, Aime Hilaire, Sarma V Pisupati. 2014. A review of thermal co-conversion of coal and biomass/waste. *Energies* **7**(3) 1098–1148.

Tharakan, Pradeep J, Timothy A Volk, Christopher A Lindsey, Lawrence P Abrahamson, Edwin H White. 2005. Evaluating the impact of three incentive programs on the economics of cofiring willow biomass with coal in new york state. *Energy Policy* **33**(3) 337–347.

Tillman, D., R. Conn, D. Duong. 2010. Coal characteristics and biomass cofiring in pulverized coal boilers. Tech. rep., Foster Wheeler North America Corp.

Tillman, D.A. 2000. Biomass cofiring: The technology, the experience, the combustion consequences. *Biomass and Bioenergy* **19** 365–384.

Toke, D. 2005. Are green electricity certificates the way forward for renewable energy? an evaluation of the united kingdom's renewables obligation in the context of international comparisons. *Environment and Planning C: Government and Policy* **23**(3) 361–374.

Touš, Michal, Martin Pavlas, Petr Stehlík, Pavel Popela. 2011. Effective biomass integration into existing combustion plant. *Energy* **36**(8) 4654–4662.

Tumuluru, J.S., J.R. Hess, R.D. Boardman, C.T. Wright, T.L. Westover. 2012. Formulation, pretreatment, and densification options to improve biomass specifications for co-firing high percentages with coal. *Industrial Biotechnology* **8**(3) 113–132.

U. S. Environmental Protection Agency. 2007. Renewable Fuel Standard (RFS). Available from: www.epa.gov/otaq/fuels/renewablefuels/index.htm.

US Energy Information Administration. 2010. State Energy Data System . Available from: http://www.eia.gov/state/seds/seds-data-complete.cfm.

U.S. Energy Information Administration (EIA). 2015. How much of US carbon dioxide emissions are associated with electricity generation? http://www.eia.gov/tools/faqs/faq.cfm?id=77&t=11 (accessed December 2015).

U.S. Environmental Protection Agency (EPA). 2017. Inventory of us greenhouse gas emissions and sinks: 1990-2015. https://www.epa.gov/ghgemissions/inventory-us-greenhouse-gas-emissions-and-sinks-1990-2015 (accessed July 2017).

US National Renewable Energy Laboratory (NREL). 2004. Biomass cofiring in coal-fired boilers. http://www.nrel.gov/docs/fy04osti/33811.pdf (accessed May 2014).

Wang, M. 2008. The greenhouse gases, regulated emissions, and energy use in transportation (GREET) model: Version 1.5. Center for Transportation Research, Argonne National Laboratory.

Wils, Andrea, Wolfgang Calmano, Peter Dettmann, Martin Kaltschmitt, Holger Ecke. 2012. Reduction of fuel side costs due to biomass co-combustion. *Journal of hazardous materials* **207** 147–151.

Wiser, Ryan, Mark Bolinger, Galen Barbose. 2007. Using the federal production tax credit to build a durable market for wind power in the united states. *The Electricity Journal* **20**(9) 77–88.

Wu, X., J. A. Niederhoff. 2014. Fairness in selling to the newsvendor. *Production and Operations Management* **23**(11) 2002–2022.

Xu, Jiuping, Liming Yao, Xiaodan Zhao. 2011. A multi-objective chance-constrained network optimal model with random fuzzy coefficients and its application to logistics distribution center location problem. *Fuzzy Optimization and Decision Making* **10**(3) 255–285.

You, F., L. Tao, D.J. Graziano, S.W. Snyder. 2012. Optimal design of sustainable cellulosic biofuel supply chains: Multiobjective optimization coupled with life cycle assessment and input-output analysis. *AIChE Journal* **58**(4) 1157–1180.

You, F., B. Wang. 2011. Life cycle optimization of biomass-to-liquid supply chains with distributed-centralized processing networks. *Industrial & Engineering Chemistry Research* **50**(17) 10102–10127.

Young, H. P. 1995. *Equity: in theory and practice*. Princeton University Press.

Yue, D., F. You, S.W. Snyder. 2014. Biomass-to-bioenergy and biofuel supply chain optimization: Overview, key issues and challenges. *Computers and Chemical Engineering* **66** 36–56.

Zamboni, A., N. Shah, F. Bezzo. 2009. Spatially explicit static model for the strategic design of future bioethanol production systems. 1. Cost Minimization. *Energy & Fuels* **23**(10) 5121–5133.

Zhang, Y., J. McKechnie, D. Cormier, R. Lyng, W. Mabee, A. Ogino, H. L. Maclean. 2009. Life cycle emissions and cost of producing electricity from coal, natural gas, and wood pellets in Ontario, Canada. *Environmental Science and Technology* **44**(1) 538–544.

Zhou, Y., L. Wang, J. D. McCalley. 2011. Designing effective and efficient incentive policies for renewable energy in generation expansion planning. *Applied Energy* **88**(6) 2201–2209.